SOFT COMPUTING TECHNIQUES IN POWER SYSTEM ANALYSIS

by

Kurukulasuriya Joseph Tilak Nihal Fernando

A thesis submitted in fulfilment of the requirements for the degree of

Doctor of Philosophy

Faculty of Health, Engineering and Science

Victoria University of Technology

Footscray, Victoria, Australia

2008

Doctor of Philosophy

Declaration

I, Kurukulasuriya Joseph Tilak Nihal Fernando, declare that the PhD thesis entitled Soft Computing Techniques in Power System Analysis is no more than 100,000 words in length, exclusive of tables, figures, appendices, references and footnotes. This thesis contains no material that has been submitted previously, in whole or in part, for the award of any other academic degree or diploma. Except where otherwise indicated, this thesis is my own work.

K. J. T. N. Fernando Date:

TABLE OF CONTENTS

ACKNOWLEDGMENTS

I wish to thank Prof. Akhtar Kalam for his excellent supervision of the research and the writing of the thesis and the help he extended even while on vacation. Thanks are also extended to Victoria University of Technology for giving me the opportunity and the facilities for research.

I wish to dedicate this thesis and research to my wife Shanthi, my children Manisha, Manjiv and Mayantha and last but not least to my late parents Norbert and Magdalene all of whom contributed in immeasurable ways that are too numerous to enumerate here.

Chapter 1

INTRODUCTION

Soft computing is a concept that has come into prominence in recent times and its application to power system analysis is still more recent [1]. This thesis explores the application of soft computing techniques in the area of voltage stability of power systems.

Soft computing, as opposed to conventional "hard" computing, is a technique that is tolerant of imprecision, uncertainty, partial truth and approximation. Its methods are based on the working of the human brain and it is commonly known as artificial intelligence. The human brain is capable of arriving at valid conclusions based on incomplete and partial data obtained from prior experience. It is an approximation of this process on a very small scale that is used in soft computing. Some of the important branches of soft computing (SC) are artificial neural networks (ANNs), fuzzy logic (FL), genetic computing (GC) and probabilistic reasoning (PR). The soft computing methods are robust and low cost.

It is to be noted that soft computing methods are used in such diverse fields as missile guidance, robotics, industrial plants, pattern recognition, market prediction, patient diagnosis, logistics and of course power system analysis and prediction. However in all these fields its application is comparatively new and research is being carried out continuously in many universities and research institutions worldwide [2, 3].

The research presented in this thesis uses the soft computing method of Artificial Neural Networks (ANN's) for the prediction of voltage instability in power systems. The research is very timely and current and would be a substantial contribution to the present body of knowledge in soft computing

and voltage stability, which by itself is a new field. The methods developed in this research would be faster and more economical than presently available methods enabling their use online.

1.1 Problem Statement

In all electrical power engineering courses rotor angle stability is invariably taught as a routine practice. However, while voltage stability has come into prominence in recent times, it is not covered in sufficient depth if at all. Most engineers in the industry are not familiar with the problem and usually confuse it with rotor angle stability or low voltage problems. This is due to the fact that in the past virtually all power systems were designed with ample redundancy and voltage stability was seldom a problem. However, in recent times with reduced investment in power system expansion, load growth particularly in areas with weak transmission and generation and deregulation of the market causing unusual load patterns, voltage stability has come into prominence and theories to explain and analyze it are now being developed [4]. Voltage instability results in voltages in parts of the system or the entire system becoming unstable or collapsing altogether causing collapse of the system. It is also different to low voltages experienced in certain parts of the network during certain conditions, when, though some voltages are low, the system is operating at a stable point. The power system dynamics that take place during voltage instability are non-linear and non-linear analytical techniques, such as Bifurcation Theory are required for its analysis [4].

Voltage instability/collapse being a recently recognized field, literature on it is somewhat limited. It is also a field that requires a thorough understanding of the relevant mathematics which is not taught in much depth in an engineering undergraduate course. This mathemaics is the mathematics of dynamical systems that studies such concepts as dynamics of and bifurcations in dynamical systems and singular perturbation.[5-13]. (Refer to Appendices 1 & 2.) The reason for mathematics of dynamical systems for not being taught at

undergraduate level is the difficulty of the subject coupled with the difficulty of its evaluation. However with the advent of personal computers more and more mathematicians and engineers are paying greater attention to it and computer programs are being written for solution and visualization of solutions, PHASER [14] and MATLAB. There is also a voltage stability specific computer program called UWPFLOW that solves voltage stability specific problems.[15]. Extensive use of this program is made in the present research along with PHASER [14].

A major outage in North America on 14th August 2003 causing major blackouts in Midwest and Northeast United States and Ontario, Canada has been at least partially due to voltage collapse according to the US-Canada Power System Outage Task Force Report [16].

A recent outage due to voltage instability has also been reported in Sri Lanka [17].

References [18, 19] describe the application of voltage stability theory to analyze the South-Brazilian and Ecuadorian Power Systems and how the results thus obtained agreed with operational experience where voltage collapse has been experienced before. Thus voltage stability is not merely a theoretical construct but reality for which there was no urgency till recent times when power systems became more and more stressed due to aforementioned reasons.

Therefore as power systems become more complex as well as operate in more stressed states, in addition to presently used security assessment methods, methods for voltage security assessment are also needed.

1.2 Aim

The aims of the research reported in this thesis are as follows.

- To make a thorough study of the theory of voltage stability (instability).

- To study the methods of soft computing in general and Artificial Neural Networks in particular.

- Analyze the IEEE 14-bus system under different contingencies to obtain proximity to voltage collapse indices. The analysis will be performed using the UWPFLOW computer program.

- To use the results of the computer analysis to develop artificial neural networks (ANN's) suitable for the prediction of pending voltage instability in power systems thus developing a soft computing method of power system security assessment. This is the main aim of this research. Though the implementation is not a part of this project, ANN's developed will be suitable for on-line use in real power systems. For this purpose the ANN's need to be embedded and trained in dedicated hardware with inputs of the suitable power system parameters which will be identified.

- To relate the results to the hypothesis (Section 1.3).

- To identify topics suitable for further research on the subject.

1.3 Hypothesis

After reading the available literature on voltage stability and soft computing methods the following hypothesis was formed.

It is possible to train Artificial Neural Networks to predict pending voltage instability in a power system.

1.4 The Research Method

The following approach which includes the method used to obtain results was used in the research.

- The relevant mathematics was studied in detail. Refer to appendices 1 & 2.

- A study was made of the theory of voltage stability/instability. Although a highly technical textbook [4], is available and is very good for the understanding of voltage stability phenomena, other sources such as journal papers and the IEEE/PES Special Publication on Voltage Stability [20], were found to be more useful in the actual research method implemented during the voltage stability computer simulations. The computer program used is UWPFLOW [15].

- Data on voltage stability for the IEEE 14-bus test system was generated using UWPFLOW to be used to train the ANN's and illustrate the phenomenon of voltage instability in power systems.

- Artificial Neural Network theory was studied and ANN's for the prediction of voltage instability in power systems were trained and tested.

- The results were related to the hypothesis.

1.5 A survey of the available literature on voltage stability in power systems

As stated before voltage stability/instability has come in to prominence or has even been recognised only in comparatively recent times. Therefore the available literature on the topic is still tentative and often repetitive. Two recent attempts at formalising the theory and facilitating its analysis are presented in References [4, 20].

Placing the voltage stability problem in context, the references [16-19] describe real life voltage stability problems, some of which caused major outages in North America, Sri Lanka, Brazil and Ecuador.

The IEEE journal article [21] giving definitions and classifications of power system stability recognises voltage stability and gives a brief description and definition.

The References [22-25] are good examples of the original efforts to develop and consolidate a dynamical systems based theory of power system stability in general and voltage stability in particular. These are initial efforts and a theory of voltage stability is only beginning to take shape.

Subsequently further study of dynamical systems theory as applied to voltage stability of power systems was made with test systems and real systems analysed References [19, 26-34]. In these papers the theory of voltage stability takes shape pointing to the later writing of a text book and an IEEE/PES Special Publication [4, 20]. The IEEE/PES Special Publication explains the phenomenon of voltage stability, its theory though not extensively and different methods of voltage stability evaluation together with definitions of different indices to measure proximity to voltage stability in a power system. It appears from the literature that the main contributors to the development of voltage stability theory and its evaluation are Canizares [15, 19, 20, 33, 35-39], Ajjarapu [22, 23, 26-29, 32, 40, 41], Van Cutsem [4] and Hill [24, 25] in the early stages.

Later a series of papers some of which are given in references [35, 36, 38, 40-50], were published that considered different methods of calculating the voltage stability of power systems. Broadly the methods fall in to two categories, direct methods and continuation methods. The different papers vary mostly only in the detail of the methods rather than the mathematical principles involved. The point of collapse and continuation power flow methods put forward in reference [35] are the methods used in the computer program UWPFLOW; both the paper and the computer program are by the same author. This computer program is the only reasonable program that is available to researchers without spending too much on purchase of the software.

Modelling of power system components such as generators, lines, loads, etc. are presented in references [4, 20, 36, 38, 43, 45, 51].

Indices for the prediction of proximity to voltage instability are presented in references [4, 20, 37, 39, 52, 53] and compared.

A mathematical function called a Lyapunov Function is used in the analysis of dynamical systems. In voltage stability analysis this function is called an Energy Function and its derivation is put forward in references [20, 24, 54-61]. Using this energy function proximity to voltage instability can be calculated as an index.

An implemented method of real time monitoring of voltage stability in a power system in China is described in reference [62]. Other methods are described or touched upon in references [20, 63]. However none of these methods use any artificial intelligence methods as proposed in this thesis.

1.6 Originality of the Thesis

The thesis contains original work of the author except where reference is made to published literature. The choice of parameters for the training of ANN's and the particular ANN architectures chosen are new in the field of voltage stability prediction as far as the author has been able to ascertain after an extensive search of the available literature. Therefore the thesis would be an original contribution to and an expansion of the present knowledge in the field of voltage stability in general and the application of soft computing or artificial intelligence to voltage stability estimation in particular.

1.7 Thesis Organisation

Chapter 1 - Introduction

This Chapter introduces the intent of the thesis. The problem of voltage stability in power systems which has recently come into prominence is briefly explained. An aim and a hypothesis for the thesis are formulated and the research method appropriate for the stated aim of the research is formulated. Section 1.5 gives a survey of the available literature on the subject. A statement of originality of the thesis is given in Section 1.6.

Chapter 2 – Voltage Stability

The theoretical concepts of voltage stability in power systems are introduced in this Chapter which starts with an introductory section that illustrates voltage stability problems in an elementary dc power system to set the stage for later more complicated voltage instability phenomena in large ac power systems explanation of which requires complicated mathematics. This Chapter is considered essential since text books on the subject have been published only in very recent times [4] and are hard to obtain in Australia without specially ordering them from overseas. Journal publications are

somewhat recent too and it is difficult to come to grips with the subject without reading a large number of them.

Chapter 3 – Methods for Evaluation of Voltage Stability in Power Systems and Indices Used to Measure Proximity to Voltage Instability

This Chapter explains methods used to evaluate the voltage stability of power systems off line and the various indices proposed in the literature to measure proximity to voltage instability in power systems with their relative merits. The methods used in this thesis will be indicated.

Chapter 4 – Soft Computing or Artificial Intelligence Methods – Brief Theory and Selection

A brief theory of soft computing or artificial intelligence methods is introduced in this Chapter. Reasons for the selection of artificial neural networks in general and the types of neural networks used in particular are explained.

Chapter 5 – Design of the Simulation Performed

This Chapter explains the design of the power system simulations performed for the evaluation of voltage stability in the IEEE 14-bus test system and its variations selected by the author of the thesis. The reasons for the particular design used are explained. The design and training of the ANN's used is also explained.

Chapter 6 – Simulation Results

Results of the voltage stability analysis of the IEEE 14-bus Test System and the results of the ANN's trained are presented in this Chapter. Graphical representations of voltage collapse of the IEEE 14-bus Test System for different contingencies and the error graphs of the different ANN's that were trained are also given in this Chapter.

Chapter 7 – Discussion of Results

A discussion of the results in the context of the aims of the research undertaken is given in this Chapter. Section 1.2 presents the aims in point form and a summary of these aims is used as the relevant section headings in this Chapter.

Chapter 8 – Conclusions and Scope for Future Work

Finally the conclusions of the research with respect to the hypothesis presented in Section 1.3 are presented here. The discussion of the results with respect to the aims of the research is presented in Chapter 7. Topics for further related research are also identified.

1.7.9 Appendices 1 & 2

These two appendices, Appendix 1 – Preliminary Mathematics and Appendix 2 – Analysis of Voltage Stability are given for completeness of the thesis. They, it is hoped will save the reader the trouble of having to locate hard to find references. In the relevant chapters of the thesis reference is made to these two Appendices.

Chapter 2

VOLTAGE STABILITY

2.1 Introduction

In the past adequate redundancy was built into power systems for voltage instability to be a major problem. Only rotor angle stability was considered in the operation and expansion of power systems. With the introduction of the new electricity market resulting in reduced investment and altered load patterns, particularly increasing load in areas with weak transmission and generation capacity, voltage stability has come into prominence [4, 20]. Voltage stability requires mathematical theory and concepts that are difficult to understand.

2.2 Some Useful Definitions.

The following two definitions of stability of a power system are given in [20].

1. *An operating point of a power system is* ***small disturbance stable*** *if, following any small disturbance, the power system state returns to be identical or close to the pre-disturbance operating point.*
2. *An equilibrium of a power system model is* ***asymptotically stable*** *if, following any small disturbance, the power system state tends to the equilibrium.*

The second definition assumes that the power system is modelled by a set of differential equations.

Voltage instability is defined in [4] as follows.

Voltage instability *stems from the attempt of load dynamics to restore power consumption beyond the capacity of the combined transmission and generation system.*

2.3 Voltage Instability

A power system operating under stable conditions keeps continuously evolving. During this process some or all of the following take place in the system. The load changes; generators and induction motors go through electromechanical transients; static VAR compensators, (SVCs), activate; on load tap changers in transformers activate; shunt capacitors are switched on and off; automatic load recovery takes place following faults; faulted components of the power system are isolated; faulted transmission and distribution lines auto-reclose; excitation limiters activate etc. Thus a power system under load is a dynamical system. During this dynamics, if the power system is to remain stable, the operating point or the equilibrium point of the system has to track a stable point in state space. However, the transmission system has a limited capacity for power transmission and generators have a limited generating capacity, on reaching these limits the system can go into voltage instability. At the point of going into voltage instability, the stable point of operation that existed before disappears. Thus the power system undergoes a transient and during this transient, the voltages decline causing a voltage collapse. It is to be noted that the state of a power system operating with low voltages but at a stable point, i.e. there is no dynamic collapse of the voltages, does not constitute a voltage stability problem.

The following example taken from [1] but solved in greater detail is an elementary example of how voltage instability takes place.

2.4 Voltage Instability in an Elementary DC Power System

Consider a simple dc power system fed by a dc power source of 1V. The line resistance is 0.5Ω, the load is a variable resistor and I is the current drawn by the load.

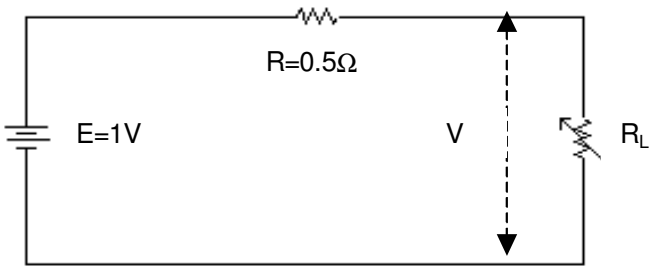

Figure 2.1 An Elementary dc Power System

The load resistance R_L is automatically varied to achieve an assumed maximum power demand of 0.55W according to the differential equation:

$$\dot{R}_L = I^2 R_L - 0.55 \tag{2.1}$$

According to elementary circuit theory, the maximum transferable power P_{max} is given by:

$$P_{\max} = \frac{E^2}{4R} = 0.50W \tag{2.2}$$

However in this example a power demand of 0.55W is placed on the system.

The trajectory of the load resistance given by the solution of the differential equation (2.1) with an initial condition of $R_L = 4.5\Omega$ is shown in Figure 2.2.

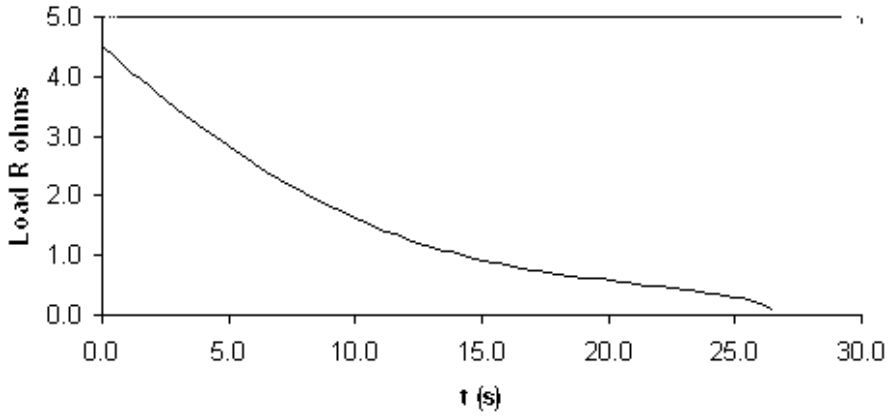

Figure 2.2 Trajectory of the Load Resistance

The variation of the load voltage and load power as the system power demand increases are shown in Figures 2.3 & 2.4.

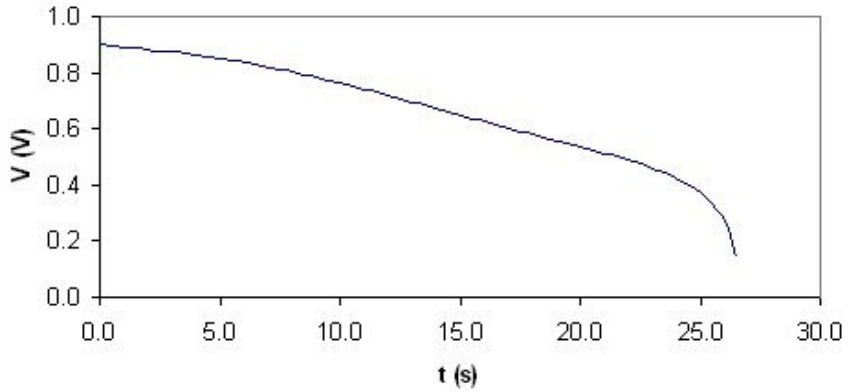

Figure 2.3 Variation of Load Voltage

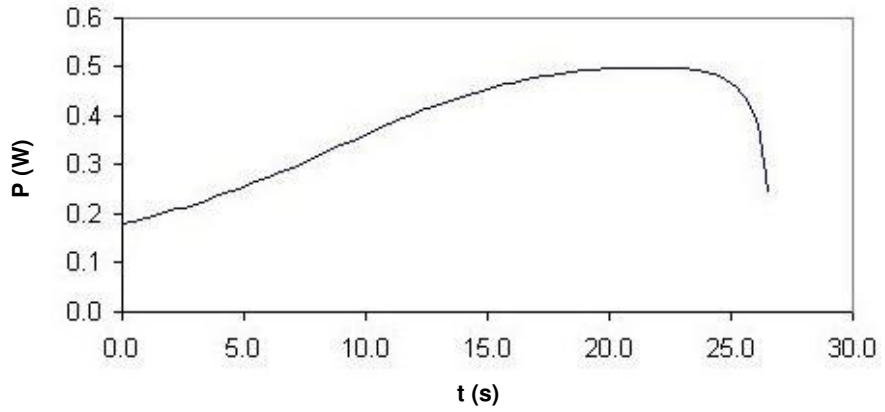

Figure 2.4 Variation of Load Power

It is seen from Figures 2.3 & 2.4 that voltage instability or collapse takes place when the demand for power increases beyond the maximum deliverable power of 0.5 W. Obviously the dynamics obtained in an actual power system is far more complicated.

The dynamics of a loaded power system, as the dynamics of many other systems in engineering, can be represented by a system of non-linear ordinary differential equations, which can be written as:

$$\dot{x} = f(x) \qquad (2.3)$$

where usually $\dot{x} = \frac{dx}{dt}$ where t is time, x is a $(n \times 1)$ vector and $f_i, (i = 1, 2, ...n)$ are generally non-linear functions of $x_i, (i = 1, 2, ...n)$. The vector x represents the state of the system at a given time and is known as the **state vector.** Systems of this type are known as **dynamical systems.**

Such dynamical systems can be solved analytically only in a very limited number of cases, however given initial conditions for the **state variables**, the equations can be solved by numerical integration. Computer programs are now available for their solution. A theory known as the qualitative or

geometric theory of ordinary differential equations allows the study of the behaviour of dynamical systems without resort to integration. [5-13].

2.5 Classification of Power System Stability

Table 2.1 shows a convenient classification of power system stability. It is similar to Table 1.1 in reference [4] but has been modified for better clarity of understanding.

Table 2.1 Classification of Power System Stability

Time Scale	General Description - generator driven	Generator driven	Load Driven
Short Term	Steady state or small signal stability. Transient or large disturbance stability	Rotor angle stability both transient and steady state	Short term voltage stability
Long Term	Insufficient generation	Frequency stability	Long term voltage stability

Here two types of mechanisms of instability, namely generator driven and load driven are identified. The column headed general description briefly describes the familiar generator driven instability. Rotor angle stability takes place in the time frame of electromechanical dynamics which lasts a few seconds. Frequency instability also generator driven takes place on a longer time frame lasting several minutes. Voltage stability also takes place both in the short term and in the long term but it is load driven. Its analysis requires a detailed network representation as will be seen below. Further, in its analysis,

no strict distinction is made between long term and short term voltage stability. [4].

The dynamic nature of a power system was touched upon in Section 2.3. The dynamics mentioned there take place in the general time scales given in table 2.1. A further elaboration of the time scales in which voltage instability may take place is as follows.

1. The time scale of electromechanical transients such as those of generators, regulators, induction machines and power electronics (eg. SVC's), takes place in the range of seconds.

2. The time scale of discrete switching devices such as on load tap changers and excitation limiters, takes place in the range of tens of seconds.

3. The time scale of load recovery processes, takes place in the range of several minutes or even hours.

The time scale 1 as aforementioned is the short term or transient time scale in voltage stability while the time scales 2 & 3 are the long term time scales. Electromagnetic transients such as dc components of short circuit currents take place in too short a time scale to be of any relevance in voltage stability and therefore are not considered. It should also be noted that a voltage collapse that starts in the long term time scale could end up as a transient or short term collapse. That is initially the voltages in the power system collapse slowly but towards the end of this collapse the rate of collapse accelerates causing a catastrophic failure of the power system. [20].

A very important but often unnoticed difference between voltage collapse and classical transient stability is that the focus of voltage collapse is voltages

and loads while the focus of classical transient stability is generators and angles.

2.6 Theory of Voltage Stability

As mentioned earlier in the thesis, a power system is a nonlinear dynamical system and in the analysis of voltage stability, mathematics of dynamical systems is used. Though in the past, engineers have from time to time used the methods of dynamical systems for problem solving, it has remained mainly the province of mathematicians due to its difficulty. Even among mathematicians not many have devoted much time to it due to its computational difficulties and the need to grasp and visualise its concepts in many dimensions. However with the advent of personal computers easing the computational burden, more and more authors are paying attention to it. Some of the available books on the subject are [6-13]. There is a computer program 'PHASER' [14] specifically designed for evaluation and visualisation of the behaviour of dynamical systems. The author of this thesis used this program to solve some of the specifically designed problems which are presented in Appendix 1. Appendices 1 & 2 present the mathematics of dynamical systems and will be referred to in the rest of this section along with other references. It should be emphasised that dynamical systems are solved, given the initial conditions, using qualitative or geometric theory of ordinary differential equations rather than analytical methods. These systems are very difficult or impossible to analyse analytically.

2.6.1 A Brief Description of Relevant Mathematics

A dynamical system is usually represented by a set of n differential equations as follows: (Refer to Appendices 1 & 2, particularly appendix 2 for detailed explanations and references.)

$$\dot{x} = f(x) \qquad (2.1)$$

Here x is a (n x 1) vector, $f(x)$ is a set of (n) nonlinear functions of x and $\dot{x}$ is the time differential of x. Given the initial conditions and under certain conditions the system can be solved to give a **trajectory** of the system over time in the n-dimensional space of x. These trajectories have **intervals of existence** that may be finite or infinite.

Equilibrium points are particular solutions of the equation (2.1) where the solutions stay at these equilibrium points for all time. Equilibrium points are given by the solutions to the following equation:

$$f(x) = 0 \qquad (2.2)$$

An equilibrium point may be **unstable**, **stable** or **asymptotically stable** with a region of attraction.

If equation (2.1) represents a nonlinear system then the following apply.

- The number of equilibria of the system may be one, more than one or none.

- The existence of a stable equilibrium is not a guarantee of the stability of the system since the region of attraction of the stable equilibrium may be limited.

The stability of an equilibrium point of a nonlinear system of the type shown in equation (2.1) may be determined by linearising the system around the equilibrium point and obtaining its Jacobian.

- If all the eigenvalues of the Jacobian have negative real parts, then that particular equilibrium point is asymptotically stable.

- If at least one eigenvalue of the Jacobian has a positive real part, then that particular equilibrium point is unstable.

2.6.1.1 Bifurcations

The instabilities of interest in power system voltage stability are bifurcations.

Consider a dynamical system of the following form.

$$\dot{x} = f(x, p) \tag{2.3}$$

where x is a (n x 1) state vector and p is a (k x 1) parameter vector. For every value of p, the equilibrium points of the system are given by:

$$f(x, p) = 0 \tag{2.4}$$

These equilibrium points fall on a k-dimensional manifold in the (n + k)-dimensional space of state and parameter vectors. At a **bifurcation** point for the given value of p, the Jacobian of equation (2.3) with respect to x is singular. A **saddle node bifurcation** (**SNB**) is a bifurcation where two branches of equilibria meet. (Refer to Appendix 2.) So at a saddle node bifurcation two equilibria coalesce and disappear. One of the equilibria has a real positive eigenvalue and the other has a real negative eigenvalue. Both become zero at the SNB.

At a **Hopf** bifurcation a pair of complex eigenvalues crosses the imaginary axis and causes an oscillatory instability.

2.6.1.2 Differential Algebraic Systems

Some dynamic systems are represented by a set of differential equations with algebraic variables where these algebraic variables are subject to a set of algebraic constraints represented by a set of algebraic equations as follows:

$$\dot{x} = f(x, y, p) \tag{2.5a}$$

$$0 = g(x, y, p) \tag{2.5b}$$

where x and p are as in equation (2.3) and y is a (m x 1) vector of algebraic variables. The algebraic equation (2.5b) defines a (n + k)-dimension **constraint manifold** which is a hypersurface where the solutions to the system occur.

At singular points of the m algebraic equations, ie. when the algebraic Jacobian is singular, the response of the system is undefined and causes **singularity induced bifurcations**.

When the algebraic Jacobian is non-singular, the response of the system can be studied by studying the **reduced Jacobian** of the system given by equation (2.5). This will give the bifurcation points and other relevant data of the system.

2.6.1.3 Singular perturbation or Time Scale Decomposition

Some systems, including power systems, have dynamics evolving in different time scales. That is these systems have dynamics evolving in slow and fast time scales. Such systems are represented as follows.

$$\dot{x} = f(x, y) \tag{2.6a}$$

$$\varepsilon \dot{y} = g(x, y) \tag{2.6b}$$

where x is a vector of slow states, y is a vector of fast states and ε is a small number.

In singular perturbation or time scale decomposition, the method used to study such systems, it is assumed that $\varepsilon \to 0$. Then the system reduces to a differential algebraic system as follows:

$$\dot{x}_s = f(x_s, y_s) \tag{2.6c}$$

$$0 = g(x_s, y_s) \qquad (2.6d)$$

This system contains only slow state variables and can be studied by the methods used for differential algebraic systems. It is assumed in the analysis that the fast dynamics is stable and that it has died out.

2.7 Application of the Theory to Power Systems

In equation 2.3 reference is made to two types of variables in a dynamical system namely states and parameters. In a power system, which as stated above is a dynamical system, examples of states are bus voltage magnitudes, bus voltage angles, machine angles and currents in generator windings. Examples of parameters are real power demands at system buses and sometimes control settings that determine how different power system and generator controls behave. [4, 18-20, 26-29, 31, 32, 35, 36, 40, 41, 44]. The choice of states and parameters used in a particular study of voltage stability is dependent on the method of analysis chosen in that instance. Refer to Chapter 3 for the method of study used in this thesis.

In the analysis of a power system for voltage stability one of the methods used is the singular perturbation method described above and in Appendices 1 and 2 is applied. Also refer to references [4, 20]. This is justified by the fact that the parameters, usually bus loads, vary slowly as the loads evolve with time and the variation in the states such as bus voltages and angles due to this load change is comparatively very fast. This method of analysis is known as the **quasi-static** or **quasi-steady-state method** and is sometimes used in practical voltage stability studies. In this method the states are calculated at each small increment of the parameters till voltage collapse occurs in the power system. The other methods are the **multi-time-scale method** where the full dynamics of the power system and its components are taken into account and a **modified load flow method**. For most studies the modified load flow method is sufficient. Refer to Chapter 3 for a discussion of this. It is

to be noted that both system states and parameters are vectors and therefore the **state space** and **parameter space** of a power system are multi-dimensional consisting of hundreds and sometimes thousands of dimensions each. Therefore the following explanation is confined to 1, 2 or 3 dimensions. Higher dimensional problems can be calculated and manipulated mathematically, (refer to Appendices 1 and 2), though they are impossible to visualise.

2.7.1 A Simple Power System

Consider the simple power system shown in Figure 2.5.

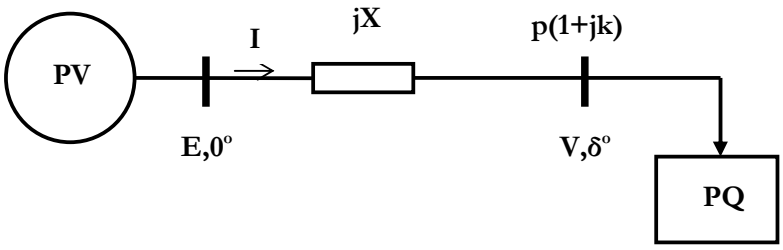

Figure 2.5 A Simple Power System

The figure shows a single PV or constant voltage or slack bus with a single generator connected to it supplying a constant power factor PQ load consisting of real and reactive parts equal to p(1+jk).

Let the impedance of the line be $(0+jX)$ as resistance is neglected. Then, if I is the line current and $(S=p+jq)$ is the load power, it can be shown that [4, 20]:

$$V = E - jXI \qquad (2.7)$$

$$S = \frac{j}{X}(EV\cos\delta + jEV\sin\delta - V^2) \qquad \text{(2.8 a and b)}$$

$$\therefore p = -\frac{EV}{X}\sin\delta$$

and

$$q = -\frac{V^2}{X} + \frac{EV}{X}\cos\delta$$

The above equations are written on the assumption of quasi-steady-state in which case they reduce to power flow equations. More will be discussed on this topic in Chapter 3.

Now, if real power p is chosen as the slowly varying parameter and V and δ are chosen as the state vector, the variation of the magnitude of V with p is as shown in Figure 2.6. Such a diagram where one of the state variables is plotted against the slowly varying parameter, p in this case, is called a **bifurcation diagram**.

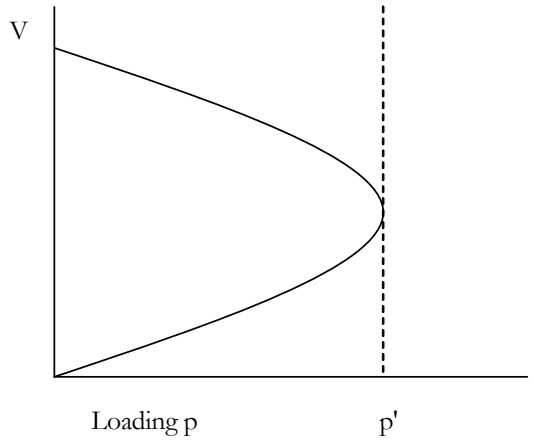

Figure 2.6 Bifurcation Diagram of State V Vs Parameter p

It is seen from the bifurcation diagram that for loads less than p' there are two equilibria, one at high voltage and therefore low current and the other at low

voltage and high current. In practice the high voltage equilibrium is the more stable and the equilibrium at which a power system operates. As the slowly varying parameter, power p, is increased at the load bus, the two equilibria come closer and coalesce at the critical power p' which is a saddle node bifurcation. Beyond p' the power system has no equilibrium points and cannot be operated. At p' voltage collapse occurs.

In Figure 2.7 both power system states V and δ are plotted against p.

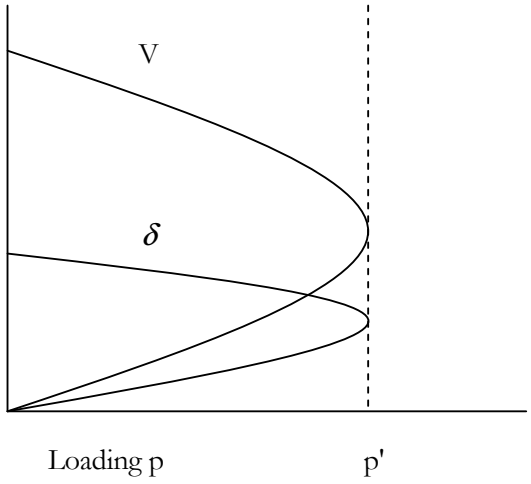

Figure 2.7 Bifurcation Diagram of States V & δ Vs Parameter p

In this diagram the lower value of angle δ refers to the stable higher value of voltage V. It is seen that the noses of both curves representing a saddle node bifurcation occur at the same critical loading p'.

The occurrence of voltage stability and instability can also be visualised in state space as follows: (It is to be emphasised that the Figures 2.6 and 2.7 are bifurcation diagrams). Figure 2.8 shows the case of the above simple power system operating at a stable equilibrium where the load power is less than p'.

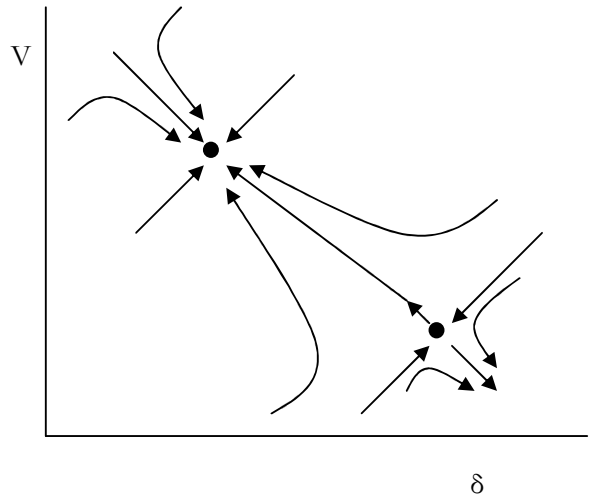

Figure 2.8 State Space at Loads Below Critical Loading p'

It is seen that any small perturbation from the upper equilibrium at the higher voltage causes system dynamics that bring the operating point back to the equilibrium. The diagram also shows that the low voltage equilibrium is unstable. Any small perturbation from this equilibrium invariably causes a catastrophic collapse of the power system unable to reach an equilibrium.

Figure 2.9 shows state space at the critical loading of p'.

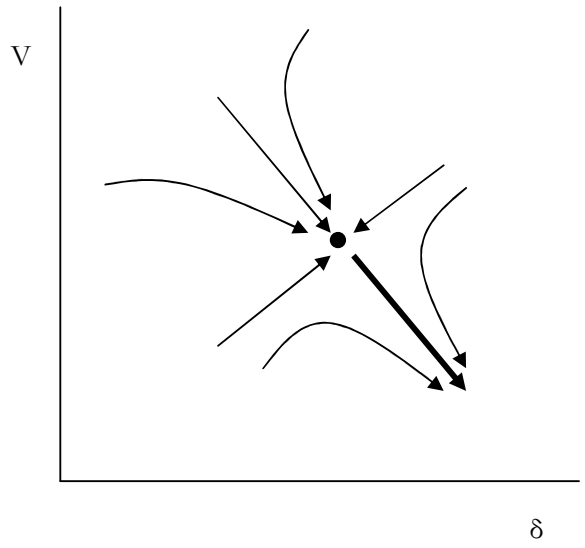

Figure 2.9 State Space at Critical Loading p'

At this loading the two equilibria have coalesced into one equilibrium. Any small perturbation from this equilibrium will cause power system states to move in the direction of the thick arrow casing a monotonic decrease in the system voltage and an increase in the angle δ. This is the mechanism of voltage collapse in a power system.

Figure 2.10 shows the state space of the simple power system above subsequent to voltage collapse at a saddle node bifurcation.

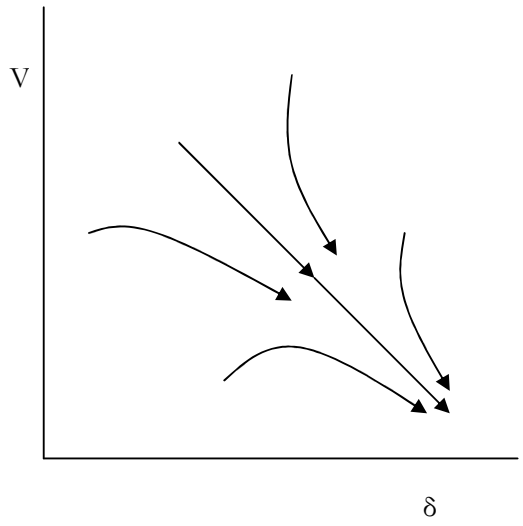

Figure 2.10 State Space Subsequent to Voltage Collapse at a Saddle Node Bifurcation

The voltages fall monotonically unable to find an equilibrium.

In a real power system the state space would be, as aforementioned, multidimensional consisting of hundreds if not thousands of states.

2.7.1.1 A Two Load Power System in Parameter Space

Figures 2.8 to 2.9 showed a single load power system in state space. Similarly a power system can also be visualised in parameter space for voltage stability studies. To do so at least two load buses need to be considered. Let the real power loads at the two buses be p1 & p2.

Referring to Figure 2.11:

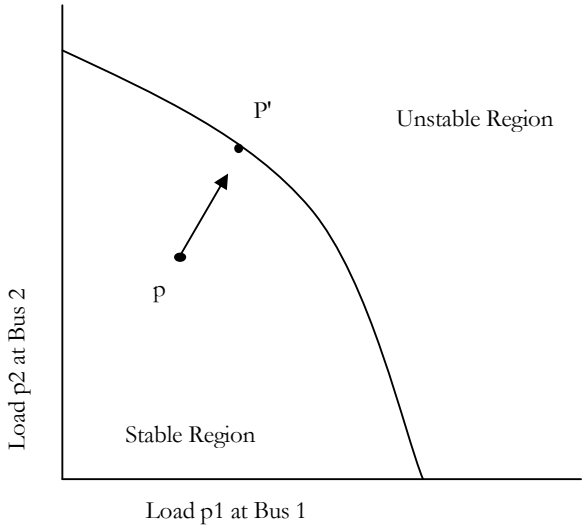

Figure 2.11 Parameter Space of a Two Load Bus Power System

In the region marked 'Stable Region' there are stable equilibrium points where the power system may be operated stably with any combination of p1 & p2 that falls in that region. However in the region marked 'Unstable Region' the power system has no equilibrium points at which it can operate stably and any loading that reaches this region will cause voltage collapse. In the figure loading point p is stable, however if the power system is stressed by increasing the load in the direction of the arrow it will reach the point p' which is a saddle node bifurcation and voltage collapse will ensue. Thus the power system always needs to be operated in the stable region. The two regions are separated by a curve called the **bifurcation set**. The bifurcation set for a power system with n real power loads (parameters) is a hyper surface of (n-1) dimensions and the parameter space is n-dimensional.

2.7.1.2 Voltage Instability Caused by a Large Disturbance

Voltage instability may result in a power system that undergoes a large disturbance such as the loss of a transmission line or a generator due to a

fault. Before the disturbance the power system is operating at a stable equilibrium, however, after the disturbance that causes the loss of a major component, the power system may be left without a stable operating point or equilibrium. This would cause a catastrophic collapse of the system voltages. In state space this is the equivalent of the power system abruptly going from the state represented in Figure 2.8 to the state represented in Figure 2.10 without first reaching the saddle node bifurcation represented in Figure 2.9. In parameter space this can be represented as the system, operating stably, as represented by the point p in Figure 2.11 and then immediately after the disturbance finding itself operating in the unstable region as shown in Figure 2.12.

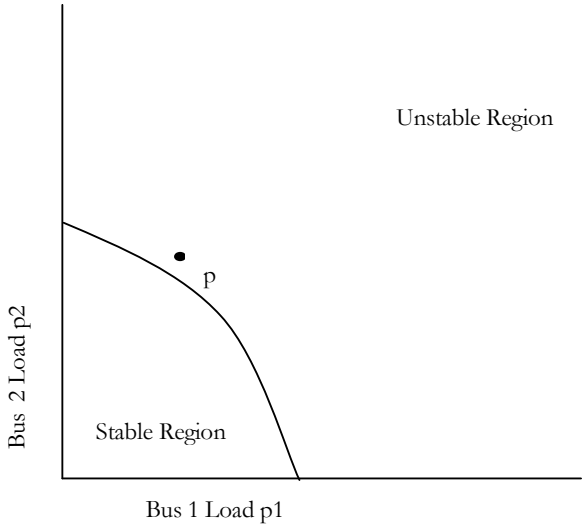

Figure 2.12 Parameter Space of a Two Load Bus Power System Operating at an Unstable Point

In Figure 2.12, the operating point p of the power system has not moved but the stable operating region of the power system has shrunk due to the disturbance and now the operating point is outside the new modified stable region.

2.7.1.3 Voltage Instability Caused by Power System Limits

During the operation of a power system various limits are invariably encountered. Examples of these limits are generators reaching their reactive power limits and on load tap changing transformers reaching the limits of the tap ranges. Consider a generator with reactive power limits and the nose curves of the power system drawn for a particular bus with the bus voltage on the y-axis and the system real power drawn on the x-axis. When so drawn, the nose curves are also bifurcation diagrams and are shown in the following Figures 2.13 and 2.14. The upper portions of the nose curves represent the stable equilibria of the power system.

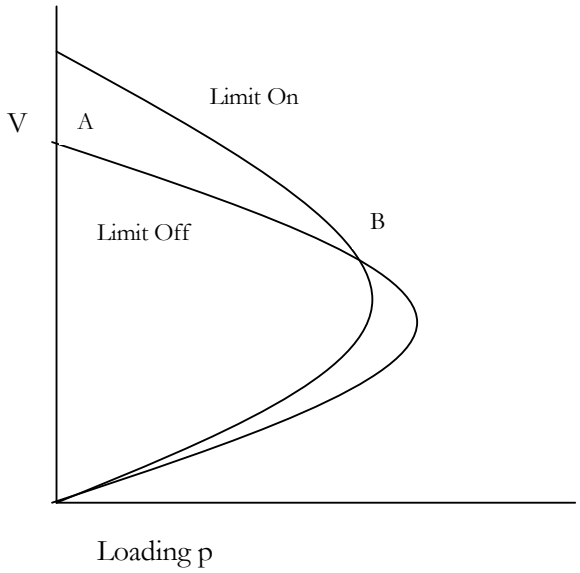

Figure 2.13 Equilibrium Point B Remains Stable On Reaching Reactive Power Limit

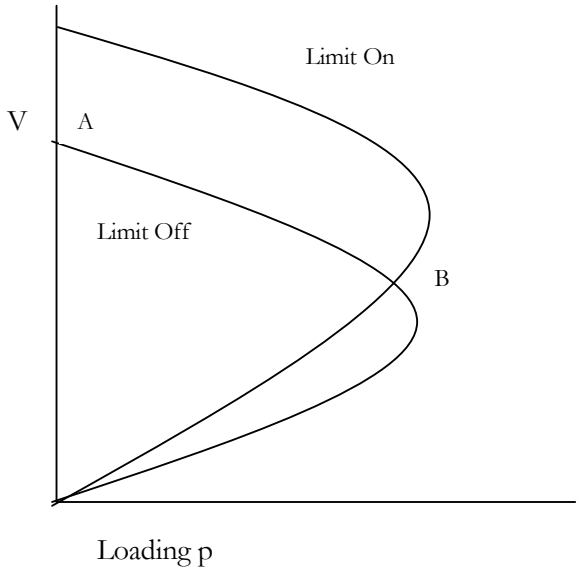

Figure 2.14 Equilibrium Point B Becomes Unstable On Reaching Reactive Power Limit

In both figures consider the system starting operation at point A. Point A is not a zero power point since the x-axis starts at a value greater than zero, the base condition of the power flow study. At this point in time, the generator reactive power limit is off, that is the generator is capable of supplying more reactive power. As the parameter p (system real power) increases, the system equilibrium or operating point moves along the 'limit off' nose curve. Now if it is assumed that the generator reaches its reactive power limit at point B, then the nose curve which is also the bifurcation diagram changes to the 'limit on' nose curve. In Figure 2.13 it is seen that the point B falls on the stable part of the 'limit on' nose curve and therefore the power system continues to function in a stable state though with a smaller margin to voltage collapse. However if the 'limit on' nose curve of the system is as shown in Figure 2.14, then the power system operating point is on the unstable part of the new nose curve and therefore the system collapses at a **limit induced bifurcation.**

2.7.1.4 Voltage Stability in a System with Both Slow and Fast Time Scales

Equations 2.6c and 2.6d represent the time scale decomposition of a system with both slow and fast time scales. In the two equations it is assumed that the fast transients are stable and that they have died out. Such a system with only one slow variable x and one fast variable y is represented in Figure 2.15 in the x-y plane.

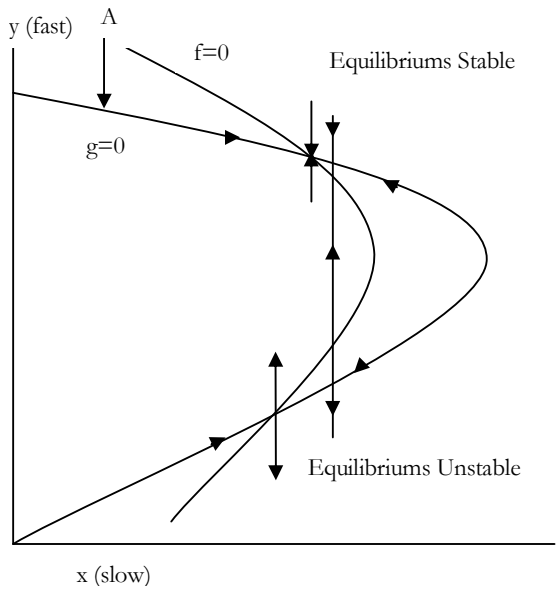

Figure 2.15 A System with Slow and Fast Time Scales

The curve g=0 is the **fast dynamics equilibrium manifold**, that is, on this manifold fast dynamics do not take place. Only the slow components of y and x vary on this curve. That is, this is a good approximation of the **slow manifold** of the two time scale system. Now the equilibria of the complete system with both slow and fast components are the intersection of the curves g=0 and f=0. The upper equilibrium is stable and the lower equilibrium is unstable. The arrows in the diagram indicate the direction of movement of the system operating point for any initial condition. As an example, if the initial condition of the system is at A in the figure, then a fast transient takes

place that brings the operating point to the upper stable part of the fast dynamics equilibrium manifold and then moves slowly along this slow manifold of the two time scale system till the stable upper equilibrium of the two time scale system is reached and continues to operate there. In an actual power system obviously there will be many variables x and y and therefore Figure 2.15 would be multi-dimensional.

In a two time scale system it can also happen that the curves g=0 and f=0 do not intersect. For example the curve f=0 may be some distance removed from the curve g=0 in the positive direction along the x-axis. If the power system has reached such a state then a **saddle node bifurcation of the fast dynamics** can take place since the two curves or manifolds do not intersect at system equilibria. In this case, for an initial condition at A, the system again is brought to the fast dynamics equilibrium manifold through a fast transient and starts moving along this manifold in search of a system equilibrium. But since no system equilibrium exists, the operating point reaches the nose of the fast dynamics equilibrium manifold which is a saddle node bifurcation of the fast dynamics causing voltage collapse.

2.8 Conclusion

In this chapter voltage stability in a power system is defined and illustrated with a simple dc power system. A classification of power system stability is given and the theory of voltage stability along with the requisite mathematics is described. Finally the application of the theory to power systems is discussed and illustrated with simple examples.

Chapter 3

METHODS FOR EVALUATION OF VOLTAGE STABILITY IN POWER SYSTEMS AND INDICES USED TO MEASURE PROXIMITY TO VOLTAGE INSTABILITY

There are a number of methods of evaluating voltage stability in a power system. However the method chosen in a particular case depends on the resources available, time constraints and the required depth of analysis. Since voltage stability is still a developing field one has to be rather cautious in the method and resources used. The program used for this thesis is UWPFLOW [15]. This chapter, as the title suggests, will examine the methods of evaluation of voltage stability in a power system and indices used to measure proximity to voltage instability in a power system with emphasis on the method used in the thesis.

3.1 Background

Until now time power system engineers have used power flow programs and transient angle stability programs in the analysis of power systems during design and operation [4, 20]. However, due to reasons mentioned in Section 2.1, it has now become necessary to consider voltage stability as well.

Power flow programs use static analysis using algebraic equations to obtain the condition of the power system at a particular point in time. This point in time may be after the active and reactive powers have changed in some or all of the buses or the system configuration has changed due operational reasons or fault conditions.

Transient angle stability programs use dynamic analysis. As mentioned in [20] and in the experience of the author of this thesis as a power systems engineer, transient stability programs use dynamic models of power system

components such as synchronous machines, excitation systems, turbines and their governors, static var compensators (SVC's), high voltage direct current transmission, loads etc. These models are suitable for analysis in the time frame of a few milliseconds to a few tens of seconds.

However voltage instability can develop in the time frame of up to many tens of minutes, references [4, 16, 20, 64]. Thus a careful choice of the method depending on resources and time available is needed in the analysis of voltage stability.

3.2 Methods Used in the Analysis of Voltage Stability

Voltage security of a power system in the context of its general security is explained very clearly in reference [4] which is summarised below.

A power system is subjected to two types of constraints:

- **Load constraints** state that the load demand is met by the system and are expressed as equality constraints.

- **Operating constraints** impose maximum and minimum limits on variables such as line currents, bus voltages, generator real and reactive power etc. These are expressed as inequality constraints.

When both load and operating constraints are satisfied the power system is in a **normal state**. On the occurrence of a disturbance the system may settle down to a new normal state or one of two abnormal states. An **emergency state** is an abnormal state when some operating constraints are not satisfied. A **restorative state** is an abnormal state when operating constraints are satisfied but some or all the load constraints are not, due to say a partial blackout or load shedding.

A **static emergency** occurs after a disturbance when a new long term equilibrium is reached but some operative conditions are violated. A

dynamic emergency occurs when a disturbance causes the system to become unstable due to say loss of synchronism. **Static security assessment** deals with the ability of the system not to enter a static emergency after a disturbance. **Dynamic security assessment** deals with the ability of the system to reach a stable operating point after a disturbance and is a prerequisite for system security.

Corrective control or corrective operator action is often possible in a static emergency but a dynamic emergency requires action by automatic devices.

Voltage stability belongs to the category of dynamic emergencies where a stable operating point is lost requiring automated action, however if a pending voltage instability could be predicted sufficiently in advance then corrective operator action may be possible. This is still beyond the state-of-the-art, reference [4], and the research presented in this thesis is an attempt at rectifying this.

In voltage security analysis, a power system is evaluated for voltage stability during credible contingencies such as the loss of transmission and generation facilities. The general rule adopted is the well-known (N-1) criterion where a power system is expected to perform without entering an emergency state for contingencies when a single transmission line or a single generator trips out. [4].

As will be seen below in this Chapter static analysis tools can be used for voltage security analysis and often is the main tool used. However this should not detract from the fact that voltage instability is a dynamic problem.

3.2.1 Dynamic or Time Domain Analysis.

As stated in section 3.1, dynamic or time domain analysis is used in the main for the analysis of transient behaviour of power systems. The computer programs designed for this purpose, in general, use dynamic models for the following power system components, [20]:

- Synchronous machines.
- Excitation systems.
- Turbines.
- Governors.
- Loads.
- High Voltage Direct Current (HVDC) transmission equipment.
- Static Var Compensators (SVC).

These dynamic models and the algorithms used in these programs are suitable only for short term analysis, that is from a few milliseconds to a few tens of seconds. The programs do not model variables in slow acting components such as on load tap changing transformers (OLTC's), generator over excitation limiters and load characteristics (ie. variation of loads with variation of voltage and frequency). Therefore they are unsuitable for voltage stability analysis which takes place in a much longer time scale one or two orders of magnitude larger. However now a new class of computer programs are being written with system component models that are suitable for long term dynamic analysis and the literature presents a few examples of analysis using such programs [4, 20, 44-46]. (In these references the power system components are modelled to varying degrees of complexity). Component modelling for voltage stability study by dynamic analysis is discussed in detail in [4]. These methods are very time and engineering effort intensive and in general do not give voltage stability indices to ascertain system security. Because of their time and engineering effort requirements they are unsuitable for the study of large numbers of contingencies in large power systems. Therefore they are used mostly for bench marking purposes and for post-mortem analysis after major incidents [4, 20].

3.2.2 Quasi Steady State (QSS) Method or Analysis

The quasi steady state method makes use of the method known as singular perturbation or time scale decomposition presented in Sections 2.6.1.3, 2.7.1.4 and A2.7.

In this method the fast dynamics of fast responding components of the power system are neglected and represented by their equilibrium equations. The long term dynamics of components such as shunt compensation, on load tap changers, secondary voltage and frequency controllers, loads etc are represented by differential or difference equations. The algorithm uses suitable time steps and at each time step (call this the present time step) calculates the values of the states assuming that the slow dynamics remains static at the value at the end of the previous time step. Then these new state values are used in the equations for slow dynamics to calculate corrected values for states at the present time step. The calculations are repeated at each time step for the required period of time [4].

The quasi steady state method has been found to be about three orders of magnitude faster than the complete time simulation by dynamic analysis [20]. Therefore it is suitable for studies of large power systems with numerous possible network and equipment configurations.

3.2.3 Use of Traditional Power Flow Analysis

The main interest in most voltage stability analyses is to determine the distance, in say real power (MW), from a given stable operating point to the nearest unstable point. Referring to Figure 2.6, this would be the distance from a stable operating point on the upper half of the nose curve to the critical power point p' at the tip of the nose curve. This may be required for a number of network and equipment configurations. A standard power flow analysis may be used for this purpose. The presence of a solution to the power flow analysis indicates a stable operating point and the absence of a solution indicates an unstable operating point. So a number of power flow

analyses can be performed with suitable increments of real power demand till an unstable operating point is reached [4, 20]. However there are a number of drawbacks to this method. A number of modelling assumptions are made in traditional power flow analysis programs, some of which are as follows [20]:

1. The real power dispatch of generators are fixed with a swing bus to handle the slack.

2. Loads are assumed to be constant P and constant Q without voltage and frequency sensitivity.

3. On load tap changer action is assumed to be instantaneous.

4. Capacitors and reactors are assumed to be either fixed to the network or switched instantaneously.

5. Generator limits are represented as maximum and minimum reactive power limits.

6. PV buses are assumed to have perfect voltage control.

The algorithms used in power flow programs tend to be unstable and non convergent as an unstable operating point is approached due to the Jacobian of the power flow equations tending to zero. Therefore it is not possible to know definitely when an unstable point is reached since the lack of a solution to the power flow equations could be due to limitations of the solution algorithm as the bifurcation point is neared rather than on reaching the bifurcation or unstable operating point.

Therefore if traditional power flow programs are used in voltage stability analysis it should be with caution and also in the knowledge that the system components are not quite adequately modelled for voltage stability analysis.

3.2.4 Energy or Lyapunov Function Analysis

In the theory of dynamical systems and control theory, Lyapunov functions, which are a family of functions that can be used to demonstrate the stability of some state points of a system, are used as one of the methods of analysis. In voltage stability analysis these functions are called **energy functions** since they have not been proved to be true Lyapunov functions. References [20, 54-61] deal with the topic. This method of analysis has not been used in this thesis since suitable computer programs are not yet available to analyse systems of suitable size for a thesis and also since the methods used in this thesis give more accurate results.

3.3 Power System Component Modelling for Voltage Stability Studies

As mentioned in Section 3.2.1 voltage stability takes place in the time scale of one or two orders of magnitude greater than that of transient stability. Therefore component models used in traditional transient stability or standard power flow analysis are inadequate for voltage stability analysis. This section describes briefly some of the methods used in voltage stability programs to take into account the behaviour of various components over the long periods of time studied in voltage stability. References [4, 20, 51, 65-67] deal with this subject in greater detail.

Ideally all components of a power system need to be modelled accurately; however, the type of data available, the limitations of the models available and the practicalities of keeping the system manageable so that the number of equations that need to be solved is kept to a minimum require some system reduction. Due to the very nature of voltage stability that makes it dependent on reactive power demand and supply it is necessary to represent these variables accurately though [4, 20].

In voltage stability analysis behaviour of loads particularly space heaters with changing voltage is of great importance due to the large interval over which voltage collapse can take place whereas in traditional power flow analysis and

transient stability analysis these effects are often neglected. As the voltage drops, loads exhibit a thermostatic effect whereby the energy consumed drops. As a result these loads tend to remain active for a longer time for example to bring the temperature to the set point. Therefore after a period of time within the voltage collapse time frame, the average load returns to the original value thus exacerbating any voltage stability problems.

In addition to the thermostatic effect, OLTC transformers and other voltage restoration devices between the transmission system and the loads on the distribution system act to restore the load voltages during a voltage collapse scenario again exacerbating the problem by restoring the loads to nominal values.

3.3.1 Load Modelling

Load modelling for voltage stability studies and the study of other power system phenomena is still an ongoing project and a number of papers [19, 65-67], have been published. As mentioned above [4, 20] also deal with the subject. The model used in this thesis is based on the polynomial load model mentioned in these references which can be accommodated in the UWPFLOW program used by the author. The model is presented briefly below and the reader is referred to the above references for details.

In the polynomial model used in this thesis the load at a given bus is divided into two parts, a constant impedance part and the balance, usually a constant current part. The effective load at a given voltage is calculated as follows:

Let,

Pl = Effective real power load at per unit voltage V of the bus,

Ql = Effective reactive power load at per unit voltage V of the bus,

Pz = Constant impedance part of the real power at the bus,

Qz = Constant impedance part of the reactive power at the bus,

Pn = Balance real power at the bus,

Qn = Balance reactive power at the bus,

a and b are given constants relevant to the load under consideration.

Then,

$$Pl = Pn.V^{a} + Pz.V^{2} \qquad (3.1a)$$

$$Ql = Qn.V^{b} + Qz.V^{2} \qquad (3.1b)$$

If a = b= 1, then Pn and Qn are constant current parts of the given load.

It is assumed that Equations 3.1a & b take into account the effects of tap changers and other voltage control devices in the distribution network.

3.3.2 Generator Modelling

Generator modelling suitable for voltage stability is an important aspect of detailed voltage collapse studies. References [4, 20, 51] deal with the subject in some detail.

The desired models are those for generator capability curves and over excitation limiters. The above references deal with the subject.

However in the computer program UWPFLOW [15], used by the author of this thesis, there is a weakness as stated by the author of the program in the manual. When detailed generator data is used the program experiences convergence difficulties. Therefore detailed generator modelling has been avoided in the present work. As mentioned in Section 3.3, in any type of analysis, certain compromises need to be made depending on resources and data available and since the aim of this thesis is to show that artificial

intelligence methods can be used to predict voltage instability in power systems, this is considered not to be a drawback. It is only a compromise in the details and with more sophisticated tools of analysis it can easily be overcome without compromising the conclusions drawn in this thesis.

3.4 Indices Used to Measure Proximity to Voltage Collapse

In voltage stability analysis it is useful to know, given a particular operating point of the power system, how far this operating point is to voltage instability. This enables the operators to anticipate and take precautionary measures to avoid any pending voltage instability. In fact the aim of this thesis is to develop an artificial intelligence method to predict the distance to voltage stability of a power system from any stable operating point.

A number of voltage stability indices have been proposed in the literature [4, 20, 26, 32-51, 53, 55, 63]. Many of these papers are repetitions in some form or slightly improved versions of a given method. Some of the methods have taken hold in the research community and some have not. Discussed briefly below, avoiding mathematical detail, are some of the more relevant indices and methods. The reader is referred to the above references particularly [4, 20] for details.

3.4.1 Loading Margin

Loading margin is the simplest and most straight forward of the indices used to measure proximity to voltage collapse in a power system. It is also the most widely accepted index of voltage collapse, [20]. However the determination of loading margin requires new and sophisticated methods that are unfamiliar to the average power system engineer. The computer program, UWPFLOW, used in this thesis can be employed to determine this index and it is this index that is used in this thesis in the design and training of artificial neural networks.

The **loading margin** to voltage collapse is defined in the above references as the change in loading between the operating point and the loading at point of voltage collapse. Considering Figure 2.6, the nose curve for a power system, the loading margin is the difference in loading between any stable operating point on the upper part of the nose curve and the tip of the same curve.

The following advantages of the load margin index to voltage collapse are given in [20]:

- The loading margin is straight forward, well accepted and easily understood.

- The loading margin is not based on a particular system model; it only requires a static power system model. It can be used with dynamic models, but it does not depend on the details of the dynamics.

- The loading margin is an accurate index that takes full account of the power system nonlinearity and limits such as reactive power control limits encountered as the loading is increased. Limits are not directly reflected as sudden changes on the loading margin.

- The loading margin accounts for the pattern of load increase.

3.4.1.1 Continuation Method of Determining Loading Margin Using Nose Curves

This method is equivalent to using successive power flow solutions with successive small increments of the parameter of interest which usually is the system power. However certain drawbacks of this method are overcome as will be apparent below. The data obtained is used to draw the nose curves for buses of interest. Figure 3.1 illustrates the procedure.

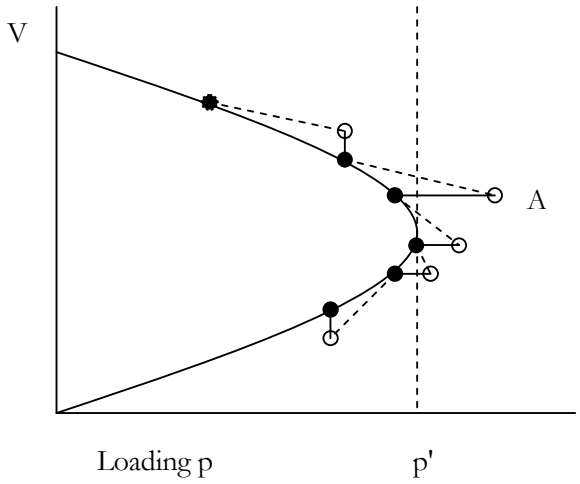

**Figure 3.1 Continuation Method –
Modified from Reference [1]**

Since it is the long term voltage stability that is of interest in voltage stability studies, a stable operating point of the power system is obtained by the following equilibrium version of the power system equations given in [4]:

$$F(z, p) = 0 \qquad (3.2)$$

Where z represents the states of the system and p is the varying parameter of interest. In the case of a power flow study, which is of interest here, z represents the vectors of bus voltages and angles and p represents varying system power.

If standard power flow methods are used, as the system approaches the bifurcation point at the nose of the nose curve, the equations exhibit convergence difficulties. Also a large number of different power flow studies with small increments of system power are computer resource and time consuming. These difficulties are overcome as described below.

The continuation method uses a predictor corrector method of drawing the nose curve for a given bus, Figure 3.1. The references [4, 20, 26, 32, 35, 36, 38, 40-45, 47, 53] deal with the subject in detail and give the mathematical theory behind the method. The method starts with a known stable operating point obtained after performing a standard power flow. From this known stable point, the method proceeds as shown in Figure 3.1 by increasing the varying parameter p in small steps and calculating predicted and corrected points on the nose curve. The white dots represent the predicted values and the black dots represent the corrected values. Suitable numerical methods are used to obtain the predicted and corrected values; refer to the above references. However there is a drawback in this method in that as the nose of the curve, which is the bifurcation point, is approached the numerical method tends not to converge as indicated by point A in Figure 3.1. To overcome this, as the nose is approached, the increment in the varying parameter p, is decreased.

3.4.1.2 Continuation Method with Parameterisation

This method is similar to the continuation method described in Section 3.4.1.1 above. The difference being, referring to Figure 3.1, when convergence problems are encountered at a point such as A, then the continuation parameter p in Equation 3.2 is swapped with a component of z. Usually the lowest magnitude voltage or the voltage with the highest rate of decrease is chosen. Thus p becomes a state in the Equation 3.2 and one of the bus voltages becomes the parameter. This is continued till the nose of the curve, where the most change occurs, is past and after passing the nose, again the standard Equation 3.2 is used. In Figure 3.2 this is illustrated by the fact that from point A, till the nose of the curve is past, the movement from the predicted value to the corrected value is horizontal, that is the movement is at constant voltage but the parameter p finds a new corrected value. References [4, 20, 33, 35, 38, 40, 41, 45, 53] describe this method in detail.

3.4.1.3 Direct or the Point of Collapse Method

Considering Equation 3.2, the bifurcation point, which is the nose of the nose curve and therefore the loadability limit, may be obtained by solving the following set of equations:

$$\begin{aligned} &F(z, p) = 0 \\ &F_z v = 0 \\ &\|v\|_\infty = 1 \end{aligned} \tag{3.3}$$

where,

F_z = Jacobian of Equation 3.2 with respect to z, the states

v = the right eigen vector

$||v||_\infty$ = mathematical L_∞ norm of v.

In Equation 3.3, the first equation is the equilibrium condition of the power system, the second equation is the singularity condition at the point of collapse and the third equation is the non-zero requirement for the right eigenvector. See references [4, 20, 23, 35, 36, 43] for detailed explanations of the method including its mathematics.

3.4.1.4 Optimisation Method

This too is a direct method in that it determines the point of collapse without tracing the complete nose curve. The problem may be expressed mathematically as follows:

$$\begin{aligned} &\max \quad p \\ &s.t. \quad F(z, p) = 0 \end{aligned} \tag{3.4}$$

This is an optimisation problem that can be solved using the following Lagrangian:

$$L = p + w^T F(z, p) \tag{3.5}$$

where, w = the vector of Lagrangian multipliers.

The first order optimality conditions, which are the derivatives of L with respect to z, w and p, are as follows:

$$\begin{aligned} D_z L &= D_z F(z, p)^T w = 0 \\ D_w L &= F(z, p) = 0 \\ \frac{\partial L}{\partial p} &= w^T \frac{\partial F}{\partial p}(z, p) + 1 = 0 \end{aligned} \tag{3.6}$$

By solving the first order optimality conditions in Equation (3.6) using numerical methods the maximum value of p which is the bifurcation point or the point of collapse can be obtained. There are computer programs for the solution of optimisation problems and an example is given in [68]. References [4, 20, 33, 34, 36, 48, 51] deal with optimisation methods to different degrees of description.

3.4.2 Other Methods

There are a number of other methods described in the literature, references [4, 18, 20, 22, 27-31, 37, 39, 42, 46-50, 52, 53], for the analysis of voltage stability and the determination of indices of proximity to voltage collapse. These are:

1. Voltage Sensitivity Factor.
2. Sensitivity Factor.
3. Singular Values.
4. Eigen Value Decomposition.
5. Voltage Instability Proximity Index.

All these can be used in post mortem analysis of power system failures. However the indices they provide are highly non-linear as system loading is increased. The loading margin as an index using any of the methods described in Sections 3.4.1.1 to 3.4.1.4 is more straight forward, widely used in research and is the method used in this thesis.

3.5 Conclusion

A number of methods of voltage stability analysis have been described in this Chapter. The method chosen in this thesis is quasi steady state analysis using continuation power flows using both step reduction and parameterisation to avoid convergence difficulties when approaching the nose of the nose curve. This method has been chosen for its adequacy in voltage stability analysis giving accurate results. The author of the thesis was also able to obtain a suitable software package that implements this method. Such software packages are just beginning to be written and can be prohibitively expensive.

This chapter also describes the requirements for power system component modelling for voltage stability analysis and explores the adequacy of various available models and the compromises that may be needed in the real world.

Voltage stability indices that indicate the distance to voltage instability of a power system are also described paying special attention to the method used in this thesis.

Chapter 4

SOFT COMPUTING OR ARTIFICIAL INTELLIGENCE METHODS – BRIEF THEORY AND SELECTION

As stated earlier in Chapter 1, soft computing, as opposed to conventional "hard" computing, is a technique that is tolerant of imprecision, uncertainty, partial truth and approximation. Its methods are based on the working of the human brain and it is commonly referred to as **Artificial Intelligence** (AI). The action of AI is similar to the human brain which is capable of arriving at valid conclusions based on incomplete and partial data obtained from prior experience. An approximation of this process on a very small scale is used in soft computing. Some of the important branches of **Soft Computing** (SC) are **Artificial Neural Networks** (ANNs), **Fuzzy Logic** (FL), **Genetic Computing** (GC) and **Probabilistic Reasoning** (PR). The soft computing methods are robust and low cost.

In the research presented in this thesis, Artificial Neural Networks branch of Soft Computing has been chosen, since, for reasons that will become apparent in this chapter, such networks are eminently suitable for the study of voltage stability. The architecture of the ANNs used are selected on intelligent criteria rather than by a "brute force" method of trial and error with different architectures.

4.1 Introduction to Artificial Neural Networks (ANNs)

Artificial Neural Networks have been inspired by biological neural networks found in the human brain though the relationship is very remote. Figure 4.1 is a rudimentary representation of human neurons.

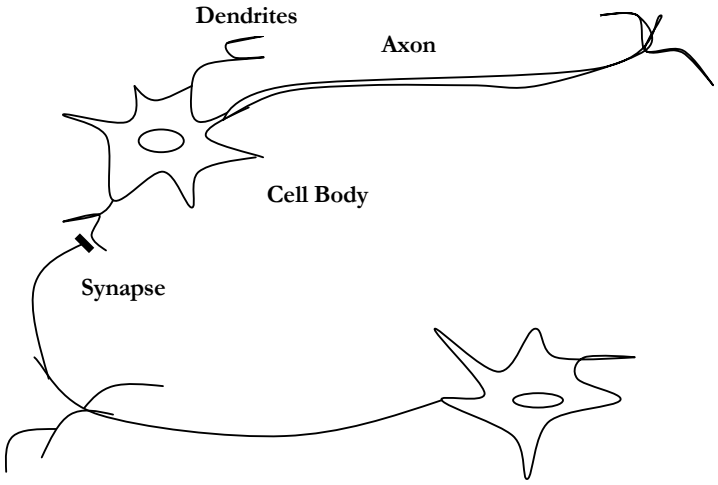

Figure 4.1 Rudimentary Representation of Human Neurons – Modified from Reference [66]

There are approximately 10^{11} neurons in the human brain with approximately 10^{15} interconnections, references [3, 69, 70]. **Dendrites** are branched receptive networks that carry electrical signals into the **cell body**. The **axon** carries the signals from the cell body to other neurons. A **synapse** is the point of contact between axon of one cell and the dendrite of another cell. The cell body thresholds and sums the incoming signals from other cells by the use of chemical processes. Some of the neural structure with interconnections through axons is present at birth. Later learning is acquired through the development of new axons and the strengthening and weakening of synapses. Reference [3] gives the following similarities between biological and Artificial Neural Networks:

- The building blocks of both networks are simple computational devices that are highly interconnected.

- Connections and the connection strengths between neurons determine the function of any given network.

Kohonen in reference [69] gives the following definition of **neural computers** or **neural networks**:

"Artificial Neural Networks are massively parallel interconnected networks of simple (usually adaptive) elements and their hierarchical organizations which are intended to interact with the objects of the real world in the same way as biological nervous systems do."

Though digital computers are used in the implementation of ANN's, both biological and Artificial Neural Networks are non-digital massively parallel computational devices. Reference [69] makes the following distinctions between digital and neural computers:

- The biological neural systems do not apply principles of digital or logic circuits.

- Neither the neurons, nor the synapses are bistable memory elements. Neurons seem to act as analogue integrators and the efficacies of the synapses change gradually without flipping back and forth.

- No machine instructions or control codes occur in neural computing.

- The neural circuits do not implement recursive computation using algorithms.

- Even on the highest level, the nature of information processing is different in the brain or neural networks and in the digital computers.

Among the many biological and mental functions of the brain, the main functions that are utilized in neural computing are sensory functions, motor functions and internal processing which is similar to thinking in humans in a rudimentary way. As such neural computers are capable of taking into account high order relationships in stochastic data and can define very

complicated dynamic phenomena. It is this property that makes ANNs, which are massively parallel interconnected computing elements, suitable for the study of power system phenomena in general and voltage stability in particular, a power system being a complicated dynamical system. Hence the choice of ANNs in the present research.

As a result of the research presented in this thesis it is envisaged that the principles involved can be used in an on-line "intelligent robot" that could predict impending voltage instabilities and take automatic corrective actions such as switching of capacitors, synchronous condensers, load shedding etc. The neural computer used in such a robot would utilize ANNs similar to the ones developed in this thesis along with sensory systems and systems for remedial actions. The sensory system would be continuously monitoring system states such as bus voltages and angles and system parameters such as loads at buses.

4.2 Notation, Neuron Models and Network Architectures

ANN's have been used in many vastly different fields and as such there are many notations used in the literature. In this thesis the notation used in reference [3] is utilised and is summarised below. This is also the notation used in the MATLAB Neural Network Toolbox which has been used in this thesis for designing and training ANNs. Neuron models and network architectures are also described briefly. References [3, 69-73] present neuron models and network architectures in detail.

A single neuron ANN may be represented as shown in Figure 4.2

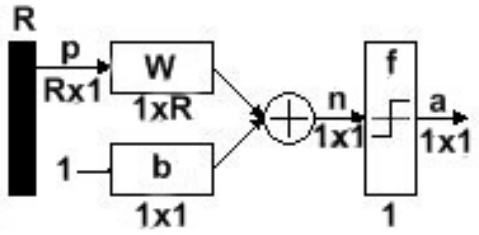

Figure 4.2 An R Input Neuron

In this figure:

p = an (Rx1) input vector. Represented by the solid bar,

W = a (1xR) weight matrix,

b = the (1x1) bias vector that multiplies the constant input of 1 to the neuron,

n = the (1x1) net input vector to the transfer function f,

a = the (1x1) output vector,

f = the transfer function.

Relating this ANN to the biological neurons shown in Figure 4.1, the cell body is the summer and the transfer function, the weight matrix is the strength of connection of the synapses and the elements of the output vector are the signals in the axons. In this thesis the standard convention of representing vector and matrix elements with simple or small letters with subscripts to indicate row and column of that element is used. The **bold** capitals indicate matrices and **bold** small letters represent vectors. f is a transfer function, many types of which are used in ANN's and the more common are discussed in this thesis. Using matrix algebra and the standard

representation for function evaluation the output of the ANN in Figure 4.2 can be represented by the following equation:

$$\mathbf{a} = \boldsymbol{f}(\mathbf{W}\mathbf{p} + \mathbf{b}) \qquad (4.1)$$

In the case of the above single neuron ANN,

$$\mathbf{n} = w_{1,1}p_1 + w_{1,2}p_2 + \ldots\ldots\ldots\ldots..+w_{1,R}p_R + b \qquad (4.2)$$

If S neurons are used the weight matrix will be of dimension (SxR) and the output vector will be of dimension (Sx1). When training an ANN, the transfer function and the number of neurons are decided by the designer. The input is repeatedly presented to the ANN and after each presentation the parameters which are the weights and biases are adjusted using a learning rule, also known as a training algorithm, till the desired result is obtained. The initial values of the weights and biases are chosen to be random small values. For example a two input single neuron ANN using the transfer function "hardlim" (refer to Section 4.2.1 for the definition of hardlim) can be trained as an AND gate by repeatedly presenting training vectors and correct target vectors till the ANN is trained producing minimum error. Though this is a simple example, once an ANN is so trained it will give correct results all the time.

Multilayer ANNs can be designed by connecting single layer ANNs together as shown in Figure 4.3.

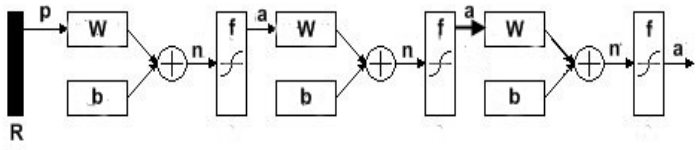

Figure 4.3 A Multilayer ANN

In the case of multilayer ANNs the convention is to use superscripts for input and output vectors and the number of neurons in each layer. These superscripts indicate the relevant layer. For example $\mathbf{W^1}$ is the (S^1xR) weight matrix of the first layer containing S^1 neurons.

Using the above convention the outputs of each of the layers of the ANN in Figure 4.3 may be written as follows:

$$\mathbf{a^1 = f^1(W^1p + b^1)} \qquad (4.3)$$

$$\mathbf{a^2 = f^2(W^2a^1 + b^2)} \qquad (4.4)$$

$$\mathbf{a^3 = f^3(W^3a^2 + b^3)} \qquad (4.5)$$

Combining these three equations the final output of the ANN can be written as follows.

$$\mathbf{a^3 = f^3(W^3f^2(W^2f^1(W^1p + b^1) + b^2) + b^3)} \qquad (4.6)$$

4.2.1 Transfer Functions

The following are the commonly used transfer functions. The figures giving the graphs of the transfer functions have been modified from reference [3]. The notation is as above.

1. The **Hard Limit** or **hardlim** transfer function:

Input/output relation:

a = 0 n or p < 0

a = 1 n or p >=0

Graph:

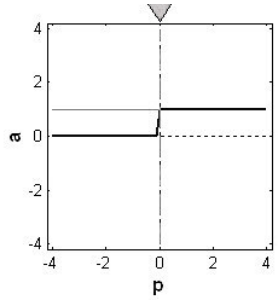

2. The **Symmetrical Hard Limit** or **hardlims** transfer function;

Input/output relation:

a = -1 n or p < 0

a = +1 n or p >= 0

Graph:

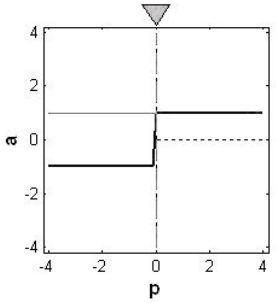

3. The **Linear** or **purelin** transfer function:

Input/output relation:

a = n or p

Graph:

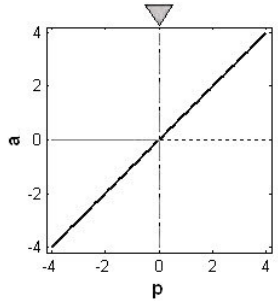

4. The **Saturating Linear** or **satlin** transfer function:

Input/output relation:

a = 0 n or p < 0

a = n 0 <= n or p <= 1

a = 1 n or p > 1

Graph:

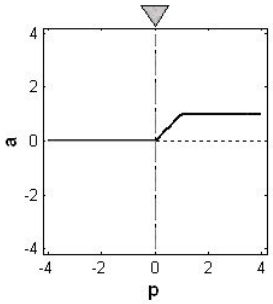

5. The **Symmetric Saturating Linear** or **satlins** transfer function:

Input/output relation:

a = -1 n or p < -1

a = n -1 <= n or p <= 1

a = 1 n or p > 1

Graph:

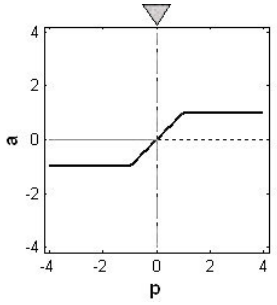

6. The **Log-Sigmoid** or **logsig** transfer function:

Input/output relation:

$$a = \frac{1}{1+e^{-n}}$$

(Note: n stands for n or p.)

Graph:

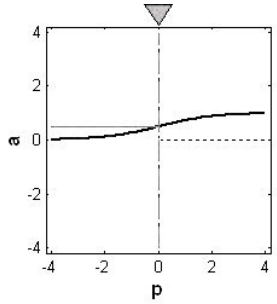

7. The **Hyperbolic Tangent Sigmoid** or **tansig** transfer function:

Input/output relation:

$$a = \frac{e^{n} - e^{-n}}{e^{n} + e^{-n}}$$

(Note: n stands for n or p.)

Graph:

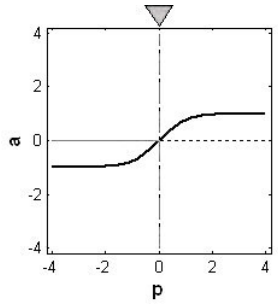

4.3 Problem Solving with Different Architectures of ANNs and Learning Rules Used

There are many architectures and learning rules described in the ANN literature. Some of these that are relevant to the research presented in this thesis are presented here. The different architectures, transfer functions and learning rules or training algorithms can be implemented in the Matlab ANN toolbox and it is this toolbox that has been used in this thesis. References [2, 3, 69-76] have been used in writing Section 4.3 along with all its sub sections. The notation used in Section 3.2 is used throughout.

4.3.1 The Perceptron Architecture

The perceptron is a **feedforward** (see Section 4.3.2.2) network that is suitable for recognising patterns that are linearly separable. Figure 4.2 represents a single neuron perceptron with a hardlims transfer function.

If we consider two element input vectors:

$\mathbf{p} = [p_1\ p_2]$,

then the perceptron once trained can separate these vectors into two categories as shown in Figure 4.4.

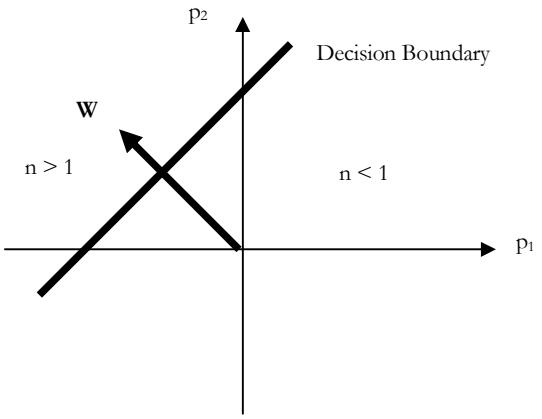

Figure 4.4 The Perceptron Decision Boundary and the Weight Matrix – Modified from [66]

The dark line crossing the p_1 and p_2 axes is the **decision boundary** and the weight matrix **W** is orthogonal to the decision boundary. When trained by repeated presentation of typical vector and their target sets, starting with small random values allocated to the weight and biases, the perceptron is able to categorise them into two categories. The perceptron learning rule modifies the weights and biases using an iterative process till the correction needed is less than a predetermined small value or zero. Referring to Figure 4.2, the value of n is greater than 0 for the region left of decision boundary in Figure 4.4 and less than 0 for the region right of the decision boundary. The output of the perceptron will be 1 for all vectors in the region where n>1 and -1 for all vectors in the region where n<1. Thus all vectors on the p_1 p_2 plane are categorised into two classes. Since the hardlims function is being used in this ANN, a perceptron, the equation to the perceptron may be written as:

$a = \text{hardlims}(\mathbf{Wp} + b)$.

If the vectors **p** are 3-dimensional, then the decision boundary will be a plane enabling the perceptron to categorise the 3-dimensional vectors.

In the case of higher dimensional vectors that require to be classified into more than two categories, multi neuron perceptrons are needed and the decision boundaries are hyper planes that are impossible to visualise. Each row vector of the weight matrix **W** will have one such hyper plane. So the power and capability of even this simple ANN is evident. References [3, 70, 72, 74, 76] provide greater detail.

4.3.1.1 Perceptron learning Rule

Consider the following set of training and target vectors presented to a perceptron: $\{\mathbf{p}_1, \mathbf{t}_1\}$, $\{\mathbf{p}_2, \mathbf{t}_2\}$,……..,$\{\mathbf{p}_Q, \mathbf{t}_Q\}$.

Then after each presentation to the perceptron of a training and target vector the weights and biases are updated according to the following rule:

$$\mathbf{W}^{new} = \mathbf{W}^{old} + \mathbf{e}\mathbf{p}^T \quad (4.7)$$

$$\mathbf{b}^{new} = \mathbf{b}^{old} + \mathbf{e} \quad (4.8)$$

Where,

$$\mathbf{e} = \mathbf{t} - \mathbf{a}. \quad (4.9)$$

The procedure is repeated till the error is zero. The perceptron learning rule or the algorithm has been proved to be convergent for all linearly separable vectors [3].

This procedure of training an ANN using sets of training and target vectors is known as **supervised training**.

4.3.2 The Backpropagation Learning Rule and Architecture

As a preliminary to the discussion of the backpropagation networks it is necessary to discuss the **Widrow-Hoff** or **Least Mean Square (LMS) Algorithm** or **Learning Rule**.

4.3.2.1 The Widrow-Hoff or Least Mean Square Learning Rule

Consider the **Linear or Adaline Network** of Figure 4.5:

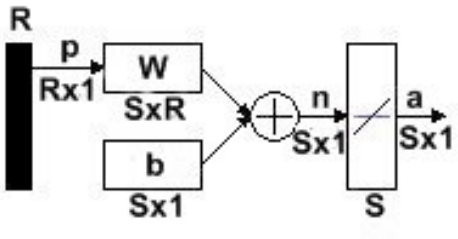

Figure 4.5 A Linear Network

This network consists of a single layer of S neurons and an input vector **p** of size (Rx1). As described in Section 4.2, these parameters decide the size of the weight matrix **W** as (SxR) and the size of the bias vector **b** as (Sx1). All neurons have the same transfer function purelin. Thus,

$$\mathbf{a} = \text{purelin}(\mathbf{Wp} + \mathbf{b}). \qquad (4.10)$$

The linear or Adaline network also uses the same method, which is **performance learning**, presented in Section 4.3.1.1. In performance learning the network is trained to optimise its performance. The performance index, which is to be minimised, used in this network is the **mean square error (mse)**. The mean square error at the k^{th} iteration is defined as follows:

Using the notation defined and used in Sections 4.2 to 4.3.1.1,

$$mse = \frac{1}{Q}\sum_{k=1}^{Q} e(k)^2 = \frac{1}{Q}\sum_{k=1}^{Q} (t(k) - a(k))^2 . \qquad (4.11)$$

The Widrow-Hoff or LMS algorithm or learning rule used to achieve this is:

$$\mathbf{W}(k+1) = \mathbf{W}(k) + 2\alpha\mathbf{e}(k)\mathbf{p}^T(k) \qquad (4.12)$$

$$\mathbf{b}(k + 1) = \mathbf{b}(k) + 2\alpha\mathbf{e}(k) \quad (4.13)$$

α which is known as the **learning rate** must be less than the reciprocal of the largest eigenvalue of the correlation matrix $\mathbf{p}^T\mathbf{p}$.

Both the perceptron and the Adaline or linear networks are single layer networks that can only solve linearly separable problems. However the linear network using the LMS algorithm is more powerful than the perceptron.

The Backpropagation Network Architecture is an extension of the linear network to solve more complicated problems as can be seen in Section 4.3.2.2.

4.3.2.2 The Backpropagation Learning Rule and Architecture Used

The "backpropagation network" is a **feedforward** multilayer perceptron. In feedforward networks the neurons are arranged in cascaded layers as shown in Figure 4.3. All neurons in a layer are connected to all neurons in the adjacent layer through unidirectional connections and therefore information can only be transmitted in a forward direction. Hence the term feedforward. An algorithm called the **Backpropagation Learning Rule or Algorithm** is used to train such netwoeks.

Referring to Figure 4.3, there are the inputs, the first layer of neurons, the second layer of neurons and the third layer of neurons. In ANN literature, by convention, the first layer of neurons is called the first layer, the second layer of neurons the second layer and so on. There is another convention; the last layer of neurons that gives the output of the ANN is called the output layer and all the other layers of neurons are called hidden layers. There can be more than three layers; however it is seldom necessary to use more than three.

As opposed to single layer perceptrons, multi layer perceptrons use differentiable transfer functions such as logsig and tansig. Reference [3] states: "In fact it has been shown that two-layer networks, with sigmoid transfer

functions in the hidden layer and linear transfer functions in the output layer, can approximate virtually any function of interest to any degree of accuracy, provided sufficiently many hidden units are available." This is the main reason for the choice of this architecture for the research presented in this thesis. This architecture has become the architecture of choice in much science and engineering research and problem solving.

The backpropagation learning rule is a modified version of the Widrow-Hoff or LMS algorithm described in Section 4.3.2.1. It is described briefly here and the references [3, 70] give its derivation in detail.

Using the notation introduced in Section 4.2,

Let M = the number of layers in the network.

Then since the network receives external inputs,

$$\mathbf{a}^0 = \mathbf{p}, \tag{4.14}$$

and,

$$\mathbf{a}^{m+1} = \mathbf{f}^{m+1}(\mathbf{W}^{m+1}\mathbf{a}^m + \mathbf{b}^{m+1}) \quad \text{for } m = 0,1,2,\ldots\ldots,M-1. \tag{4.15}$$

The network outputs at the last layer are:

$$\mathbf{a} = \mathbf{a}^M. \tag{4.16}$$

Define,

$\mathbf{s}^m$ = sensitivity of the error at layer m to elements of the net input $\mathbf{n}^m$ to that layer. The mathematical derivation of an expression for **s** is given in [3, 70].

Now during training, the desired outputs at the neurons in the hidden layers are not known and therefore the error at the hidden layers cannot be calculated. However the desired or target output at the last or output layer is

known. So using the sensitivities **s** at this last layer, the sensitivities for other layers are calculated. For example the sensitivity at layer m is calculated using the sensitivity at layer m+1 as shown in Equation 4.18. It is this recursive calculation or back propagation of the sensitivities of the error to net inputs **n** that gives the algorithm its name **backpropagation algorithm or learning rule**.

To propagate the sensitivities backwards the Jacobian matrix represented by Equation 4.17 is needed.

$$\frac{\partial \mathbf{n}^{m+1}}{\partial \mathbf{n}^{m}} = \mathbf{W}^{m+1}\dot{\mathbf{F}}^{m}(\mathbf{n}^{m})$$

where

$$\dot{\mathbf{F}}^{m}(\mathbf{n}^{m}) = \begin{bmatrix} \dot{f}(n_1^m) & 0.....0 \\ 0 & \dot{f}(n_2^m).....0 \\ . & \\ . & \\ 0 & 0.....\dot{f}^m(n_{s^m}^m) \end{bmatrix} \qquad (4.17)$$

and where considering the (i, j)*th element of the vector* **n**,

$$\dot{f}^m(n_j^m) = \frac{\partial f^m(n_j^m)}{\partial n_j^m}$$

Then it can be proved that, (references [3, 70]),

$$\mathbf{s}^m = \dot{\mathbf{F}}(\mathbf{n}^m)(\mathbf{W}^{m+1})^T\mathbf{s}^{m+1},\ m = M-1,.....,2,1. \qquad (4.18)$$

Now the weights and biases can be updated as follows:

$$\mathbf{W}^m(k+1) = \mathbf{W}^m(k) - \alpha \mathbf{s}^m (\mathbf{a}^{m-1})^T,$$
$$\mathbf{b}^m(k+1) = \mathbf{b}^m(k) - \alpha \mathbf{s}^m.$$
k represents the k^{th} iteration (4.19)
α is the learning rate as for the LMS algorithm.

4.3.2 Generalisation of Backpropagation ANNs

When a backpropagation ANN is trained, it is trained using a representative and known sample of input/output (target) pairs. However the purpose of training the ANN is so that it can predict correctly the output for related inputs it was not trained for. When an ANN can do this, the ANN is said to be **generalised** [2, 3, 70]. There can be cases where the ANN has more parameters, ie. weights and biases, than data points in the training set; then the ANN could become over fitted and give inaccurate results for some inputs that it was not trained on. If that happens the ANN is not generalised. When designing an ANN it is difficult to know whether it would be generalised, but the following general rule is given in reference [3]:

"For a network to be able to generalise, it should have fewer parameters than there are data points in the training set."

This rule has been adhered to in the research presented here.

There are also other methods, reference [2], described briefly in Sections 4.3.2.1 and 4.3.2.2, that ensures good generalisation and were used in this research.

4.3.2.1 Regularisation

In **regularisation**, the performance function for training, which is usually the mean sum of the squares of the errors, is algorithmically modified during training to obtain generalisation. MATLAB Neural Network Toolbox provides an automated regularisation training algorithm called 'trainbr' to achieve this [2]. This is one of the methods used in this thesis. It is claimed in

reference [2] that using this method, the network response would never over fit the data. MATLAB help file defines the trainbr algorithm as follows: (In the research presented in this thesis it was found to give the most accurate results.)

"trainbr is a network training function that updates the weight and bias values according to Levenberg-Marquardt optimization. It minimizes a combination of squared errors and weights, and then determines the correct combination so as to produce a network that generalizes well. The process is called Bayesian regularization."

4.3.2.2 Pre-processing and Post-processing of Data

To avoid over-fitting, the MATLAB Neural Network Tool box also provides two methods of processing the input data, ie. pre-processing. If these methods are used the outputs have to be processed to obtain the correct results, ie. post-processed.

One method is to process training input/target pairs so that their values fall within the range [-1, 1]. The process is reversed with the outputs to obtain the correct results. The other method is to scale the training input/target pairs so that the mean and the standard deviation of the training set is normalised. Again the outputs have to be post-processed to obtain the correct results.

The first method been used in this thesis and Chapters 5 and 6 further elaborate on the method.

4.4 Conclusion

This chapter has presented the theory of Artificial Neural Networks with emphasis on the Backpropagation Networks that are used in the research presented in this thesis. The theory of ANNs being a vast subject, the presentation has been brief; however relevant references have been sited.

Various methods of training relevant to the present research have been presented with comments where necessary on their suitability.

Chapter 5

DESIGN OF THE SIMULATION PERFORMED

5.1 Choice and Analysis of a Power System

The power system chosen for voltage stability analysis is the IEEE 14-Bus Test System. Figure 5.1 shows the single line diagram and Table 5.1 gives the bus and branch data for this system. It consists of five synchronous machines three of which are synchronous compensators for reactive power support; eleven loads totalling 259 MW and 81.3 MVAR; and lines and transformers as shown.

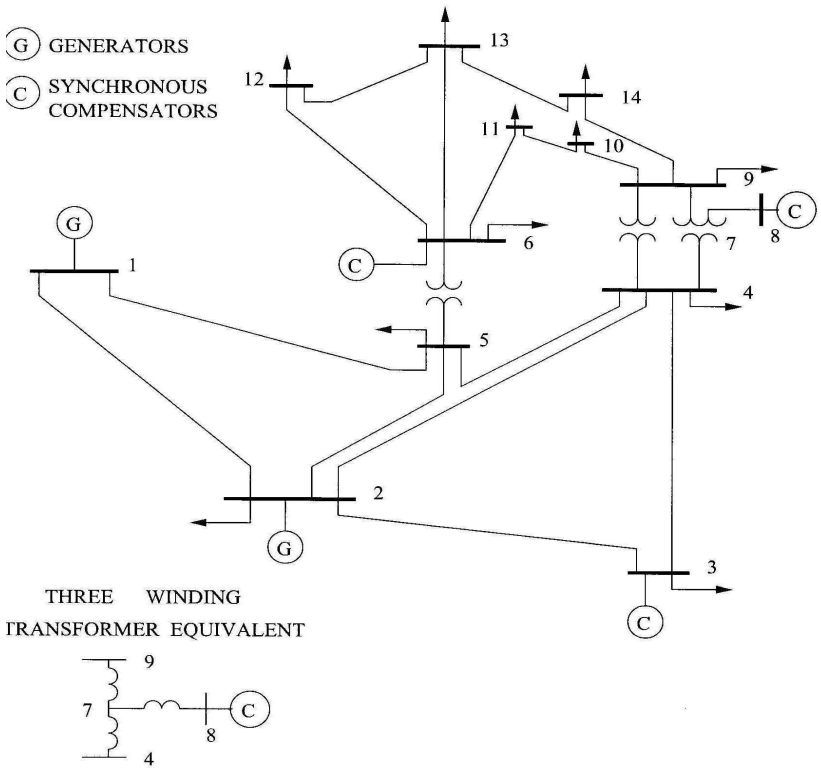

Figure 5.1 The IEEE 14 Bus Test System

IEEE 14 Bus Test System Bus Data

A	B	C	D	E	F	G	H	I	J	K	L	M	N	O	P	Q	R	S	T	U
1	Bus 1	1	HV	1	1	3	1	0	0	0	0	0	0	1.06	100	-100	0	0	0	
2	Bus 2	2	HV	1	1	2	1.045	0	21.7	12.7	40	0	0	1.045	50	-40	0	0	0	
3	Bus 3	3	HV	1	1	2	1.01	0	94.2	19	0	0	0	1.01	40	0	0	0	0	
4	Bus 4	4	HV	1	1	0	1	0	47.8	-3.9	0	0	0	0	0	0	0	0	0	
5	Bus 5	5	HV	1	1	0	1	0	7.6	1.6	0	0	0	0	0	0	0	0	0	
6	Bus 6	6	LV	1	1	2	1.07	0	11.2	7.5	0	0	0	1.07	24	-6	0	0	0	
7	Bus 7	7	ZV	1	1	0	1	0	0	0	0	0	0	0	0	0	0	0	0	
8	Bus 8	8	TV	1	1	2	1.09	0	0	0	0	0	0	1.09	24	-6	0	0	0	
9	Bus 9	9	LV	1	1	0	1	0	29.5	16.6	0	0	0	0	0	0	0	0.19	0	
10	Bus 10	10	LV	1	1	0	1	0	9	5.8	0	0	0	0	0	0	0	0	0	
11	Bus 11	11	LV	1	1	0	1	0	3.5	1.8	0	0	0	0	0	0	0	0	0	
12	Bus 12	12	LV	1	1	0	1	0	6.1	1.6	0	0	0	0	0	0	0	0	0	
13	Bus 13	13	LV	1	1	0	1	0	13.5	5.8	0	0	0	0	0	0	0	0	0	
14	Bus 14	14	LV	1	1	0	1	0	14.9	5	0	0	0	0	0	0	0	0	0	

IEEE 14 Bus Test System Branch Data

1	2	1	1	1	0	0.01938	0.05917	0.0528	0	0	0	0	0	0	0	0	0	0	0	0
1	5	1	1	1	0	0.05403	0.22304	0.0492	0	0	0	0	0	0	0	0	0	0	0	0
2	3	1	1	1	0	0.04699	0.19797	0.0438	0	0	0	0	0	0	0	0	0	0	0	0
2	4	1	1	1	0	0.05811	0.17632	0.034	0	0	0	0	0	0	0	0	0	0	0	0
2	5	1	1	1	0	0.05695	0.17388	0.0346	0	0	0	0	0	0	0	0	0	0	0	0
3	4	1	1	1	0	0.06701	0.17103	0.0128	0	0	0	0	0	0	0	0	0	0	0	0
4	5	1	1	1	0	0.01335	0.04211	0	0	0	0	0	0	0	0	0	0	0	0	0
4	7	1	1	1	0	0	0.20912	0	0	0	0	0	0	0.978	0	0	0	0	0	0
4	9	1	1	1	0	0	0.55618	0	0	0	0	0	0	0.969	0	0	0	0	0	0
5	6	1	1	1	0	0	0.25202	0	0	0	0	0	0	0.932	0	0	0	0	0	0
6	11	1	1	1	0	0.09498	0.1989	0	0	0	0	0	0	0	0	0	0	0	0	0
6	12	1	1	1	0	0.12291	0.25581	0	0	0	0	0	0	0	0	0	0	0	0	0
6	13	1	1	1	0	0.06615	0.13027	0	0	0	0	0	0	0	0	0	0	0	0	0
7	8	1	1	1	0	0	0.17615	0	0	0	0	0	0	0	0	0	0	0	0	0
7	9	1	1	1	0	0	0.11001	0	0	0	0	0	0	0	0	0	0	0	0	0
9	10	1	1	1	0	0.03181	0.0845	0	0	0	0	0	0	0	0	0	0	0	0	0
9	14	1	1	1	0	0.12711	0.27038	0	0	0	0	0	0	0	0	0	0	0	0	0
10	11	1	1	1	0	0.08205	0.19207	0	0	0	0	0	0	0	0	0	0	0	0	0
12	13	1	1	1	0	0.22092	0.19988	0	0	0	0	0	0	0	0	0	0	0	0	0
13	14	1	1	1	0	0.17093	0.34802	0	0	0	0	0	0	0	0	0	0	0	0	0

Table 5.1 The IEEE 14 Bus Test System Data

The column labels, A, B, C,…etc., in Table 5.1 represent the following:

Bus data:

A – Introduced by the author of this thesis to identify row numbers.

B – Introduced by the author of the thesis to identify each bus.

C – Bus number as per IEEE Common Format. The following are as per IEEE Common Format.

D – Bus name. (To suit the user.)

E – Load flow area number. (Not used in present analysis.)

F – Loss zone number. (Not used in present anlysis.)

G – Bus type.

(0 – Unregulated bus, ie. load, PQ

1 – Hold MVAR generation within voltage limits, ie. gen., PQ,

2 – Hold voltage within VAR limits, ie, gen., PV,

3 – Hold voltage and angle, swing bus.)

H – Final Voltage in p.u.

I – Final angle in degrees

J – Load MW

K – Load MVAR

L – Generation MW

M – Generation MVAR

N – Base kV, no particular voltage chosen since p.u. values are used

O – Desired volts in p.u.

P – Maximum MVAR limit

Q – Minimum MVAR limit

R – Shunt conductance G p.u.

S – Shunt susceptance B p.u.

T – Remote controlled bus number, not used in present analysis.

Branch data:

A – Start bus of transmission line

B – End bus of transmission line

C – Load flow area number, not used in present analysis

D – Loss zone number, not used in present analysis

E – Circuit number

F – Type of branch, 0 – transmission line

G – Branch resistance, R p.u.

H – Branch reactance, X p.u.

I – Line charging susceptance, B p.u.

J – Line No. 1 MVA rating, not used

K – Line No. 2 MVA rating, not used

L – Line No. 3 MVA rating, not used

M – Control bus number, not used

N – Control side, not used

O – Transformer final turns ratio

P – Transformer final angle, not used

Q – Minimum tap on transformer, not used

R – Maximum tap on transformer, not used

S – Transformer tap step size, not used

T – Minimum voltage limit, not used

U – Maximum voltage limit, not used.

The IEEE 14-Bus Test System, hereafter referred to as the power system, was analysed for voltage stability as the load at each load bus was progressively increased using the UWPFLOW computer program, [15].

5.1.1 Power System Configurations and Contingencies Used in the Voltage Stability Analysis

The full configuration of the power system as given for the IEEE 14 Bus Test System is used. However certain assumptions as to the detail of the configuration are made and a number of operational contingencies are introduced in the analysis.

It is assumed that each line of the power system is a double circuit line consisting of two identical circuits. Therefore doubling of the line resistance and reactance for any line is equivalent to one circuit of that line being out of service.

The voltage stability analysis was conducted for the full power system and the following contingencies of one circuit in some lines being out of service.

5.1.1.1 Contingencies Considered

The following contingencies were chosen at random:

1. One circuit from bus 1 to bus 2 out of service.
2. One circuit from bus 6 to bus 11 out of service.
3. One circuit from bus 11 to bus 10 out of service.
4. One circuit from bus 12 to bus 6 out of service.

5. One circuit from bus 12 to bus 13 out of service.

6. One circuit from bus 13 to bus 14 out of service.

However after these six contingencies were analysed, it was noted that case 1 above, the case of one circuit from bus 1 to bus 2 out of service, was more onerous than the rest due to the fact that most of the generation is concentrated on bus 1. Therefore another contingency as below was considered.

7. One circuit from bus 1 to bus 5 out of service.

5.1.1.2 How the UWPFLOW Program was Used in the Voltage Stability Studies

The UWPFLOW contains a number of features that can be used in the study of voltage stability. The following describes how it was used in the present research:

1. The program was used to determine the point of collapse of the power system by the direct method, (refer to Section 3.4.1.3), for the full system and all the seven contingencies described above.

2. Then the parameterised continuation method, (refer to Section 3.4.1.2), was used to determine the point of collapse and the nose curves at the most vulnerable buses for the full system and all the seven above contingencies. The conditions under which the continuation power flow was run are as follows:

    - The input power system data was in the IEEE format.

    - A distributed slack bus was used for which a generation direction file, which gives the direction the generation at each bus is to be increased, is required. (See Chapter 6).

- Load modelling to take into account the variation in load as the voltage at each bus changes during load increase (continuation method) was implemented. (See Chapter 6).

- The **loading factor**, λ, was increased in increments of 0.01 times the load at each bus after the base load flow analysis. The base load flow analysis being the load flow run to meet the nominal initial loads at the bus as given in Table 5.1.

5.2 The Artificial Neural Networks used for Training

For reasons given in Section 4.3.2.2 the backpropagation ANN architecture has been chosen for the research presented in this thesis. The notation, R – S1 – S2 – S3…, where R is the number of inputs to the ANN and S1, S2 etc. are the number of neurons in layer 1, layer 2, etc. is used to represent the structure of each network.

5.2.1 The Backpropagation ANN Architectures Used

1. The backpropagation ANN architectures described below in Section 5.2.1.1 were used with the intention of selecting the best architecture among them.

2. Since the study is for voltage collapse under increasing system load, the inputs to the ANNs were chosen to be the voltage V, real power P and reactive power Q at the most affected buses. Once the parameterised continuation power flows were performed under the stipulated conditions in Section 5.1.1.2 for the full power system and the seven contingencies the seven buses whose voltages were most affected were found to be the buses 6, 9, 10, 11, 12, 13 and 14. Therefore V, P and Q at these buses were chosen as the inputs to the ANNs giving a total of 21 inputs.

3. Two thirds of the operating points obtained from each study were chosen as the training set. Their order of outputs from the UWPFLOW program was scrambled arbitrarily so that the inputs to the ANNs are not in any logical order to facilitate generalisation by the ANNs.

4. The third of operating points that are furthest away from voltage collapse were allocated the target vector $\mathbf{[1\ 0\ 0]^T}$ for **very safe**, the next third that is nearer the point of voltage collapse were allocated the target vector $\mathbf{[0\ 1\ 0]^T}$ for **safe** and the third that is nearest the point of collapse were allocated the target vector $\mathbf{[0\ 0\ 1]^T}$ for **critical**. Thus there are 3 ANN outputs. Therefore if a suitable backpropagation ANN from the number trained in this thesis were used in the IEEE 14 bus test power system in a real life situation, (assuming that this system actually exists), and the relevant inputs fed into it during operation, then the ANN would predict how close the system is to voltage collapse by its output. Depending on this an operator would be able to take any necessary corrective action. The ANN would be able to correctly predict even for situations that it was not trained for as was seen by testing the ANN with the test set. Refer to Chapter 6.

5. The remaining third of the operating points after the training set was selected were chosen as the test or validation set. This validation set was used in testing the ANNs and the results were compared against the known target vectors with successful results. Refer to Chapter 6.

5.2.1.1 The Selected Backpropagation ANN Architectures

Using the notation introduced in Section 5.2, the ANNs described below were trained. The number of data sets used for training was 928. Therefore the ANNs were selected such that the total number of parameters, ie. the total number of weights and biases, in each net was less than the number of

training data sets. This would facilitate generalisation of the ANNs. Refer to Section 4.3.2.

ANN 1:

21 – 25 – 3.

Number of parameters = 649.

Layer 1, logsig transfer function, layer 2 purelin transfer function.

Training function, trainlm. This is a backpropagation algorithm modified for low computer memory use. Reference [2].

ANN 2:

21 – 25 – 3.

Number of parameters = 649.

Layer 1, tansig transfer function, layer 2 purelin transfer function.

Training function, trainlm.

ANN 3:

21 – 25 – 3.

Number of parameters = 649.

Layer 1, tansig transfer function, layer 2 tansig transfer function.

Training function, trainlm.

ANN 4:

21 – 25 – 3.

Number of parameters = 649.

Layer 1 tansig transfer function, layer 2, purelin transfer function.

Training function, traincgf. This is a backpropagation algorithm modified for low computer memory use by a method different to trainlm. Reference [2].

ANN 5:

21 – 30 – 3.

Number of parameters = 774.

Layer 1, tansig transfer function, layer 2, purelin transfer function.

Training function, trainlm.

ANN 6:

21 – 35 – 3.

Number of parameters = 899.

Layer 1, tansig transfer function, layer 2, purelin transfer function.

Training function, trainlm.

ANN 7:

21 – 25 – 3.

Number of parameters = 649.

Layer 1, tansig transfer function, layer 2, purelin transfer function.

Training function, trainbr. Refer to Section 4.3.2.1.

ANN 8:

21 – 50 – 3.

Number of parameters = 1250.

Layer 1, tansig transfer function, layer 2, purelin transfer function.

Training function, trainbr.

The trainbr algorithm, by its design, is not dependent on having lesser network parameters than training points and it generalises extremely well. [2].

ANN 9:

21 – 25 – 25 – 3. (This is an ANN with two hidden layers.)

Number of parameters = 1374.

Layer 1, tansig transfer function, layer 2, tansig transfer function, layer 3 purelin transfer function.

Training function, trainbr.

For ANNs 7, 8 and 9 all data was used in training because of the assured ability of the training function trainbr to generalise correctly.

5.3 Conclusion

In this chapter the design of the simulations carried out for the research is described.

The selected power system for analysis is the IEEE 14-Bus Test Power System. Configurations of the power system and contingencies selected for the voltage stability studies are described.

Finally the architectures of the ANNs selected for the research is described.

Chapter 6

SIMULATION RESULTS

All the simulation data used and the results are presented in this Chapter and Appendix 3 along with the relevant graphs. Appendix 3 is saved in the accompanying CD due to the large quantity of data that cannot be fitted in printed pages. Greatly summarised results are presented in Chapter 7 – Discussion of Results – to give a general overview of the results.

6.1 Voltage Stability Analysis of the IEEE 14 Bus Test Power System

Voltage stability analysis was conducted on the IEEE 14-Bus Test Power System. The circuit diagram of the power system is shown in Figure 5.1 and the data for the power system is shown in Table 5.1.

The generation and load direction file, referred to in Section 5.1.1.2, used in the UWPFLOW program, is shown in Table 6.1.

Table 6.1 The Generation and Load Direction File for UWPFLOW Program in Required Format

```
C
C                IEEE 14 BUS AC TEST SYSTEM:
C              Generation and Load Direction
C                   Nihal Fernando
C This file contains the generation (DPg) and load (Pnl, Qnl, and optional
C Pzl and Qzl) direction, and the maximum P generation (PgMax) needed for
C finding the bifurcation point.  Since the IEEE Common Format does not
C allow for the definition of PgMax, this value is ignored in this file
C by making it equal to 0.
C
C
C The unformatted data is given in the following order:
C
```

```
C BusNumber  BusName       DPg      Pnl       Qnl      PgMax [ Smax Vmax
Vmin Pzl  Qzl – The quantities within square brackets not used. ]
   1          0          2.33     0          0         0
   2          0          0.40     0.217      0.127     0
3  0  0  0.942   0.19    0
4  0  0  0.478  -0.039   0
5  0  0  0.076   0.016   0
6  0  0  0.112   0.075   0
7  0  0  0  0  0
8  0  0  0  0  0
9  0  0  0.295  0.166  0
10  0  0  0.09  0.058  0
11  0  0  0.035  0.018  0
12  0  0  0.061  0.016  0
13  0  0  0.135  0.058  0
14  0  0  0.149  0.05   0
```

The load model file referred to in Section 5.1.1.2 and used in the UWPFLOW program, is shown in Table 6.2.

Table 6.2 The Load Model File
UWPFLOW Program in Required Format

```
C
C                IEEE 14 BUS TEST SYSTEM:
C                Steady State Load Data
C
C                Nihal Fernando
C
C
C This file is used to define the steady state load characteristics
C for bifurcation studies.
C The data is assumed to be given in SSSP (Ontario Hydro) format.
C The program only reads the information between the keywords NLBS
C and EDATA, the rest is ignored.
C This data describes the steady state load power as:
C
C                    Pl = Pn*V^a + Pz*V^2    (Pn and Qn represent the % of
nominal load)
C                Ql = Qn*V^b + Qz*V^2 (Pz and Qz the balance)
C
C and this information is given in the following FORTRAN format:
C
C             BusNumber    PnQna       b
C               [I5]      [I5]    [I5]   [F10.5]  [F10.5]
```

```
C
 DGEN
EDATA
!
 NLBS
C
C Bus|   |   |        |        |
C-Num<--Pn<--Qn<--------a<--------b
C  I5   I5   I5    F10.5    F10.5
     2  100           1.0
     3  100           1.0
     4  100           1.0
     5  100   30      1.0      1.0
     6  100   30      1.0      1.0
     9  100   30      1.0      1.0
    10  100   30      1.0      1.0
    11   60   60      0.0      0.0
    12   60   60      0.0      0.0
    13   60   60      0.0      0.0
    14   60   60      0.0      0.0
EDATA
!
 NDCL
EDATA
  END
```

6.1.1 Base Load Flow Analysis

A base load flow analysis was performed on the full power system. That is no contingencies were considered. The UWPFLOW program automatically performs a base power flow for the power system each time a voltage stability analysis is performed before it starts increasing the load at each bus up to the nose of the nose curve or point of collapse both of which are the same point. This base power flow would give the same results for all the contingencies considered as well, since the base load at each bus remained the same. Table A3.1 in Appendix 3 gives the results of this base power flow. Due to the large number of operating points of the power system that were evaluated most of the tables in Chapter 6 are provided in Appendix 3. This Appendix is placed in the accompanying CD in MS Excel format.

6.1.2 Voltage Stability Analysis

6.1.2.1 Full Power System

The point of collapse loading factor λ by the direct method = 0.763745

As stated in Section 5.1 the base load (or the nominal load) of the power system is:

P = 259 MW

Q = 81.3 MVAR

The point of collapse loading factor of 0.763745 obtained by the direct method indicates that the following total load was reached by the power system at the point of voltage collapse:

P = (1 + 0.763745)259 = 456.809955MW

Q = (1 + 0.763745)81.3 = 143.392469MVA

The results of the parameterised continuation power flow are shown in Appendix 3, Excel Sheet 1.

The UWPFLOW program provides the voltages for the 8 weakest buses in the power system at each operating point and these are shown in the Tables in Appendix 3, Excel Sheets 1, 3, 5, 7, 9, 11, 13 and 15. The weakest buses are 7, 6, 9, 11, 10, 12, 13 and 14, 14 being the weakest bus. The operating point loading factor and load are also shown.

Data generated by the UWPFLOW program for the nose curves at the weak buses is shown in Appendix 3, Excel Sheet 2.

Figure 6.1 shows the voltage profile or the nose curves for the buses 7, 6, 9 and 11, the four worst affected buses. Voltage at each bus in p.u. is plotted against the loading factor λ in p.u.

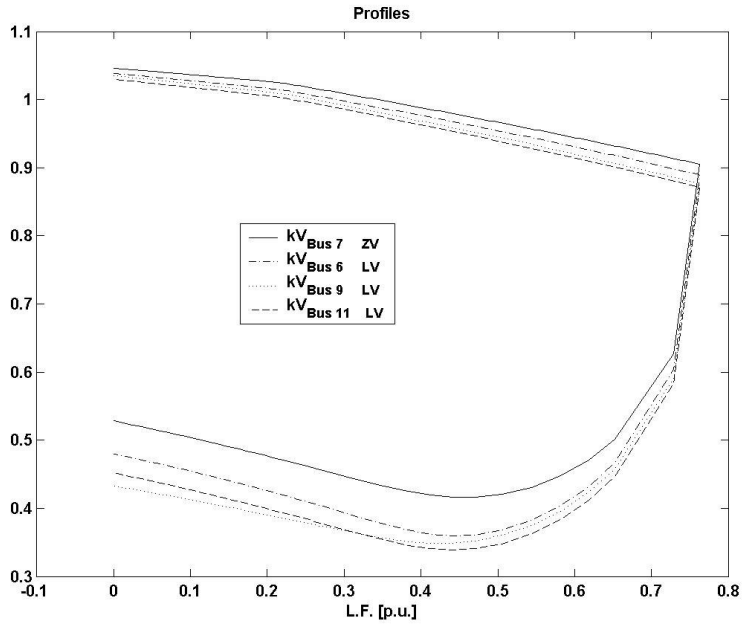

Figure 6.1 The Voltage Profile or Nose Curves for Four Buses – Full Circuit

Point of collapse loading factor by this method = 0.76321

Therefore at point of collapse:

P = (1 + 0.76321)259 = 456.67139 MW

Q = (1 + 0.76321)81.3 = 143.348973 MVA

Summarising:-

Base P_{load} = 259 MW

Base Q_{load} = 81.3 MVA

Point of collapse by direct method occurs at $\lambda = 0.763745$.

Therefore voltage collapse occurs at system power:

P = 456.809955 MW

Q = 143.392469 MVA

Point of collapse by continuation method occurs at $\lambda = 0.76321$.

Therefore voltage collapse occurs at system power:

P = 456.67139 MW

Q = 143.348973 MVA

6.1.2.2 Power System with One Circuit from Buses 1 to 2 Out of Service

This is the contingency 1 in Section 5.1.1.1. It was simulated by assuming the line to be a double circuit line and doubling the impedance of the line between buses 1 and 2.

Point of collapse by direct method occurs at $\lambda = 0.675355$

Therefore voltage collapse occurs at system power:

P = 433.916945 MW

Q = 136.206362 MVA

Point of collapse by the parameterised continuation method occurs at:

$\lambda = 0.67444$.

Therefore voltage collapse occurs at system power:

P = 433.67996 MW

Q = 136.131972 MVA

The weakest buses are buses 7, 6, 9, 11, 10, 12, 13 and 14.

The results of the parameterised continuation power flow are shown in Appendix 3, Excel Sheet 3.

Data generated by the UWPFLOW program for the nose curves at the weak buses is shown in Appendix 3, Excel Sheet 4.

Figure 6.2 shows the voltage profile or the nose curves for the buses 7, 6, 9 and 11, the four worst affected buses. Voltage at each bus in p.u. is plotted against the loading factor λ in p.u.

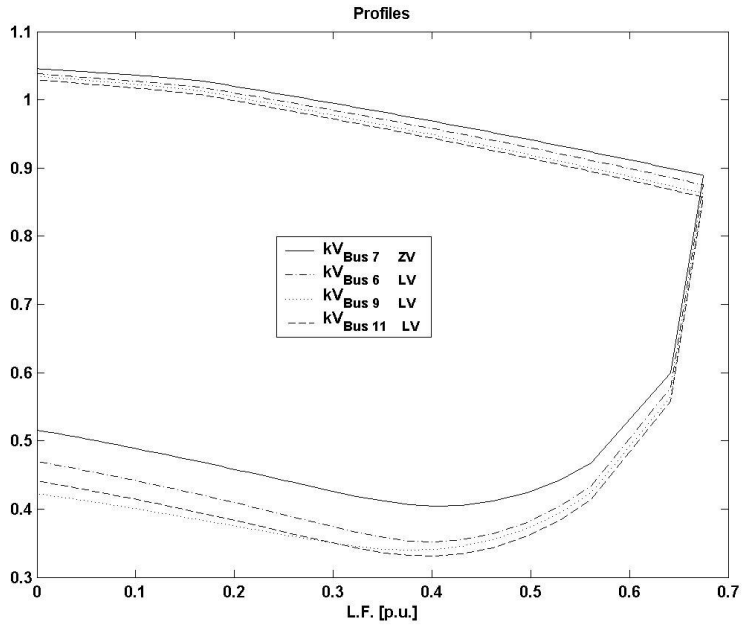

Figure 6.2 The Voltage Profile or Nose Curves for Four Buses – One Circuit Buses 1 to 2 Out

6.1.2.3 Power System with One Circuit from Buses 6 to 11 Out of Service

This is the contingency 2 in Section 5.1.1.1. It was simulated by assuming the line to be a double circuit line and doubling the impedance of the line between buses 6 and 11.

Point of collapse by direct method occurs at $\lambda = 0.763141$

Therefore voltage collapse occurs at system power:

P = 456.65352 MW

Q = 143.34336 MVA

Point of collapse by the parameterised continuation method occurs at:

$\lambda = 0.76255$.

Therefore voltage collapse occurs at system power:

P = 456.50045 MW

Q = 143.29531 MVA

The weakest buses are buses 7, 6, 9, 11, 10, 12, 13 and 14.

The results of the parameterised continuation power flow are shown in Appendix 3, Excel Sheet 5.

Data generated by the UWPFLOW program for the nose curves at the weak buses is shown in Appendix 3, Excel Sheet 6.

Figure 6.3 shows the voltage profile or the nose curves for the buses 7, 6, 9 and 12, the four worst affected buses. Voltage at each bus in p.u. is plotted against the loading factor λ in p.u.

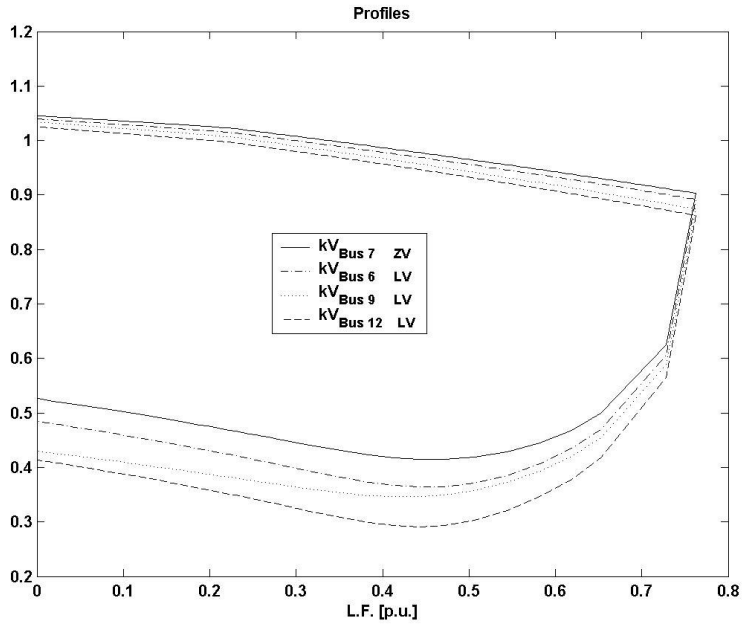

Figure 6.3 The Voltage Profile or Nose Curves for Four Buses – One Circuit Buses 6 to 11 Out

6.1.2.4 Power System with One Circuit from Buses 6 to 12 Out of Service

This is the contingency 3 in Section 5.1.1.1. It was simulated by assuming the line to be a double circuit line and doubling the impedance of the line between buses 6 and 12.

Point of collapse by direct method occurs at $\lambda = 0.761305$

Therefore voltage collapse occurs at system power:

P = 456.177995 MW

Q = 143.190965 MVA

Point of collapse by the parameterised continuation method occurs at:

$\lambda = 0.76094$.

Therefore voltage collapse occurs at system power:

P = 456.08386 MW

Q = 143.164422 MVA

The weakest buses are buses 7, 6, 9, 11, 10, 13, 12 and 14.

The results of the parameterised continuation power flow are shown in Appendix 3, Excel Sheet 7.

Data generated by the UWPFLOW program for the nose curves at the weak buses is shown in Appendix 3, Excel Sheet 8.

Figure 6.4 shows the voltage profile or the nose curves for the buses 7, 6, 9 and 11, the four worst affected buses. Voltage at each bus in p.u. is plotted against the loading factor λ in p.u.

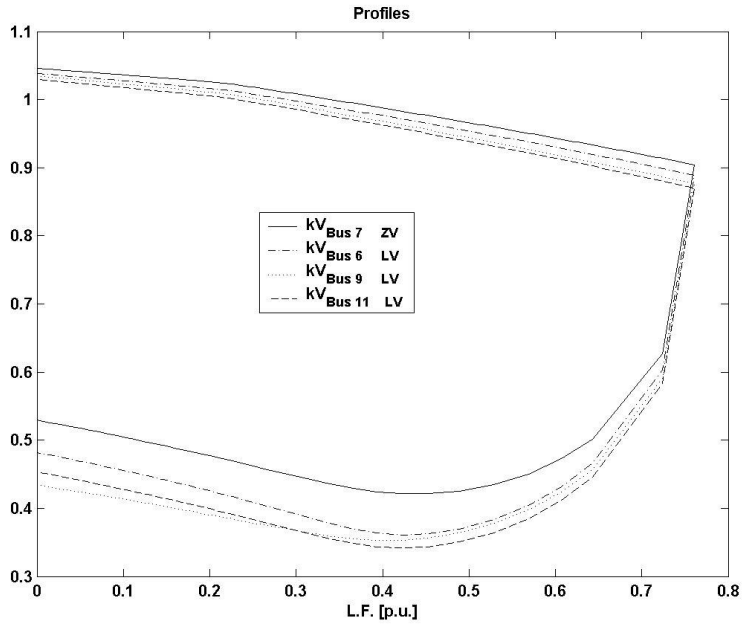

Figure 6.4 The Voltage Profile or Nose Curves for Four Buses – One Circuit Buses 6 to 12 Out

6.1.2.5 Power System with One Circuit from Buses 10 to 11 Out of Service

This is the contingency 4 in Section 5.1.1.1. It was simulated by assuming the line to be a double circuit line and doubling the impedance of the line between buses 10 and 11.

Point of collapse by direct method occurs at $\lambda = 0.763767$

Therefore voltage collapse occurs at system power:

P = 456.815653 MW

Q = 143.394257 MVA

Point of collapse by the parameterised continuation method occurs at:

$\lambda = 0.76094$.

Therefore voltage collapse occurs at system power:

P = 456.08386 MW

Q = 143.164422 MVA

The weakest buses are buses 7, 6, 9, 11, 12, 10, 13 and 14.

The results of the parameterised continuation power flow are shown in Appendix 3, Excel Sheet 9.

Data generated by the UWPFLOW program for the nose curves at the weak buses is shown in Appendix 3, Excel Sheet 10.

Figure 6.5 shows the voltage profile or the nose curves for the buses 7, 6, 9 and 11, the four worst affected buses. Voltage at each bus in p.u. is plotted against the loading factor λ in p.u.

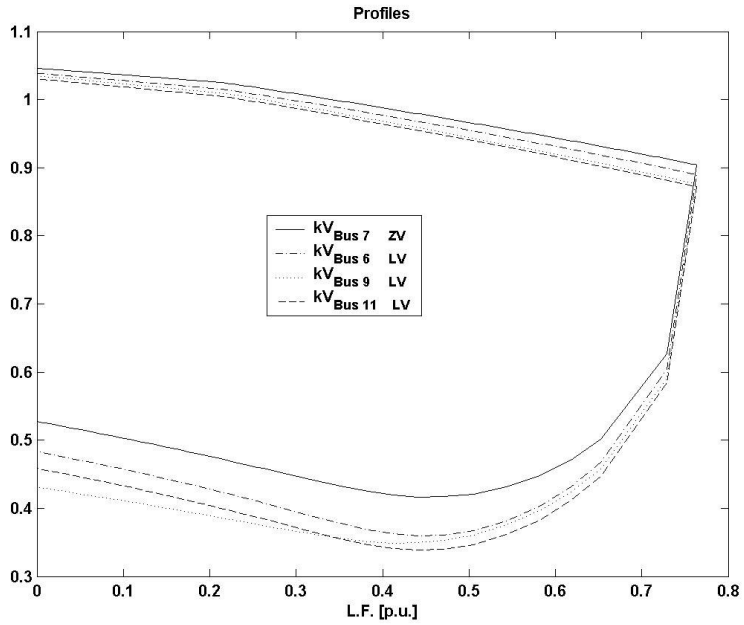

Figure 6.5 The Voltage Profile or Nose Curves for Four Buses – One Circuit Buses 10 to 11 Out

6.1.2.6 Power System with One Circuit from Buses 12 to 13 Out of Service

This is the contingency 5 in Section 5.1.1.1. It was simulated by assuming the line to be a double circuit line and doubling the impedance of the line between buses 12 and 13.

Point of collapse by direct method occurs at $\lambda = 0.763653$

Therefore voltage collapse occurs at system power:

P = 456.786127 MW

Q = 143.384989 MVA

Point of collapse by the parameterised continuation method occurs at:

$\lambda = 0.76312$.

Therefore voltage collapse occurs at system power:

P = 456.64808 MW

Q = 143.341656 MVA

The weakest buses are buses 7, 6, 9, 11, 12, 10, 13 and 14.

The results of the parameterised continuation power flow are shown in Appendix 3, Excel Sheet 11.

Data generated by the UWPFLOW program for the nose curves at the weak buses is shown in Appendix 3, Excel Sheet 12.

Figure 6.6 shows the voltage profile or the nose curves for the buses 7, 6, 9 and 11, the four worst affected buses. Voltage at each bus in p.u. is plotted against the loading factor λ in p.u.

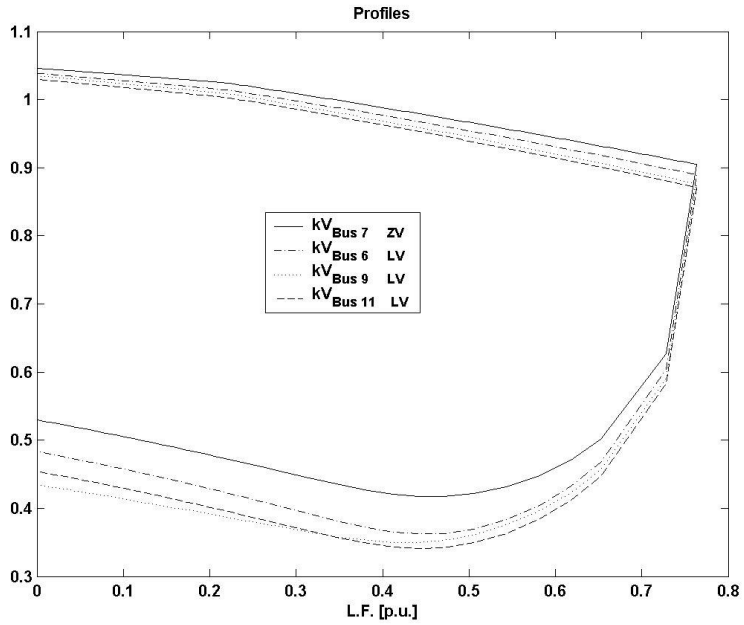

Figure 6.6 The Voltage Profile or Nose Curves for Four Buses – One Circuit Buses 12 to 13 Out

6.1.2.7 Power System with One Circuit from Buses 13 to 14 Out of Service

This is the contingency 6 in Section 5.1.1.1. It was simulated by assuming the line to be a double circuit line and doubling the impedance of the line between buses 13 and 14.

Point of collapse by direct method occurs at $\lambda = 0.762671$

Therefore voltage collapse occurs at system power:

P = 456.531789 MW

Q = 143.305152 MVA

Point of collapse by the parameterised continuation method occurs at:

$\lambda = 0.76216$.

Therefore voltage collapse occurs at system power:

P = 456.39944 MW

Q = 143.263608 MVA

The weakest buses are buses 7, 6, 9, 11, 12, 10, 13 and 14.

The results of the parameterised continuation power flow are shown in Appendix 3, Excel Sheet 13.

Data generated by the UWPFLOW program for the nose curves at the weak buses is shown in Appendix 3, Excel Sheet 14.

Figure 6.7 shows the voltage profile or the nose curves for the buses 7, 6, 9 and 11, the four worst affected buses. Voltage at each bus in p.u. is plotted against the loading factor λ in p.u.

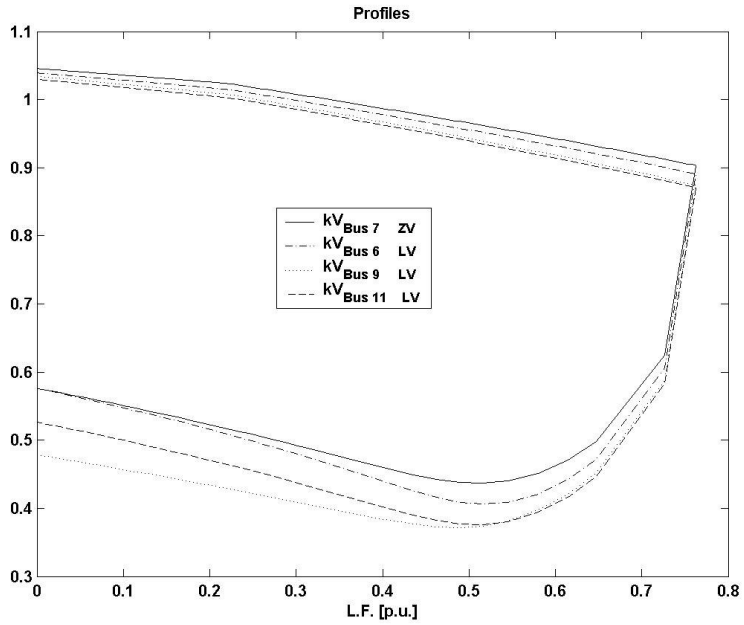

Figure 6.7 The Voltage Profile or Nose Curves for Four Buses – One Circuit Buses 13 to 14 Out

6.1.2.8 Power System with One Circuit from Buses 1 to 5 Out of Service

This is the contingency 7 in Section 5.1.1.1. It was simulated by assuming the line to be a double circuit line and doubling the impedance of the line between buses 1 and 5.

Point of collapse by direct method occurs at $\lambda = 0.691537$

Therefore voltage collapse occurs at system power:

P = 438.108083 MW

Q = 137.521958 MVA

Point of collapse by the parameterised continuation method occurs at:

$\lambda = 0.69140$.

Therefore voltage collapse occurs at system power:

P = 438.0726 MW

Q = 137.51082 MVA

The weakest buses are buses 7, 6, 9, 11, 10, 12, 13 and 14.

The results of the parameterised continuation power flow are shown in Appendix 3, Excel Sheet 15.

Data generated by the UWPFLOW program for the nose curves at the weak buses is shown in Appendix 3, Excel Sheet 16.

Figure 6.8 shows the voltage profile or the nose curves for the buses 7, 6, 9 and 11, the four worst affected buses. Voltage at each bus in p.u. is plotted against the loading factor λ in p.u.

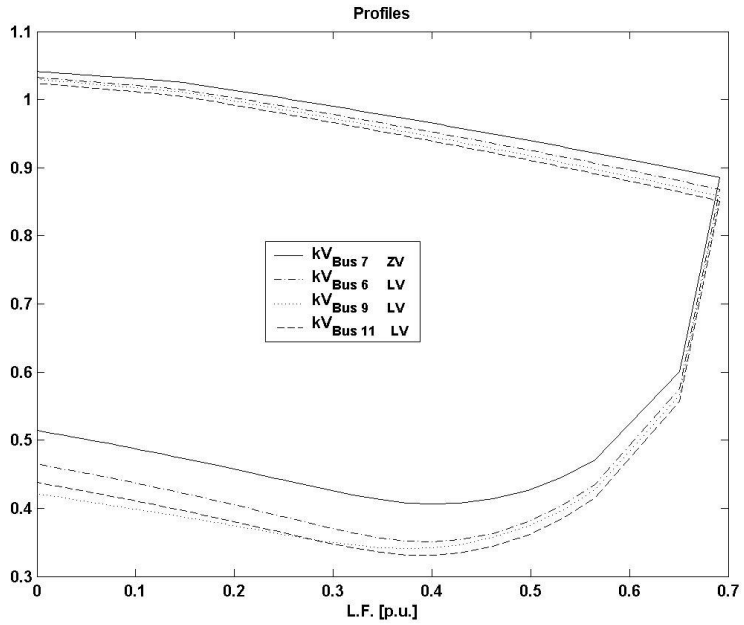

Figure 6.8 The Voltage Profile or Nose Curves for Four Buses – One Circuit Buses 1 to 5 Out

The results of Section 6.1.2 are tabulated in Table 7.1.

6.2 Training of Backpropagation ANNs and Their Final Errors

1. Section 5.2.1 describes the ANN architectures used, the training and target sets used, the test or validation sets used and how they were selected. The seven weakest buses whose parameters real power in MW, reactive power in MVAr and voltage in p.u. at each operating point were chosen as the training and validation sets are buses 6, 9, 10, 11, 12, 13 and 14. Buses 7 and 8 were not chosen since they are a transformer internal bus and a synchronous condenser bus respectively.

2. The target set is derived from the load margin. Load margin is defined in Section 3.4.1 and is calculated for each parameterised continuation

power flow operating point and shown in Appendix 3, Excel Sheets 1, 3, 5, 7, 9, 11, 13 and 15. Each operating point was allocated one of three target vectors as described in Section 5.2.1, each of the three target vectors representing a very safe, safe or critical operating condition.

3. Two thirds of the operating points from each power flow were used as the training set and the balance one third was used as the validation set.

4. Finally each ANN is tested with the validation test and the error plotted using a Matlab program written by the author of this thesis.

6.2.1 Training of Backpropagation ANNs

The training set for all ANNs was derived as follows:

- Two thirds of each set of operating points for the seven weakest buses, namely buses 6, 9, 10, 11, 12, 13 and 14, obtained from the parameterised continuation power flow for the full power system and all the contingencies (refer to Section 5.1.1) were selected as the training set. The remaining one third was reserved for testing the trained ANNs and is referred to as the simulation set.

- The training sets for the power flows were designated p1, p2,…,p8. Their target vector sets as explained in Section 5.2.1 were designated t1, t2,…,t8. Refer to the tables in Appendix 3, Excel Sheet 17.

- Similarly the testing or simulation or testing sets were designated s1, s2,…,s8 and the respective target vectors were designated t'1, t'2,…,t'8.

- The final training set was designated P1 (= p1 + p2 +…+p8) with the order of operating points arbitrarily shuffled for better generalisation of the ANNs.

- The final target set was designated T1 (= t1 + t2 +…+t8) the order of the target vectors shuffled in the exact order of shuffling used for P1.

- The simulation set S and its correct target vector set Ts was similarly derived but the sets were not shuffled as this is unnecessary for a test set.

The matrices P1, T1, S and Ts, since they are too large for MS Excel or MS Word, are included in Appendix 3 in MATLAB format and can be opened by the MATLAB program.

6.2.1.1 The MATLAB Program to Draw Error graphs of the Simulation Results

After the ANNs were trained they were tested with the simulation set to test the accuracy and generalisation of the ANNs. It is emphasized that the simulation set is separate from the training set and the trained ANNs have not encountered the simulation set during training. Therefore it is a valid test of the accuracy of the ANNs to correctly predict the voltage stability state of the power system for any of the possible operating points and therefore it is also a test of the generalisation of the ANNs.

The MATLAB program given below was written to give two different graphical representations of the simulation errors and the average value of the simulation errors. The graph titled 'Error Vector Magnitude' gives the magnitude of the error plotted against each simulation set point. The graph titled 'Error Matrix Visual' gives an overall view of how the errors are distributed though an estimation of the error is difficult with this representation.

The Matlab Program:

```
% Matlab Program to Calculate Error Between Target and Simulated Result

% 1. a = simulation results, T = Targets

% 2. Subtract elements of 'a' from elements of 'T'=A

% 3. Square each element of 'A'=Esq

% 4. Add all columns of Esq=Esqsum

% 5. Get sqrt of each element of Esqsum=E

% 6. Average error magnitude Eav = sum(E)/462

% 7. Graph E Vs column or target number

% 8. Graph error matrix A for visualisation



A = Ts - a;

Esq = A .^ 2;

Esqsum = sum(Esq);

E = Esqsum .^ 0.5;

Eav = sum(E)/462

plot(E), title('Error Vector Magnitude'), xlabel('Target No.'),...

   ylabel('Error Vector Magnitude')

figure     % Creates new figure window for second figure
```

contour3(A), title('Error Matrix Visual'), xlabel('Target No.'),...

ylabel('Matrix Row No.'), zlabel('Error')

6.2.1.2 ANN 1

(Section 5.2.1.1 explains the different ANN architectures such as ANN 1 used in the research).

The trained ANN 1 is given in Appendix 3 as Backprop1.mat, a Matlab file. (Note: All ANNs were trained in the Matlab Neural Network Toolbox). Trained for 1000 episodes when minimum error was reached.

The simulation results are given in Appendix 3, ANN 1 Simulation Results.doc.

Average error = 0.1753

Figure 6.9 shows the error vector magnitude graph.

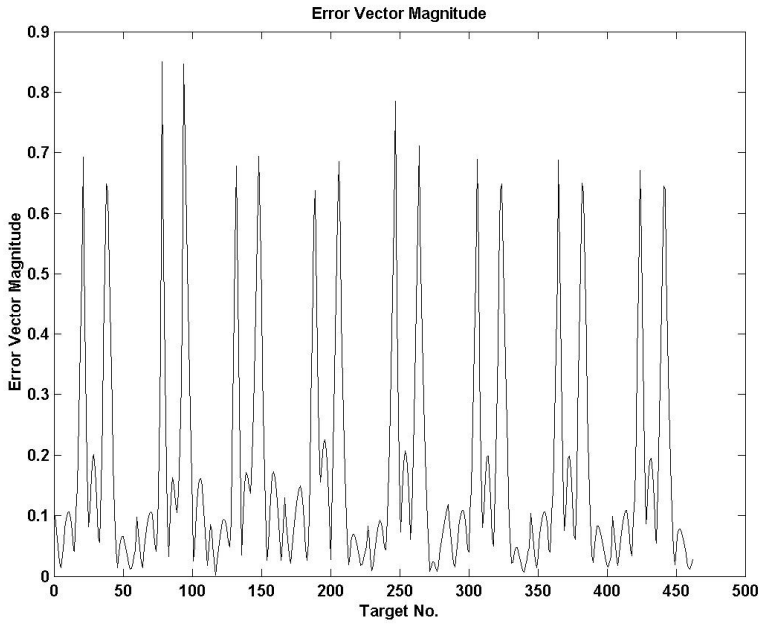

Figure 6.9 ANN 1 Simulation Error Magnitude

Figure 6.10 shows the error matrix visual graph.

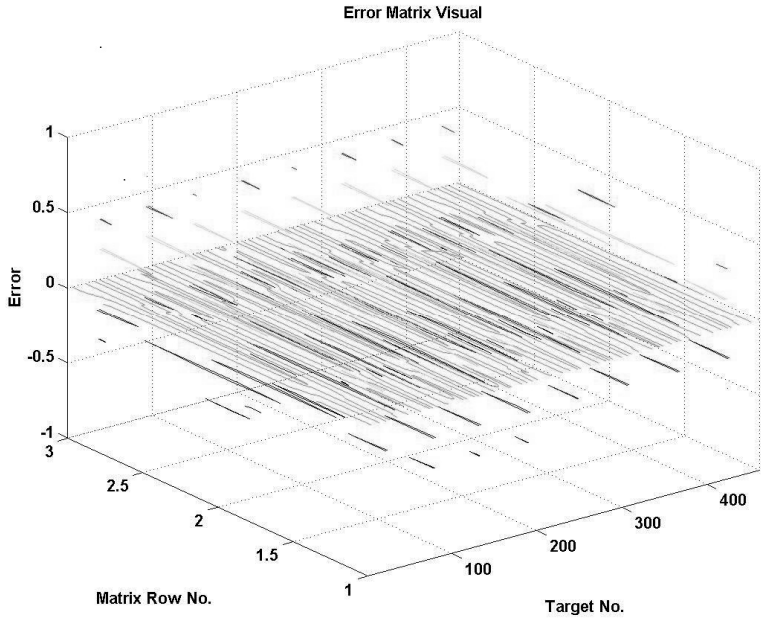

Figure 6.10 ANN 1 Simulation Error Matrix Visual

Note that Figure 6.10 is to given as a visual aid to show where the errors lie. It is seen that most of the errors represented by the shaded plane is very close to zero with a much fewer number of errors lying away from the zero error plane.

6.2.1.3 ANN 2

The trained ANN 2 is given in Appendix 3 as Backprop2.mat, a Matlab file. Trained for 1000 episodes when minimum error was reached.

The simulation results are given in Appendix 3, ANN 2 Simulation Results.doc.

Average error = 0.0555

Figure 6.11 shows the error vector magnitude graph.

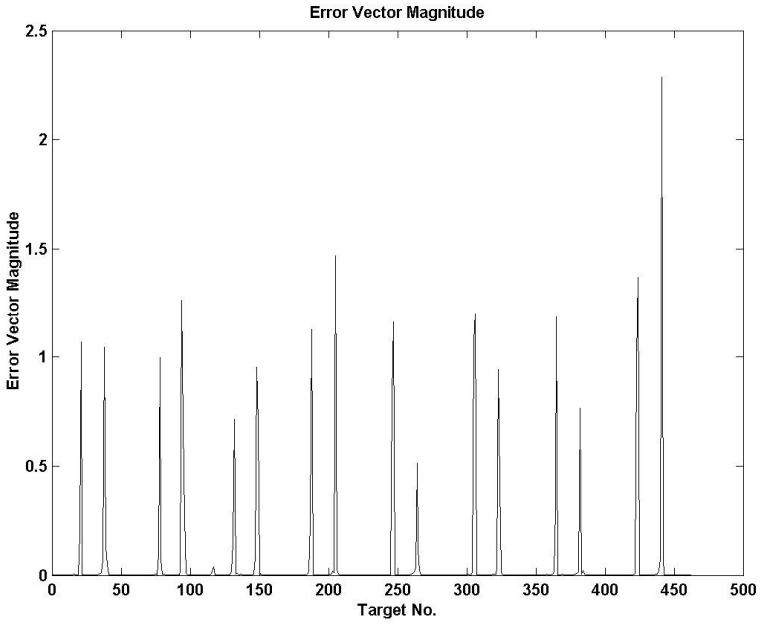

Figure 6.11 ANN 2 Simulation Error Magnitude

Figure 6.12 shows the error matrix visual graph.

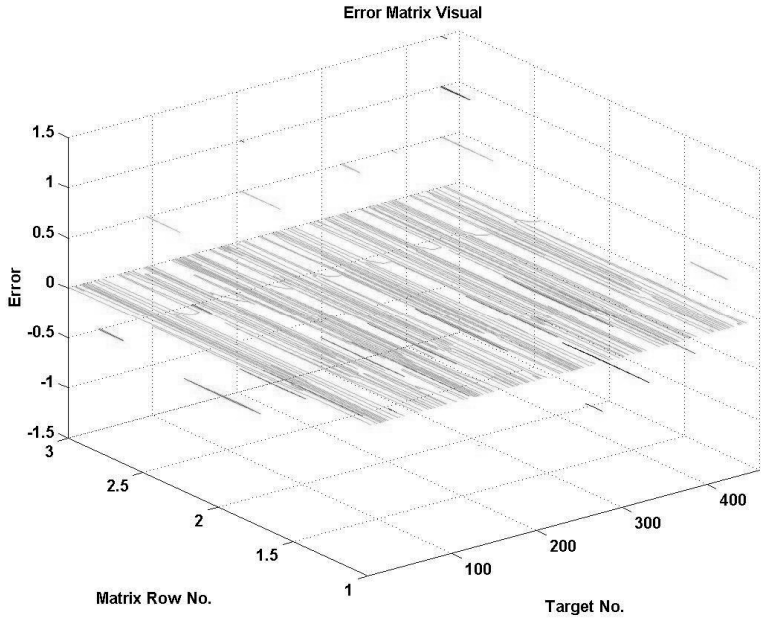

Figure 6.12 ANN 2 Simulation Error Matrix Visual

6.2.1.4 ANN 3

The trained ANN 3 is given in Appendix 3 as Backprop3.mat, a Matlab file. Trained for 1000 episodes when minimum error was reached.

The simulation results are given in Appendix 3, ANN 3 Simulation Results.doc.

Average error = 0.0347

Figure 6.13 shows the error vector magnitude graph.

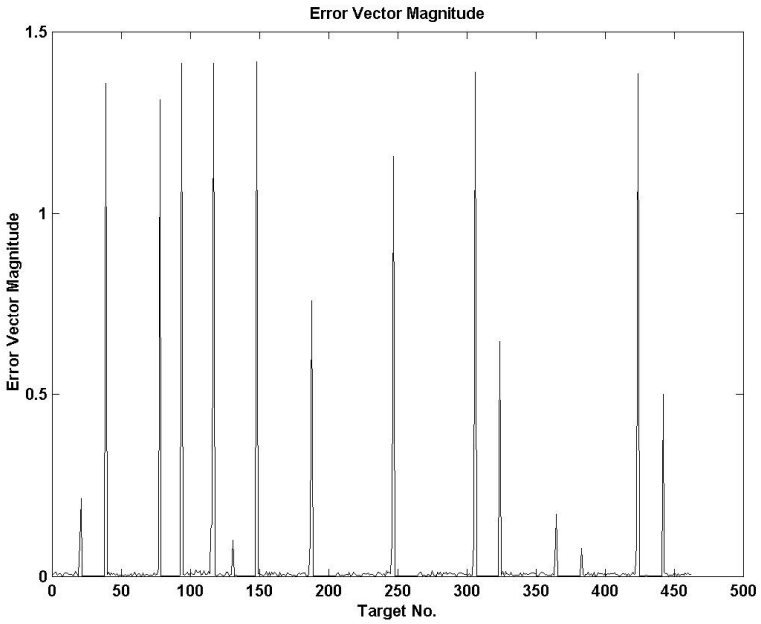

Figure 6.13 ANN 3 Simulation Error Magnitude

Figure 6.14 shows the error matrix visual graph.

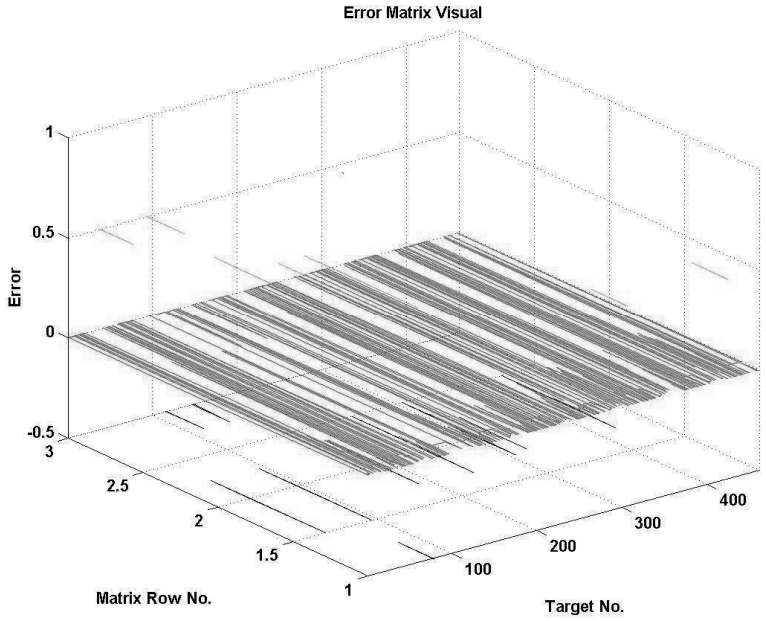

Figure 6.14 ANN 3 Simulation Error Matrix Visual

6.2.1.5 ANN 4

The trained ANN 4 is given in Appendix 3 as Backprop4.mat, a Matlab file. Trained for 630 episodes when minimum error was reached.

The simulation results are given in Appendix 3, ANN 4 Simulation Results.doc.

Average error = 0.02534

Figure 6.15 shows the error vector magnitude graph.

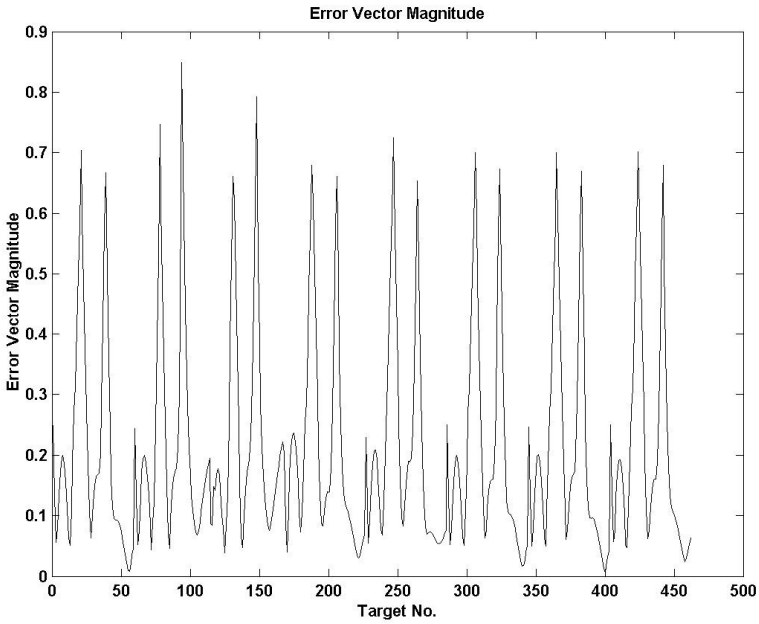

Figure 6.15 ANN 4 Simulation Error Magnitude

Figure 6.16 shows the error matrix visual graph.

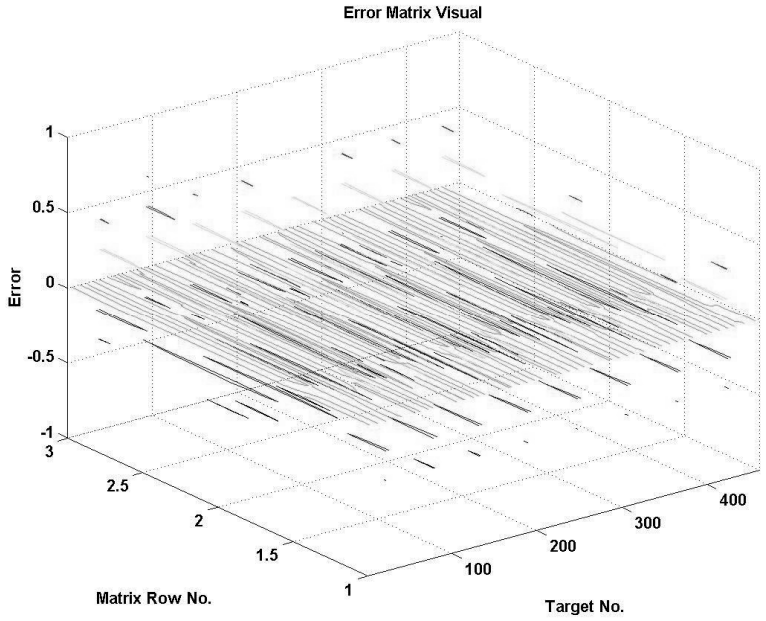

Figure 6.16 ANN 4 Simulation Error Matrix Visual

6.2.1.6 ANN 5

The trained ANN 5 is given in Appendix 3 as Backprop5.mat, a Matlab file. Trained for 1000 episodes when minimum error was reached.

The simulation results are given in Appendix 3, ANN 5 Simulation Results.doc.

Average error = 0.0850

Figure 6.17 shows the error vector magnitude graph.

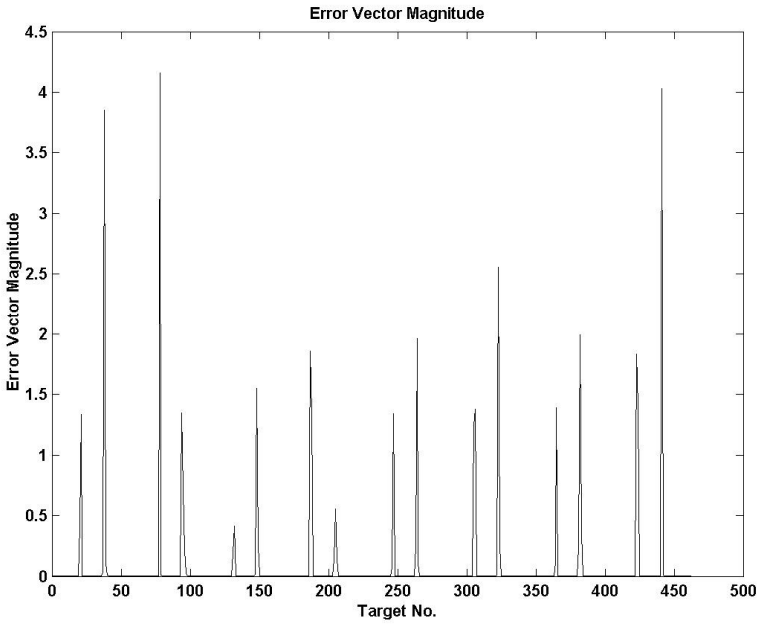

Figure 6.17 ANN 5 Simulation Error Magnitude

Figure 6.18 shows the error matrix visual graph.

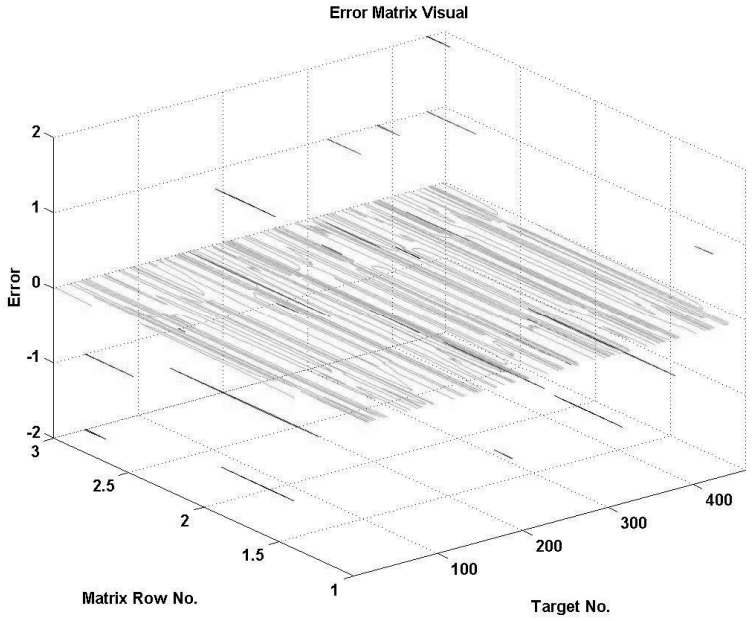

Figure 6.18 ANN 5 Simulation Error Matrix Visual

6.2.1.7 ANN 6

The trained ANN 6 is given in Appendix 3 as Backprop6.mat, a Matlab file. Trained for 1000 episodes when minimum error was reached.

The simulation results are given in Appendix 3, ANN 6 Simulation Results.doc.

Average error = 0.1714

Figure 6.19 shows the error vector magnitude graph:

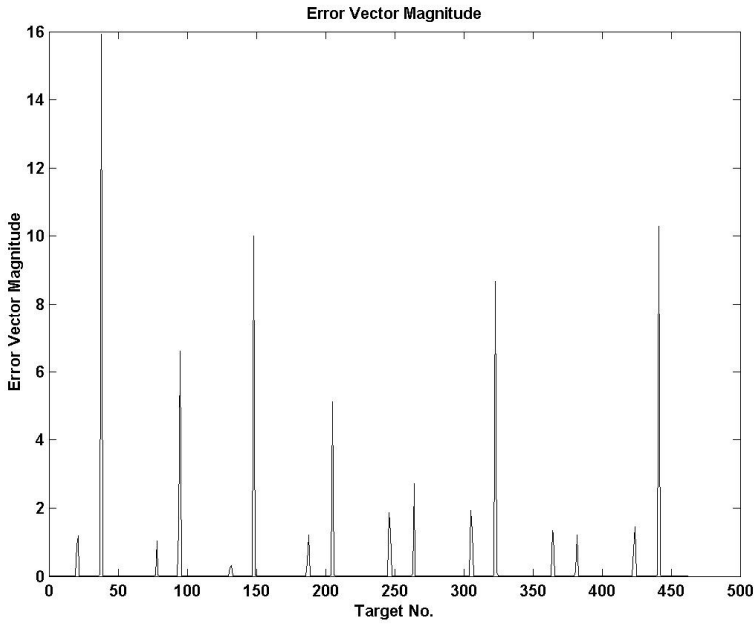

Figure 6.19 ANN 6 Simulation Error Magnitude

Figure 6.20 shows the error matrix visual graph:

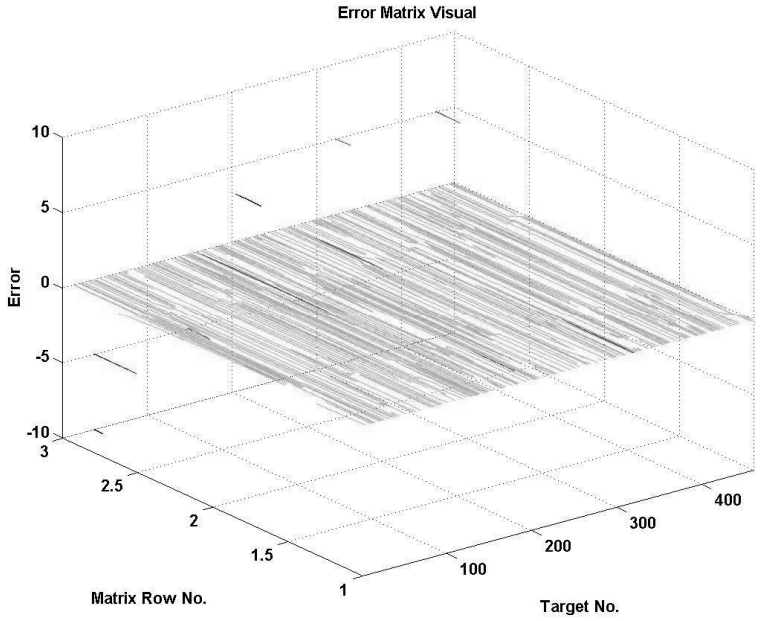

Figure 6.20 ANN 6 Simulation Error Matrix Visual

6.2.1.8 ANN 7

The trained ANN 7 is given in Appendix 3 as Backprop7.mat, a Matlab file. Trained for 220 episodes when minimum error was reached.

The simulation results are given in Appendix 3, ANN_7_Simulation_Results.mat. (This is a Matlab file and is too large to be displayed in full on the computer screen and therefore cannot be copied and pasted as a MS document). Both for training and simulation of ANN 7 all 1390 operating points of the power system were used. The reason being as stated in Section 4.3.2.1 the trainbr training function used in this ANN generalises the ANN extremely well. This is borne out by the fact that the average error is extremely small in this case.

Average error = 3.5789×10^{-4}.

Figure 6.21 shows the error vector magnitude graph.

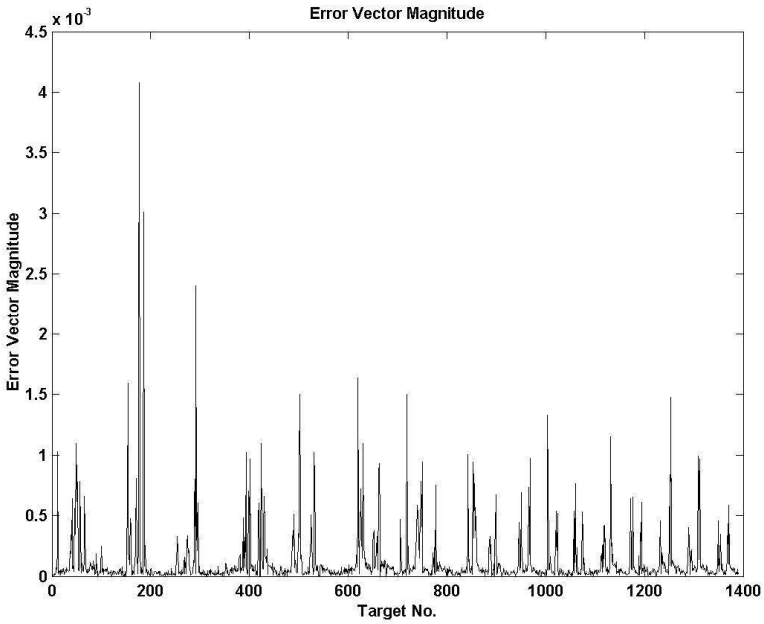

Figure 6.21 ANN 7 Simulation Error Magnitude

Figure 6.22 shows the error matrix visual graph.

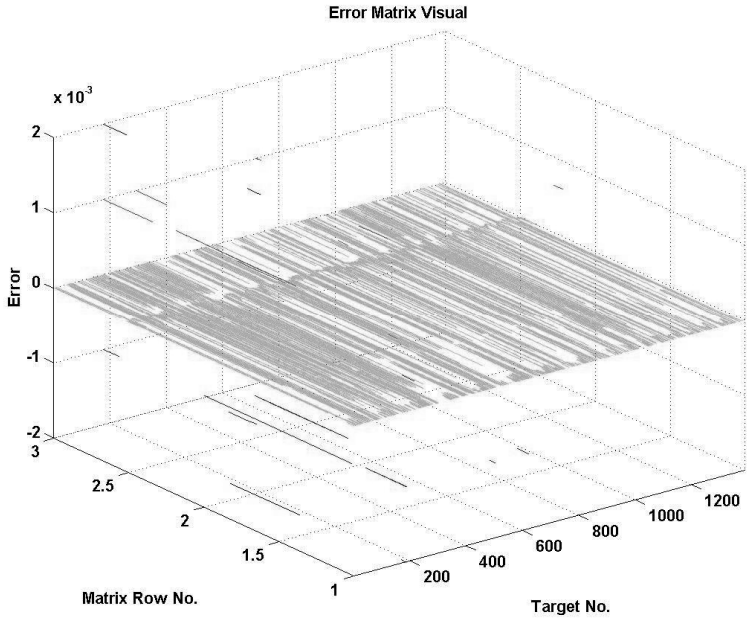

Figure 6.22 ANN 7 Simulation Error Matrix Visual

6.2.1.9 ANN 8

The trained ANN 8 is given in Appendix 3 as Backprop8.mat, a Matlab file. Trained for 500 episodes when minimum error was reached.

The simulation results are given in Appendix 3, ANN_8_Simulation_Results.mat. (This is a Matlab file and is too large to be displayed in full on the computer screen and therefore cannot be copied and pasted as a MS document). Both for training and simulation of ANN 8 all 1390 operating points of the power system were used. The reason being as stated in Section 4.3.2.1 the trainbr training function used in this ANN generalises the ANN extremely well. This is borne out by the fact that the average error is extremely small in this case.

Average error = 2.7596×10^{-4}.

Figure 6.23 shows the error vector magnitude graph.

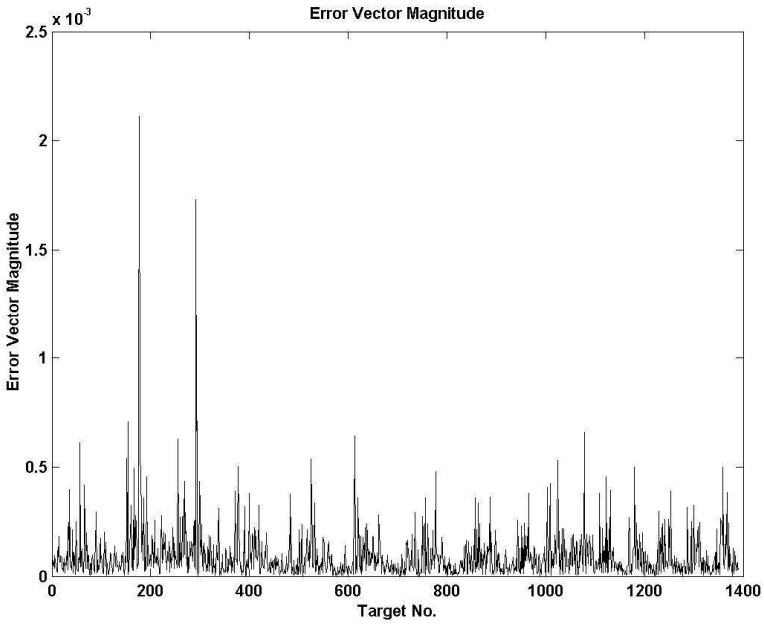

Figure 6.23 ANN 8 Simulation Error Magnitude

Figure 6.24 shows the error matrix visual graph.

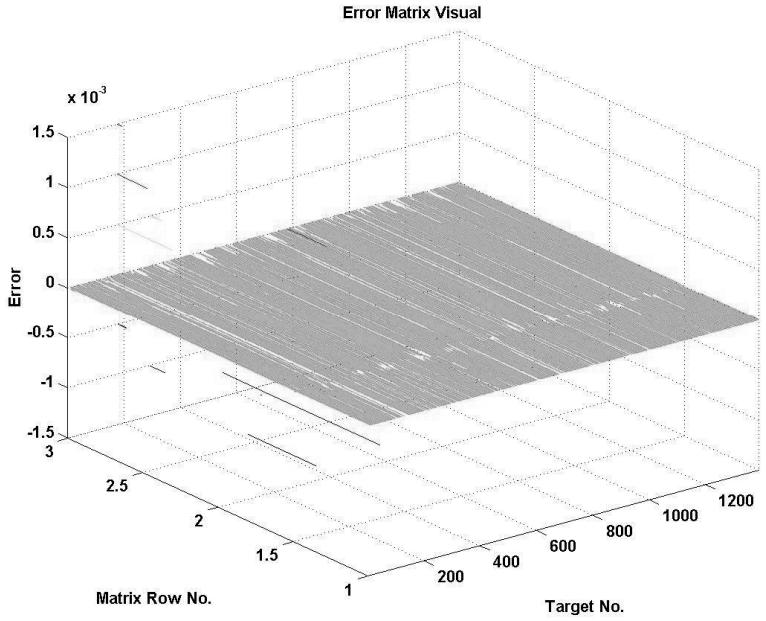

Figure 6.24 ANN 8 Simulation Error Matrix Visual

6.2.1.10 ANN 9

The trained ANN 9 is given in Appendix 3 as Backprop9.mat, a Matlab file. Trained for 231 episodes when minimum error was reached.

The simulation results are given in Appendix 3, ANN_9_Simulation_Results.mat. (This is a Matlab file and is too large to be displayed in full on the computer screen and therefore cannot be copied and pasted as a MS document). Both for training and simulation of ANN 9 all 1390 operating points of the power system were used. The reason being as stated in Section 4.3.2.1 the trainbr training function used in this ANN generalises the ANN extremely well. This is borne out by the fact that the average error is extremely small in this case.

Average error = 2.2170×10^{-5}.

Figure 6.25 shows the error vector magnitude graph.

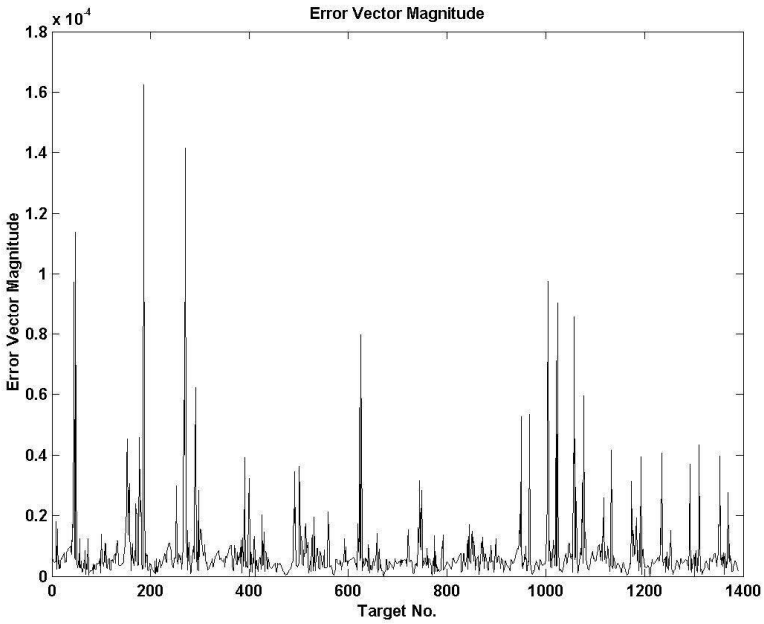

Figure 6.25 ANN 9 Simulation Error Magnitude

Figure 6.26 shows the error matrix visual graph.

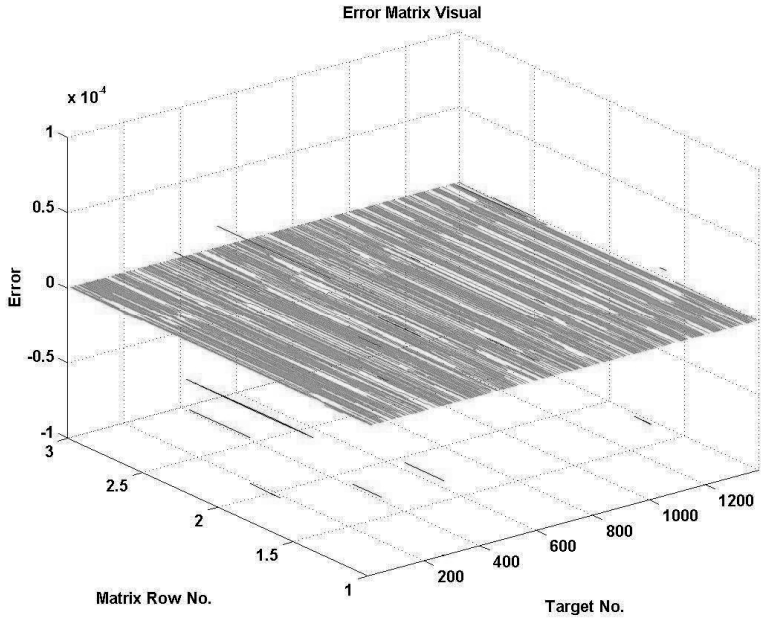

Figure 6.26 ANN 9 Simulation Error Matrix Visual

Results of Section 6.2.1 are tabulated in Table 7.2

6.3 Conclusion

This chapter presented the results for the following procedures:

- Voltage stability analysis using the parameterised continuation method of the IEEE 14 Bus Test Power System. This analysis was conducted for the full system and seven contingency configurations of the power system.

- Voltage stability analysis of the same power system to determine the point of collapse of the system by the direct method. This analysis was also conducted for the same power system configurations as above.

- Training of nine backpropagation ANNs each with a different architecture. The error plots of their simulation are also presented.

- Appendix 3 in the enclosed CD contains the files of tables of data and the trained ANNs in formats referred to in this chapter and obvious from a glance at the files. These files are too large to be included in printed paper format.

Chapter 7

DISCUSSION OF RESULTS

A discussion of the results with respect to the aims of the research laid down in Section 1.2 is presented in this chapter. Section 1.2 presents the aims in point form and a summary of these aims is used as the relevant section headings. The discussion relevant to the hypothesis laid down in Section 1.3 and suitable topics for future research in the field are presented in Chapter 8.

7.1 A Study of the Theory of Voltage Stability

Voltage stability and collapse being a power system phenomenon that has come into prominence in recent times, its theory is not well known and was developed only in recent times, refer to Section 1.5. In fact the theory has been formalised by IEEE only as recently as 2003 in its publication [20]. Therefore it was necessary to make a thorough study of the theory before proceeding with the research. It was also considered necessary to present the theory in the thesis for completeness and to place the main aims in context.

Voltage stability theory utilises a rather difficult branch of mathematics called the theory of dynamical systems. This is presented in Appendices 1 and 2. The theory of voltage stability itself, being part of the subject of this thesis, is presented in Chapter 2.

7.2 Voltage Stability Analysis of the IEEE 14-Bus Test Power System in Full and Under Different Contingencies

The results of the UWPFLOW voltage stability analysis from Section 6.1.2 for the full power system and the power system under the different contingencies in Section 5.1.1.1 are summarised below in Table 7.1.

Table 7.1 Voltage Stability Analysis
Summary

Contigency Line Out	Direct Method			Parameterised Continuation Method		
	λ	P MW	Q MVA	λ	P MW	Q MVA
Full System	0.76375	456.80996	143.39247	0.76321	456.67139	143.34897
Conting. 1 1-2 Out	0.67536	433.91695	136.20636	0.67444	433.67996	136.13197
Conting. 2 6-11 Out	0.76314	456.65352	143.34336	0.76255	456.50045	143.29531
Conting. 3 6-12 Out	0.76131	456.17799	143.19097	0.76094	456.08386	143.16442
Conting. 4 10-11 Out	0.76377	456.81565	143.39426	0.76094	456.08386	143.16442
Conting. 5 12-13 Out	0.76365	456.78613	143.38499	0.76312	456.64808	143.34166
Conting. 6 13-14 Out	0.76267	456.53179	143.30515	0.76216	456.39944	143.26361
Conting. 7 1-5 Out	0.69154	438.10808	137.52196	0.69140	438.07260	137.51082

- The point of collapse loading λ in Table 7.1 is the additional load above the base power flow load, (Section 6.1.1), expressed as a fraction of the base power flow load at which the system voltages collapse losing voltage stability.

- Two methods were used to establish the point of collapse of the power system namely, the direct method and the parameterised continuation method. (Refer to Sections 3.4.1.3 and 3.4.1.2 respectively.)

- It is seen from Table 7.1 that the values of the point of collapse obtained from the two methods agree within a small tolerance, mutually validating both methods.

- The nose curves of Section 6.1.2 are drawn for the four worst affected buses for the full power system and the seven contingencies. It is seen from these nose curves that there is a catastrophic failure of the power system at the nose of the nose curve, (refer to Section 2.7), when the loads at the buses are progressively increased as would happen in a power system as demand increases.

- The parameterised continuation power flow results for the 8 worst affected buses are shown in Appendix 3, Excel Sheets 1 to 16.

- It is seen that the order of the worst affected buses change somewhat as different contingencies are considered. There can be wider changes when different power systems are considered depending on the robustness of different areas of those power systems with respect to voltage stability.

- It is evident from Table 7.1 that contingency 1, when one line between buses 1 and 2 is out, is worse than contingencies 2 to 6 with respect to voltage stability. This led to the selection of contingency 7 in the same area of the power system as in contingency 1 as a check. Again it is found that this contingency is worse than contingencies 2 to 6. Therefore it is evident that this area of the power system is weak

with respect to voltage stability and requires strengthening in terms of transmission lines and reactive power compensation.

7.3 A Study of the Theory of Soft Computing or Artificial Intelligence

Application of soft computing or artificial intelligence methods to power system analysis in general and voltage stability in particular is new. Due to reasons given in Chapter 4, the use of artificial neural networks (ANNs), was chosen as the most suitable artificial intelligence method for the study of voltage stability in power systems. Thus it was necessary to make a thorough study of ANNs. ANNs have been developed over the years in many widely differing fields and the knowledge is scattered over many publications. The theory of ANN's that is relevant to the research presented in this thesis is presented in Chapter 4.

7.4 Training of Artificial Neural Networks for the Prediction of Voltage Instability in the IEEE 14 Bus Test Power System

Nine different ANN architectures, ANN 1 – 9, were trained to determine their suitability for the prediction of voltage instability in the IEEE 14 Bus Test Power System. Training and validation sets were chosen from the parameterised power flow studies done for the full power system and the contingencies described in Section 5.1.1.1 for the buses 6, 9, 10, 11, 12, 13 and 14. The training parameters for each bus are its, real power in MW, reactive power in MVA and voltage in p.u. Target vectors were selected for each power system operating point derived from its load margin as described in Section 3.4.1. Refer to Appendix 1, Chapter 6 Tables, Sheets 1, 3, 5, 7, 9, 11, 13 and 15.

Two types of error graphs for each trained ANN, namely Error Vector Magnitude and Error Matrix Visual, were drawn using a Matlab program written by the author of this thesis and are shown in Figures 6.9 to 6.26.

The trained ANNs are included in Appendix 3 as Matlab files Backprop1.mat…Backprop.9.mat. The simulation results are given in Appendix 3 in MS Word format as ANN1 Simulation Results.doc…ANN9 Simulation Results.doc.

Each trained ANN architecture, average error and the number of episodes taken to train the ANN are summarised below in Table 7.2.

Table 7.2 ANN Training Summary

ANN	ANN Architecture			Average Error	No. of Episodes
	Layers	Transfer Functions	Train Algorithm		
ANN 1	21-25-3	Logsig/Purelin	Trainlm	0.1753	1000
ANN 2	21-25-3	Tansig/Purelin	Trainlm	0.0555	1000
ANN 3	21-25-3	Tansig/Tansig	Trainlm	0.0347	1000
ANN 4	21-25-5	Tansig/Purelin	Traincgf	0.0253	630
ANN 5	21-30-3	Tansig/Purelin	Trainlm	0.0850	1000
ANN 6	21-35-3	Tansig/Purelin	Trainlm	0.1714	1000
ANN 7	21-25-3	Tansig/Purelin	Trainbr	3.5789×10^{-4}	220
ANN 8	21-50-3	Tansig/Purelin	Trainbr	2.7596×10^{-4}	500
ANN 9	21-25-25-3	Tansig/Tansig/ Purelin	Trainbr	2.2170×10^{-5}	231

From the error graphs in Figures 6.9 to 6.26 the following observations may be drawn:

ANN 1:

There are errors in all resultant simulation vectors with the error magnitude approaching or exceeding 0.7 in 16 cases. This led to discarding logsig as a suitable transfer function and adopting tansig transfer function for subsequent architectures. ANN 1 also has the highest average error.

ANN 2:

There is very low error in the majority of the resultant simulation vectors with the error magnitude approaching or exceeding 1 in 12 cases. This low error justifies the change of transfer function to tansig.

ANN 3:

There are low but not very low errors in majority of the resultant simulation vectors with the error magnitude approaching 1.5 in 10 cases. In this case the output layer of neurons also had tansig transfer functions as opposed to purelin in all the other cases. Since there were errors in the majority of the resultant simulation vectors, using tansig in the output layer was abandoned. This was justified by better results in subsequent ANNs.

ANN 4:

There is a low but distributed error in all the resultant simulation vectors with the error magnitude approaching 0.7 in 16 cases. The difference in this case was the training function used namely traincgf. Since it produced too many errors this training function was abandoned in favour of trainlm and trainbr training functions. This is justified by better results with these training functions.

ANN 5:

This produced very low errors in the resultant simulation vectors. However the magnitude of the error in 3 cases approached or exceeded 4.0 and in 10 cases it approached or exceeded 1.5. But since there were 462 simulation data sets the errors occurred only in a very small percentage of them. Therefore

this ANN may be considered acceptably trained. It could also be that ANN 5 with 30 neurons in the hidden layer and therefore a larger number of parameters is becoming over fitted compared to ANN 2 which has only 25 neurons in the hidden layer.

ANN 6:

This ANN produced very low errors in the majority of the resultant simulation vectors. However in 14 cases the error was between 1.0 and 16.0 indicating that the ANN is over fitted lacking generalisation due to an excess of ANN parameters.

ANN 7, ANN 8 and ANN 9:

These three ANNs produced extremely low errors, the largest errors being in the order of 10^{-3} to 10^{-4} with much smaller average errors. The reason for this being the use of the trainbr training function which uses regularisation during training as explained in Section 4.3.2.1.

Thus it is seen that the architectures, transfer functions and training functions used in ANN 2, ANN 7, ANN 8 and ANN 9 are suitable to be trained as soft computing or artificial intelligence objects to predict the state of a power system with respect to its voltage stability.

7.5 Conclusion

A discussion of the results of the research is presented in this chapter. A justification of the research undertaken is evident from the positive results obtained. The ANNs 2, 7, 8 and 9, from their results, are the most suitable ANNs for the prediction of voltage instability in a power system. The power system used in this research is the IEEE 14 Bus Test Power System. For different power systems, the same architectures with the same transfer functions and training functions may be used. However the number of

neurons in each layer will have to be different depending on the complexity of the power system and the number of training points available for training.

Chapter 8

CONCLUSIONS AND SCOPE FOR FUTURE WORK

8.1 Conclusions

In Chapter 1, Section 1.2 the aims of the research presented in this thesis was identified. Section 1.3 stated the hypothesis that was to be verified or otherwise. Section 1.4 identified the research method to be used. **The research was carried out as stated and the hypothesis has proved correct.**

The hypothesis stated in Section 1.3 is as follows:

It is possible to train Artificial Neural Networks to predict pending voltage instability in a power system.

A summary of the ANN architectures used, their test or simulation results and relevant comments are discussed in Section 7.5. Chapter 6 presents all the results of the research with Chapter 7 giving a discussion of all the results.

As discussed in Sections 7.4 and 7.5, ANN 2, ANN 7, ANN 8, and ANN 9 are the most suitable for the prediction of pending voltage instability in a power system.

All ANNs used in this thesis have the Backpropagation architecture but differ in the transfer function used in different layers, the number of layers, the number of neurons in the hidden layers and the training functions used. Refer to Section 5.2.1.1.

Using the notation given in Section 5.2, ANN 2 has the following architecture:

21 – 25 – 3.

Number of parameters = 649.

Layer 1, tansig transfer function, layer 2, purelin transfer function.

Training function, trainlm.

Thus out of all the ANNs that do not use the trainbr transfer function, ie. ANN 1 to ANN 6, ANN 2 gives the best results. It is to be noted that the training set contains 928 data sets, (refer to Section 5.2.1.1), while ANN 2 contains 649 parameters. This is in accordance with the general rule quoted in Section 4.3.2.

ANN 7 has the following architecture:

21 – 25 – 3.

Number of parameters = 649.

Layer 1, tansig transfer function, layer 2, purelin transfer function.

Training function, trainbr.

ANN 8 has the following architecture:

21 – 50 – 3.

Number of parameters = 1250.

Layer 1, tansig transfer function, layer 2 purelin transfer function.

Training function, trainbr.

ANN 9 has the following architecture:

21 – 25 – 25 – 3.

Number of parameters = 1374.

Layer 1, tansig transfer function, layer 2, tansig transfer function, layer 3, purelin transfer function.

Training function, trainbr.

The common feature of ANNs 7, 8, and 9 is that they all have trainbr as the training function and all of them give acceptable results in voltage instability prediction even though the number of parameters in each of the ANNs 8 and 9 are greater than the number of training data sets. This is in agreement with what is stated in Section 4.3.2.1, which is, that, when using the training function trainbr, the network would never over fit the data.

It is also seen that in all cases the tansig transfer function in the hidden layers, purelin transfer function in the output layer and the trainlm or trainbr training function give the best results for Backpropagation ANNs for use in the prediction of voltage instability in power systems.

Any trained ANN is specific to the power system it was trained for and in the event of additions to the power system being made or even parts of it operating islanded, different ANNs need to be trained or the same ANNs retrained. If the operating configuration of the power system is otherwise drastically changed it may again be necessary to retrain the ANNs.

8.2 Scope for Future Work

- In the research presented in this thesis the ANNs were tested using data obtained from previous parameterised continuation power flows performed on the power system under different contingencies. It is possible for ANNs to be embedded in dedicated hardware with suitable power system parameters such as real and reactive powers at

selected buses and their voltages being fed into it in real time through SCADA. The output of the ANNs, in a suitable form, would be the proximity of the power system to voltage instability. This is a suitable topic for future research.

- There was a certain limitation in the UWPFLOW program used in the present research in that power at all the buses in the power system was incremented by the same amount at each step of the continuation power flow. Though this does not detract from the validity of the results presented in this thesis, it would be more accurate to increment the bus powers differently at different buses. There may be more expensive commercially available computer programs to achieve this. If so further research can be conducted on the subject.

- Certain models, as stated in the body of the thesis, were used for power system components in this research. Further research could be conducted with different models.

- Research also could be conducted on other IEEE Test Bus Systems with numbers of buses greater or less than 14.

- Further research could be conducted on real life power systems to be compared to known previous voltage instability incidents using parameters and configuration of the power system existing at the time. This would give a very good opportunity to evaluate different power system component models and how sophisticated these models need to be.

- A versatile voltage stability computer program with an easy to use graphical user interface and a bank of suitable component models can be a future project.

- The research presented in this thesis was conducted using the Backpropagation ANN architecture. Further research could be conducted using different ANN architectures.

Appendix 1

PRELIMINARY MATHEMATICS

Scalar Autonomous Differential Equations

The references [4-13] have been consulted in the writing of this Appendix. Some of the examples used have been designed by the author of this thesis. Almost all the problems have been solved by the same author using the computer program Phaser [14].

Many of the concepts of the geometry of solutions of ordinary differential equations can be understood by a study of **scalar autonomous differential equations**.

Consider an equation of the form:

$$\dot{x} = f(x) \qquad \text{(A1.1)}$$

This equation is **scalar** if x is one dimensional and **autonomous** if $f(x)$ is independent of t (time) though x is an unknown function of t the **independent variable**. Thus the term **scalar autonomous differential equations**. Therefore x is a real variable with co-ordinates in one dimensional space and $\dot{x}$ is termed a **velocity function**.

A 1.1 Solution of Scalar Autonomous Differential Equations

When solving an equation of the type shown in Equation (A1.1), often the interest is in a specific solution that passes through an **initial value** x_0 at time t_0. Such a problem is called an **initial value problem.** Therefore the initial value problem may be expressed as:

$$\dot{x} = f(x), \qquad x(t_0) = x_0 \tag{A1.2}$$

The method of separation of variables given by the following formula may be used to find a solution to the initial value problem.

$$\int_{x_0}^{x} \frac{1}{f(s)} ds = t - t_0 \tag{A1.3}$$

But in many cases it is impossible to perform the required integration though numerical integration using a computer program can give a solution. However the interest in most cases is in the qualitative behaviour of dynamical systems and this can be studied by geometrical methods without actually solving the differential equations.

A 1.1.1 An Example

Consider the following initial value problem.

$$\dot{x} = x^2, \qquad x(0) = x_0 \tag{A1.4}$$

This is a problem where the formula (A1.3) can be used. Using this formula the following solution is obtained.

$$x(t) = \frac{x_0}{1 - x_0 t}$$

On examination of this solution certain conclusions can be drawn regarding the behaviour of $x(t)$. [4]. For $x_0 > 0$, the solution is valid or defined only on the interval $\left(-\infty, \frac{1}{x_0}\right)$; for $x_0 = 0$, the solution is defined on the interval $(-\infty, +\infty)$ and for $x_0 < 0$, the solution is defined only on the interval $\left(\frac{1}{x_0}, +\infty\right)$. **Trajectories** of the solution of the equation (A1.4) for the initial values $x_0 = -1.5, -1.0, -0.5, 0.0, 0.5, 1.0 \,\&\, 1.5$ are shown in Fig. A1.1.

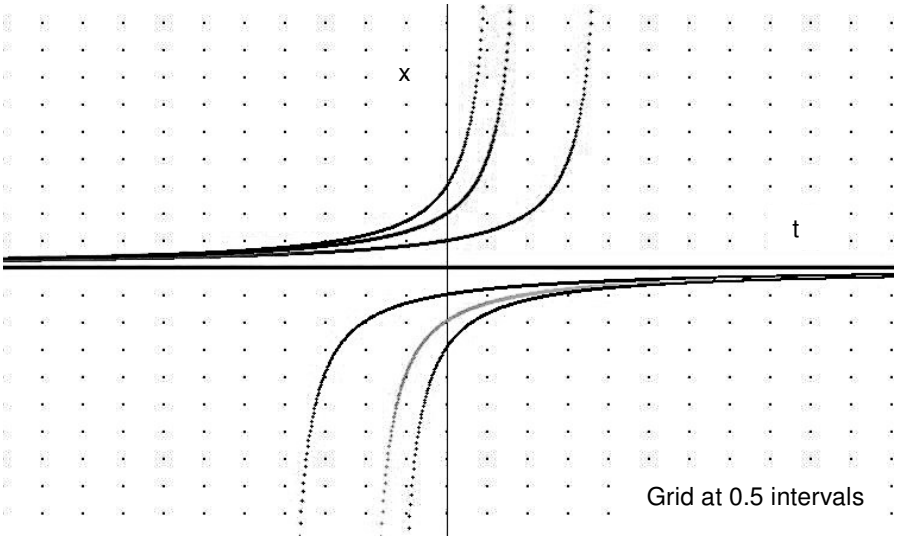

Figure A1.1 Trajectories of $\dot{x} = x^2$ for Different Initial Conditions.

It is now evident that a solution to an initial value problem has an interval of validity of its solution. This interval is called the **maximal interval of existence** and may be infinite in some cases. It is usually represented as $I_{x_0} \equiv (\alpha_{x_0}, \beta_{x_0})$ where $\alpha_{x_0} < t < \beta_{x_0}$.

Sometimes it is convenient to represent the solution $x(t)$ to the initial value problem of equation (A1.2) as $\varphi(t, x_0)$ to show its dependence on the initial value.

The following theorem, called the **theorem of existence and uniqueness of solutions**, given without proof, establishes the conditions for the existence and uniqueness of solutions to initial value problems.

A 1.1.2 Theorem A1.1: The Theorem of Existence and Uniqueness of Solutions

1. If $f(x)$ is continuous in the domain U, a sub set of the domain of real numbers R, then there exists a solution $\varphi(t, x_0)$ for all x_0 in U

with a maximal interval of existence of $I_{x_0} \equiv (\alpha_{x_0}, \beta_{x_0})$ dependent on x_0.

2. If in addition to the above, the first derivative of $f(x)$ is continuous in U, then the solution $\varphi(t, x_0)$ is unique in I_{x_0}.

A 1.2 The Direction Fields, Vector Fields, Orbits and Phase Portraits of Differential Equations

The geometry of the flow of a differential equation can be studied by a study of its direction field, vector field and phase portrait which concepts are defined below.

Considering the equation (A1.1) it is seen that the right hand side gives the slope of the trajectory of its solution in the (t, x)-plane at any given point on the (t, x)-plane where $f(x)$ is defined. Figure A1.2 below shows a collection of line segments, ignoring the arrows, representing the slope at different points on the (t, x)-plane for the example A1.1. The collection of such line segments is called the **direction field** of that particular differential equation. The direction field is always tangential to the any given trajectory at every point on that trajectory.

Now since $f(x)$ is independent of x, along every line parallel to the t-axis on the (t, x)-plane, the direction field has the same slope. If this slope is projected on to the x-axis with its direction indicated, the **vector field** or the **velocity field** is obtained. The vector field together with its direction field for the equation:

$$\dot{x} = -x \qquad \text{(A1.5)}$$

is shown on Figure A1.2. The trajectories are for initial values –1.0, -0.5, 0.0, 0.5 and 1.0.

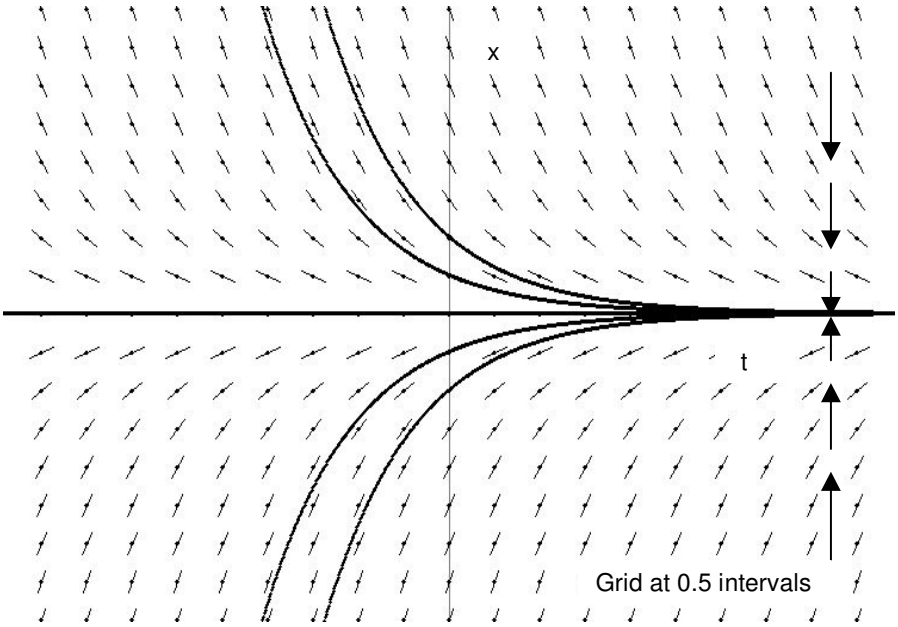

Figure A1.2 Direction Field and Vector Field of $\dot{x} = -x$.

The **orbit** $\gamma(x_0)$ of the trajectory of a differential equation passing through the initial condition x_0 is the projection of that trajectory between $t = \alpha_{x_0}$ and $t = \beta_{x_0}$ on to the x-axis.

The **positive orbit** $\gamma^+(x_0)$ of the trajectory of a differential equation passing through the initial condition x_0 is the projection of that trajectory between $t = 0$ and $t = \beta_{x_0}$ on to the x-axis.

The **negative orbit** $\gamma^-(x_0)$ of the trajectory of a differential equation passing through the initial condition x_0 is the projection of that trajectory between $t = \alpha_{x_0}$ and $t = 0$ on to the x-axis.

The Figure A1.3 shows the orbits for the trajectory of equation (A1.5) passing through a positive initial value.

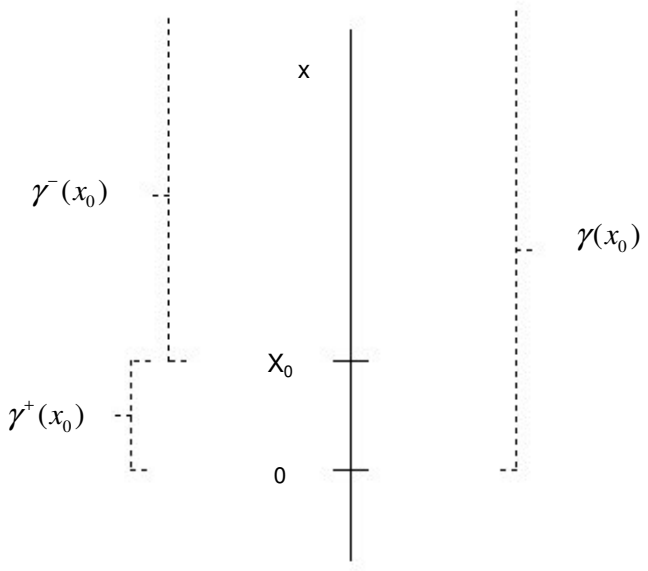

Figure A1.3 Orbits Through x_0 of
$\dot{x} = -x$.

On the orbit $\gamma(x_0)$ of a differential equation arrows can be inserted to indicate the direction in which its solution $\varphi(t, x_0)$ is changing as time t increases. The collection of all the orbits of a differential equation together with the arrows gives the **phase portrait** of the differential equation representing its flow. (Refer to Figure A1.4).

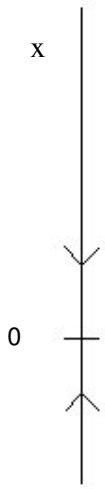

Figure A1.4 Phase Portrait of $\dot{x} = -x$

A 1.3 Equilibrium Points of Scalar Autonomous Differential Equations

An **equilibrium point** also known as a **critical point,** usually represented by $\overline{x}$, of a differential equation occurs at a point where $f(x) = 0$. A system on reaching a critical point stays at that point for all time. However any given equilibrium point may or may not be stable as seen below.

A 1.4 Methods of Drawing the Orbits and Phase portraits of Differential Equations [7]

1. The graph of x Vs $f(x)$ gives an easy method of drawing the orbits with the direction of motion and therefore the phase portrait of a differential equation. When $f(x) > 0$, the solution increases in t and therefore approaches an equilibrium point or $+\infty$ as $t \to \beta_{x_0}$. When $f(x) < 0$, the solution decreases in t and therefore approaches an equilibrium point or $-\infty$ as $t \to \beta_{x_0}$.

2. In the second method the **potential function,** $F(x)$ of equation (A1.1) is defined as follows.

$\dot{x} = f(x) = -\dfrac{d}{d(x)} F(x)$**.** Therefore,

$$F(x) = -\int_0^x f(s)ds\,.$$

Now if a graph of the potential function $F(x)$ is drawn, its extreme points, that is, its maxima and minima, will be the equilibrium points of the differential equation. If a particle is imagined to travel freely along this graph, the likely direction in which it travels, at any point on the graph, will give the phase portrait of the differential equation.

The following figures illustrate the two methods.

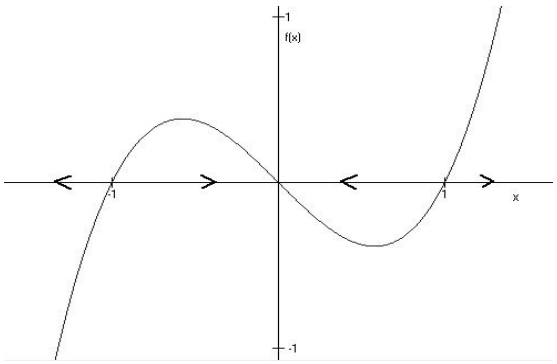

Figure A1.5a Phase Portrait of
$\dot{x} = -x + x^3$ **Using the Function**
$f(x) = -x + x^3$.

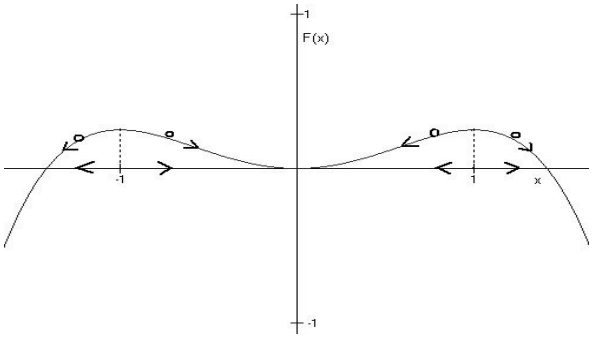

Figure A1.5b Phase Portrait of $\dot{x} = -x + x^3$ Using the Potential Function $F(x) = x^2/2 - x^4/4$.

On examination of the above graphs certain conclusions can be drawn on the behaviour of the differential equation.

The differential equation has equilibrium points at $x = -1, 0 \& +1$. The equilibrium point at $x = 0$ is stable. The equilibrium points at $x = -1 \& +1$ are unstable.

A 1.5 Stability of Equilibrium Points

An equilibrium point $\bar{x}$ is stable if all solutions to the differential equation starting near $\bar{x}$ stay near to it. An equilibrium point is asymptotically stable if all solutions near $\bar{x}$ tend to $\bar{x}$ as $t \to \infty$.

A 1.5.1 Theorem A1 .2

If $\bar{x}$ is an equilibrium point of $\dot{x} = f(x)$ and $f'(x)$ exists, that is, $f(x)$ is differentiable, then, $\bar{x}$ is **asymptotically stable** if $f'(\bar{x}) < 0$ and **unstable** if $f'(\bar{x}) > 0$.

When $f'(\bar{x}) \neq 0$, the equilibrium point is called a **hyperbolic equilibrium point** and when $f'(\bar{x}) = 0$, the equilibrium is called a **nonhyperbolic point**.

A 1.6 Bifurcations in Differential Equations

Bifurcation of its differential equations is a very important aspect of voltage instability in power systems. The behaviour of these differential equations represents the behaviour of the power system.

Consider the behaviour of the following differential equation.

$$\dot{x} = c + x^2 = F(c, x) \tag{A1.6}$$

Where c is a real number variable parameter. The graph of this equation for c=0, passes through the origin (0, 0) which is an equilibrium point. When other values are assigned to c, the resultant graph is similar to the graph with c=0, but with the x-axis shifted vertically by –c. Refer to Figure A1.6.

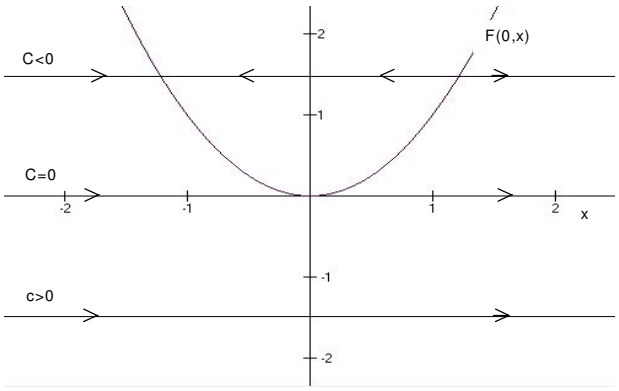

Figure A1.6 Phase Portraits of $\dot{x} = c + x^2$ for different values of c.

Using method 1 of Section A1.4, the phase portrait of equation (2.3) can be drawn for different values of c as shown. For $c < 0$, there are two equilibrium points, for $c > 0$, there are no equilibrium points and for $c = 0$, there is one equilibrium point, the origin. Now for small variations of c around 0, the number of equilibrium points change suddenly. Such a value of

the parameter is called a **bifurcation value**, the equation being at a **bifurcation point** causing a **saddle node bifurcation**.

A 1.7 Second Order Autonomous Differential Equations [7]

A 1.7.1 Linear Harmonic Oscillator

Consider the **linear harmonic oscillator** represented by the following equation.

$$\begin{aligned} \dot{x}_1 &= x_2 \\ \dot{x}_2 &= -x_1 \end{aligned} \qquad \text{(A1.7)}$$

The vector field and the phase portraits of this equation for initial values (x_1, x_2) = (1.0, 1.0), (0.75, 0.75), (0.5, 0.5) are as shown in Figure A1.7.

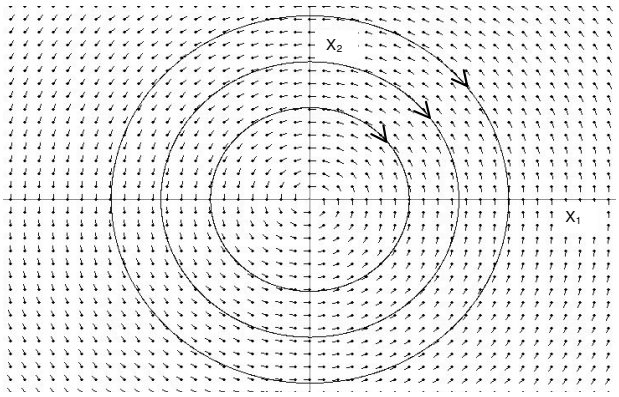

Figure A1.7 Vector Field and Phase Portraits of Linear Harmonic Oscillator.

The equation has an equilibrium point at (0, 0) and the orbits for nearby initial conditions are circular orbits round this equilibrium point. Such an equilibrium point is stable but not asymptotically stable and is called a **center**.

A 1.7.2 Van der Pol Oscillator

Consider the Van der Pol oscillator represented by the following equation.

$$\dot{x}_1 = x_2 \qquad \text{(A1.8)}$$
$$\dot{x}_2 = (1.0 - x_1^2)x_2 - x_1$$

The phase portraits of this equation for initial values $(x_1, x_2) = (-0.1, 0.1)$, (-2.0, 2.0), (2.0, -2.0) are as shown in Figure A1.8.

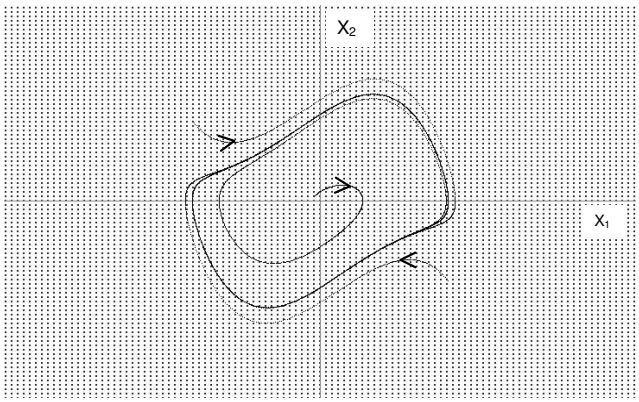

Figure A1.8 Phase Portraits of Van der Pol Oscillator.

It is seen that this equation has an isolated periodic solution called a **limit cycle.** All trajectories starting at any initial condition approach this limit cycle.

A 1.7.3 Linear Product Syatem

Consider the linear product system represented by the following equation.

$$\dot{x}_1 = ax_1 \qquad \text{(A1.9)}$$
$$\dot{x}_2 = bx_2$$

The phase portraits for b<a<0, b=a<0 and a<0<b are shown in Figures A1.9a,b &c.

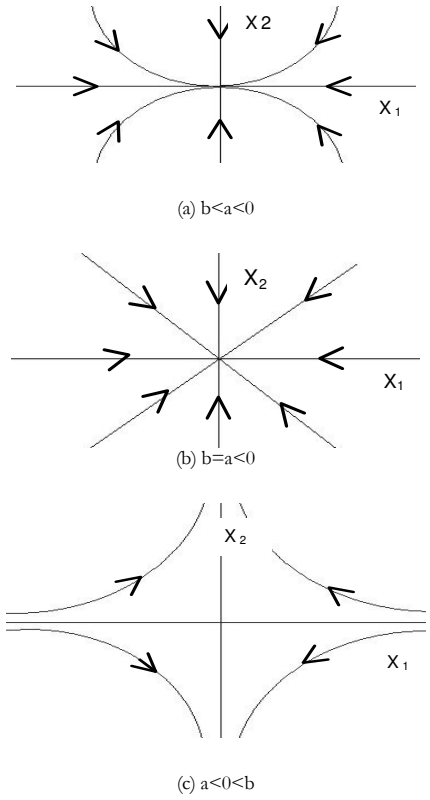

Figure A1.9 Phase Portraits of the Linear Product System

It is seen that for b<a<0, both $x_1(t)$ and $x_2(t) \to 0$ exponentially as $t \to \infty$. For b=a<0, they tend to 0 along straight lines. Therefore the equilibrium point is called a **stable node**. For a<0<b, the origin is still an equilibrium point but all orbits other than the point orbit at the origin leave the origin as shown in Figure A1.9c. Such an equilibrium point is called a **saddle**.

In a power system often the state varies as parameters vary. This variation in parameters can cause voltage collapse. A very simple case is a product system where λ is the parameter:

$$\dot{x}_1 = \lambda + x_1^{\,2}$$
$$\dot{x}_2 = -x_2 \qquad \text{(A1.10)}$$

For such a system it can be shown that for $\lambda < 0$, there are two equilibriums, one a node and the other a saddle. As λ is varied and reaches 0, the equilibriums coalesce. As λ is further increased making $\lambda > 0$, the equilibrium disappears. Such a bifurcation is called a **saddle node bifurcation**.

A 1.7.4 Hopf Bifurcation

Consider the single parameter system below.

$$\dot{x}_1 = x_2 + x_1(\lambda - x_1^2 - x_2^2) \qquad \text{(A1.11)}$$
$$\dot{x}_2 = -x_1 + x_2(\lambda - x_1^2 - x_2^2)$$

It can be shown by drawing the phase portraits, that in such a system, when $\lambda \le 0$, all solutions spiral in to the origin as $t \to \infty$ and when $\lambda > 0$ all solutions spiral in to a periodic orbit, that is a limit cycle. Such a bifurcation is called a **Hopf bifurcation**.

A 1.8 Stability in Systems of Nonlinear Differential Equations and Other Dynamical Systems

In the analysis of power systems to determine voltage stability one comes across more complicated systems of non-linear differential equations and differential algebraic systems of equations. Refer to references [4, 5, 12] and Appendix 2.

Appendix 2

ANALYSIS OF VOLTAGE INSTABILITY

Analysis of voltage stability and many other engineering problems require the solution of nonlinear ordinary differential equations and algebraic differential equations. Such systems are notoriously difficult to solve and many can only be solved numerically when the initial conditions are known. The mathematical theory presented below is based on references [4, 20], however the author of this thesis attempts to make it more understandable. The fundamentals of the concepts presented here are explained in appendix 1. The figures shown in this appendix are from reference [4].

A2.1 Solution of Differential Equations.

Voltage stability involves the solution of nonlinear ordinary differential equations of the type:

$$\dot{x} = f(x) \qquad \text{(A2.1)}$$

x is a n×1 vector and f(x) is a nonlinear function of x. The state space which is an n-dimensional hyperspace is defined by the n-dimensional state vector x. The elements of the vector x are called the state variables. The vector x is time variable and its initial value at t = 0 is given by:

$$x(0) = x_0 \qquad \text{(A2.2)}$$

When this initial value is known the ordinary differential equation (ODE) (A1.1) is known as an initial value problem. Many ODEs can only be numerically solved and then only when the initial conditions are known, ie. as initial value problems. The solution x(t) of the ODE is a curve or trajectory

passing through the initial value x_0 in state space. When t>0, it is called the **forward trajectory** and when t<0, it is called the **backward trajectory**. The theorem of existence and uniqueness of solutions states the conditions under which a solution exists for each initial condition (see below).

Let f(x) be defined in domain U in the n-dimensional real number domain R^n. Then U is a subset of R^n. From the above theorem one can make the following statements. These statements also serve as a statement of the theorem.

1. If f is continuous in U, then there exists a solution x(t) of (A2.1) for all initial conditions x_0 in U. Each solution has a maximum interval of existence I_{x_0} dependant upon the initial condition and is written as:

$$I_{x_0} : \alpha_{x_0} < t < \beta_{x_0} \qquad \text{(A2.3)}$$

   Both or one of α_{x_0} and β_{x_0} can be infinite when the solution exists for all positive and/or negative values of t.

2. If f is smooth, then it is a sufficient condition for f to have a unique solution through x_0.

3. If the maximal interval of existence of the solution is finite, then the limit points of the solution x(t) for $t \to \beta^-$ or $t \to \alpha^+$, belong to the boundary of U when U is bounded and infinite when U is unbounded.

An example taken from [4] is explained here to illustrate the above. Consider the following ODE.

$$\dot{x} = -x^2 \qquad \text{(A2.4)}$$

This ODE has a time solution as follows.

$$x = 0 \quad for \quad x_0 = 0 \tag{A2.5}$$

$$x = \frac{1}{t + \frac{1}{x_0}} \quad for \quad x_0 \neq 0 \tag{A2.6}$$

x_0 being the initial condition for t=0.

Figure A2.1 shows the time response of x for different initial values of x, ie. for different values of x at t=0.

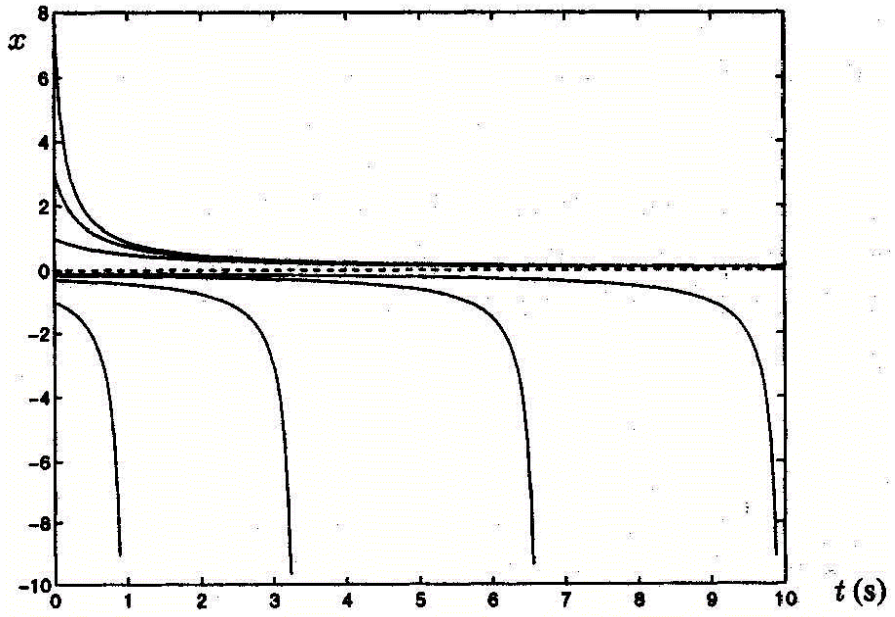

Figure A2.1 – Time Solutions of Equation A2.4 [4]

It is seen that for positive values of x_0, x eventually reduces to zero and for negative values of x_0, x collapses before reaching the critical time β_{x_0}, where:

$$\beta_{x_0} = -\frac{1}{x_0} \quad for \quad x_0 < 0. \tag{A2.7}$$

Therefore (A2.4), when the initial condition is positive, has a solution that exists for all time t>0. For t<0, it has a finite lower bound α_{x_0} of its interval of existence given by:

$$\alpha_{x_0} = -\frac{1}{x_0} \quad for \quad x_0 > 0. \tag{A2.8}$$

A2.2 Equilibria and Stability of Equilibria.

The equilibrium points, x^*, of the ODE (A2.1) are given by the solution of the equation:

$$f(x) = 0. \tag{A2.9}$$

For all initial conditions $x_0 = x^*$, the solution of (A2.1) is given by:

$$x(t) = x^*$$

for all time.

An equilibrium is said to be **stable** if all solutions of the ODE for initial conditions near x^* remain near x^* for all time t>0. An equilibrium is **asymptotically stable** if all trajectories of the solution of the ODE with initial conditions near x^*, approach x^*, as t tends to infinity. The largest region round an asymptotically stable equilibrium, x^*, for which the trajectory, with initial conditions in that region, eventually approach x^* is called the **region of attraction** or **domain** or **basin of attraction** of x^*.

Now consider a linear system of ODEs given by the following equation.

$$\dot{x} = Ax \tag{A2.10}$$

Such a system has only one equilibrium point at $x^* = 0$. The stability of the system is determined by the eigenvalues of the **state matrix** A. If all the real parts of the eigenvalues are negative the equilibrium is asymptotically stable and if the real part of at least one eigenvalue is positive then the equilibrium is unstable. The region of attraction of an asymptotically stable equilibrium in such a system is the entire state space, all trajectories approaching the origin.

On the other hand a nonlinear system of ODEs may have one, more than one or no equilibria. Also the region of attraction of a stable equilibrium may be limited causing instability of the equilibrium for initial conditions around the equilibrium.

It has been shown that the stability of an equilibrium x^* in a nonlinear system can be determined by examining the linearised system around the equilibrium point. To illustrate consider a point x near the equilibrium point x^*. Then one can write:

$$\Delta x = x - x^* \tag{A2.11}$$

Now using Taylor's expansion and retaining only the first order term we arrive at the linear system:

$$\Delta\dot{x} = A\Delta x. \tag{A2.12}$$

The state matrix A is called the **Jacobian** or **state Jacobian** of f with respect to x evaluated at x^* and is given by:

$$A = \left.\frac{\partial f}{\partial x}\right|_{x=x^*} = f_x(x^*) \tag{A(2.13)}$$

That is $A = \begin{bmatrix} \frac{\partial f_1}{\partial x_1} \ldots\ldots \frac{\partial f_1}{\partial x_n} \\ . \\ . \\ . \\ \frac{\partial f_n}{\partial x_1} \ldots\ldots \frac{\partial f_n}{\partial x_n} \end{bmatrix}$

Now if the eigenvalues of A all have negative real parts, then the equilibrium x^* is asymptotically stable but if at least one eigenvalue has a positive real part then the equilibrium x^* is unstable.

When an equilibrium is asymptotically stable, with all eigenvalues having negative real parts, it is called a **stable node** or **sink**. If it is unstable with all the eigenvalues having positive real parts, then it is called an **unstable node** or **source**. If the equilibrium has eigenvalues some having positive real parts and all the others having negative real parts, then such an equilibrium is called a **saddle**.

An interesting case arises when the Jacobian f_x has one or more eigenvalues with zero real parts. An example is the case of the system represented by equation (A2.4). It has an equilibrium point at the origin ($x^* = 0$). Linearising the system around this equilibrium at the origin we obtain the Jacobian to be zero as shown below.

$$\Delta \dot{x} = -2x^* \Delta x = 0 \qquad \text{(A2.14)}$$

Now, as seen in Figure A2.1, in the neighbourhood of $x^* = 0$, there are initial conditions $x_0 < 0$, for which the forward trajectory is unbounded and therefore the system collapses during this forward trajectory. This type of unstable equilibrium is called a **saddle node**. Figure A2.2 shows the three types of nodes for a first order, ie. a single variable system.

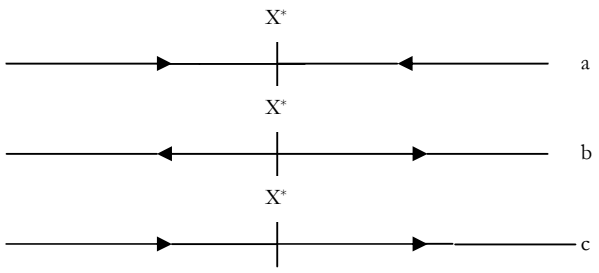

Figure A2.2, a – stable node, b – unstable node, c – saddle node.

When a multi-order system, ie. a system with multiple variables, has a Jacobian with a zero eigenvalue, then that particular equilibrium is a saddle node. Note that when the Jacobian has a zero eigenvalue, then the determinant of that Jacobian is also zero. Near such equilibrium points there are trajectories similar to that in Figure A2.2c. If the Jacobian has a complex conjugate pair of eigenvalues with zero real parts at a point of equilibrium, then such an equilibrium point is called a **center**.

In power systems where many operating points are studied, one comes across both stable and unstable equilibria.

A2.3 Eigenvectors, Manifolds and Invariance.

As seen above the linearised system of a non-linear system can provide information on the stability of equilibrium points. Similarly eigenvectors of the linearised system can be generalised in the non-linear system. Eigenvectors and eigenspaces of the linearised system correspond to the manifolds of the non-linear system.

It can be shown mathematically that the response of a linear system of the type represented by equation (A2.10) can be expressed in terms of the right and left eigenvectors v and w respectively of the state matrix A. The eigenvectors are known to satisfy the following equations.

$$Av_i = \lambda_i v_i \quad for \quad i = 1, ..., n \tag{A2.15}$$

$$w_i^T A = \lambda_i w_i^T \quad for \quad i = 1, ..., n \tag{A2.16}$$

where λ_i = the eigen values.

To simplify the theory it is assumed that the linearised system has n distinct eigenvalues. Then the left and right eigenvectors for different eigenvalues are orthogonal to each other. That is,

$$w_i^T v_j = 0 \quad for \quad i \neq j. \tag{A2.17}$$

For an initial value x_0 the response of the linear system is given by:

$$x(t) = \sum_{i=1}^{n} e^{\lambda_i t} v_i w_i^T x_0 \tag{A2.18}$$

Now if we consider an initial condition collinear with the right eigenvector v_i we have:

$$x_0 = a v_i \tag{A2.19}$$

Substituting this in equation (A2.18) and applying equation (A2.17) we have:

$$x(t) = a e^{\lambda_i t} (w_i^T v_i) v_i = b v_i \tag{A2.20}$$

Equation (A2.20) demonstrates that once a trajectory is on a right eigenvector, it is always on that right eigenvector. This is known as the invariance property of a right eigenvector.

It is also observed that if λ_i has a negative real part, then, since $e^{\lambda_i t} \to 0 \quad as \quad t \to \infty$, the trajectory x(t) approaches the equilibrium point at the origin during its forward trajectory. Similarly if the eigenvalue has a

positive real part, the backward trajectory x(t) originates at the equilibrium point as $t \to -\infty$.

If a number of right eigenvectors is considered, it is seen that they span a subspace in the space of the variables x. Consider two eigenvectors v_i and v_j spanning a plane and an initial point in this space given by:

$$x_0 = av_i + bv_j \tag{A2.21}$$

The trajectory x(t) is given by:

$$x(t) = [ae^{\lambda_i t}(w_i^T v_i)]v_i + [be^{\lambda_j t}(w_j^T v_j)]v_j = cv_i + dv_j. \tag{A2.22}$$

From this it is seen that the trajectory lies entirely on the plane defined by v_i and v_j. Thus it is seen that the invariance property holds for subspaces defined by eigenvectors as well.

In a linearised system the subspace spanned by eigenvectors corresponding to eigenvalues with negative real parts is called the **stable eigenspace**, the subspace spanned by eigenvectors corresponding to eigenvalues with positive real parts is called the **unstable eigenspace** and the subspace spanned by eigenvectors corresponding to eigenvalues with zero real parts is called the **center eigenspace**. All trajectories in a stable eigenspace approach the origin as $t \to \infty$, and all trajectories in an unstable eigenspace originate from the equilibrium point.

The equivalent in nonlinear systems, of the concept of invariant eigenspace in linear systems, is the concept of **invariant manifolds**. The word manifold refers to a smooth curved line, surface or hypersurface with no singular points such as self-intersections. A trajectory starting on an invariant manifold stays on the manifold for all time. At the equilibrium point the stable, unstable and center manifolds are tangential to the respective eigenspaces of the linearised system. Figure A2.3 shows the different types of manifolds.

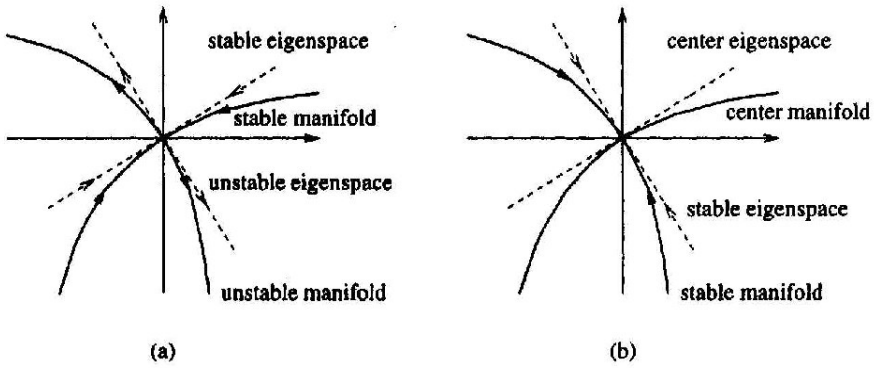

Figure A2.3 Different Types of Manifolds for a Second Order System [4].

Figure A2.3a shows an equilibrium, which is a saddle with the Jacobian having one positive and one negative real eigenvalue. Figure A2.3b shows an equilibrium with one negative and one zero eigenvalue. The direction of the trajectory of the center manifold cannot be assigned without knowledge of the nonlinear characteristics of the system.

An example taken from reference [4] is given here to illustrate the above. Consider the system of non-linear, second order (two state variables) ODEs given below which is similar to the representation of a single generator, infinite bus system with no damping.

$$\dot{x}_1 = a^2 x_2 \quad a > 0 \tag{A2.23a}$$

$$\dot{x}_2 = 0.5 - \sin x_1 \tag{A2.23b}$$

It can be shown that this system has two equilibria as follows.

$$x^{(1)} = [\pi/6 \quad 0]^T$$
$$x^{(2)} = [5\pi/6 \quad 0]^T$$

The Jacobian of the system is derived to be as follows.

$$f_x = \begin{bmatrix} 0 & a^2 \\ -\cos x_1^* & 0 \end{bmatrix}$$

Therefore the eigenvalues of the linearised system can be calculated and are:

$$\lambda_{1,2}^{(1)} = \pm j0.931a$$
$$\lambda_{1,2}^{(2)} = \pm 0.931a.$$

The eigenvalues of the equilibrium $x^{(1)}$ are complex conjugates with zero real parts. Therefore it is a center. The eigenvalues of the equilibrium $x^{(2)}$ are both real and one is negative while the other is positive. Therefore it is a saddle.

Figure A2.4 shows the trajectories of the system represented by equations (A1.23a,b) for a number of initial conditions.

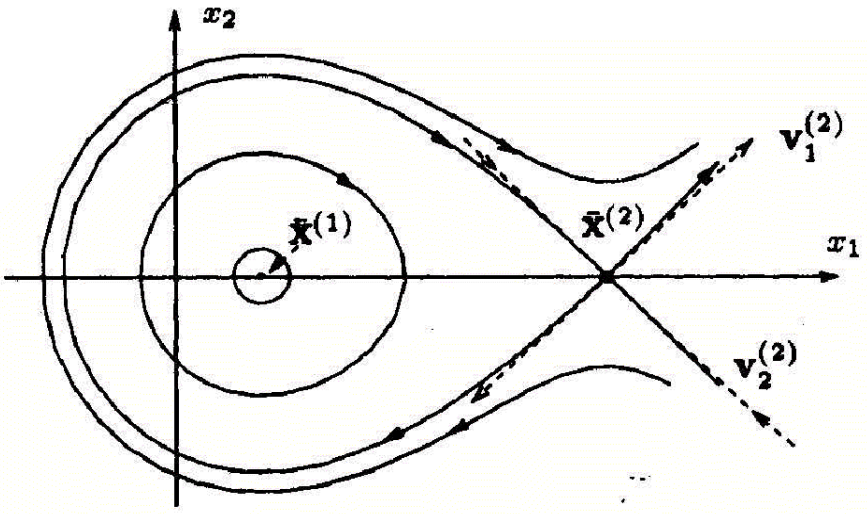

Figure A2.4 Phase Portrait of the system
[4]

The orientation or direction of the trajectories are as shown. It can be verified that the trajectories near the center $x^{(1)}$ are periodic oscillations with constant amplitude. Therefore the equilibrium $x^{(1)}$ is stable but not asymptotically stable. The trajectories near unstable saddle point $x^{(2)}$ are as shown. The eigenvalue $\lambda_1^{(2)} = +0.931a$ gives the eigenvector representing the unstable eigenspace of the saddle point, which is:

$$v_1^{(2)} = [a \quad 0.931]^T$$

This eigenspace is tangential to the unstable manifold.

The eigenvalue $\lambda_2^{(2)} = -0.931a$ gives the eigenvector representing the stable eigenspace of the saddle point, which is:

$$v_2^{(2)} = [a \quad -0.931]^T$$

This eigenspace is tangential to the stable manifold.

A2.4 Limit Cycles and the Stability of Limit Cycles.

If a periodic solution x(t) exists for the ODE given in equation (A2.1), then it satisfies the following condition.

$$x(t+T) = x(t) \qquad \text{(A2.24)}$$

The smallest value of T for which equation (A2.24) is satisfied is the period of the cycle. If a trajectory starts at a point x_0 on a periodic solution, then after time T, the trajectory will pass through x_0 again and keep on retracing its path over and over again. Thus the solution forms a closed curve in n dimensional space. An isolated periodic solution of this type is called a **limit cycle**. The periodic solutions shown in Figure A2.4 are not limit cycles since they have an infinite number of periodic solutions near each one of them and therefore are not isolated. A limit cycle is asymptotically stable if a trajectory starting near

the limit cycle eventually ends up on that limit cycle. A limit cycle is unstable if a trajectory starting near it eventually diverges away from it.

Two examples taken from reference [4] are explained here to illustrate stable and unstable limit cycles.

Consider the following second order system.

$$\dot{x}_1 = x_2 \qquad \text{(A2.25a)}$$

$$\dot{x}_2 = 10(-x_1 + x_2 - x_2^3) \qquad \text{(A2.25b)}$$

This system has an equilibrium at $x^* = 0$ and linearising around this equilibrium we obtain:

$$\Delta\dot{x}_1 = \Delta x_2 \qquad \text{(A2.26a)}$$

$$\Delta\dot{x}_2 = -10\Delta x_1 + 10\Delta x_2 \qquad \text{(A2.26b)}$$

The eigenvalues of the state matrix are $\lambda_1 = +8.87 \quad and \quad \lambda_2 = +1.13$. Therefore the equilibrium is unstable. A graph of the solution is as shown in Figure A2.5.

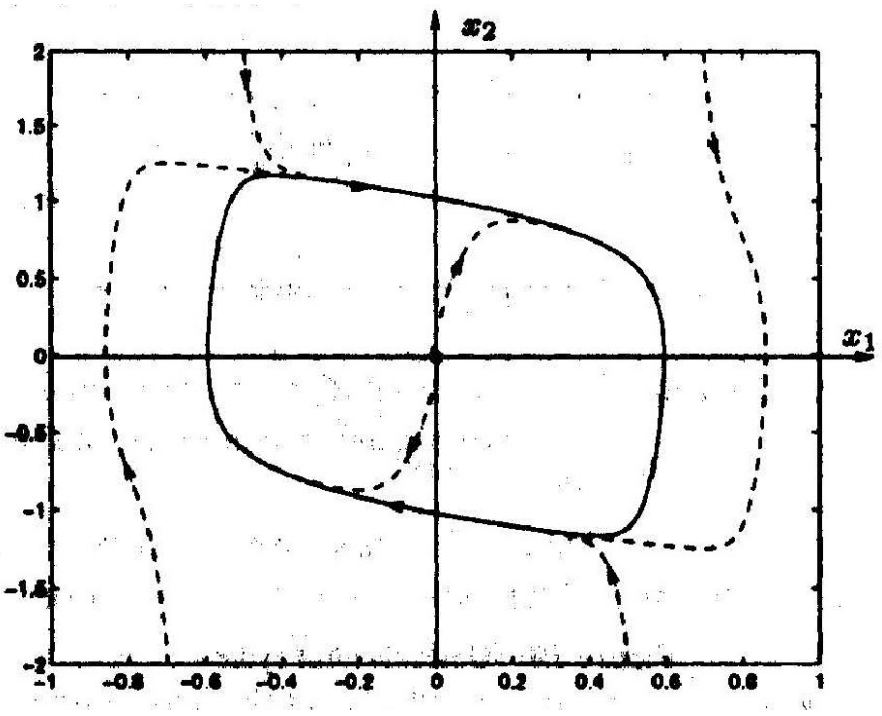

Figure A2.5 – Stable Limit Cycle [4]

It is seen from this figure that trajectories starting near the equilibrium eventually end up in an isolated periodic oscillation. Therefore it is a limit cycle and since trajectories starting both inside and outside the limit cycle eventually end up on it, it is asymptotically stable. The stable manifold of this stable limit cycle is the whole of state space.

Now consider the following system.

$$\dot{x}_1 = 10x_2 \qquad \text{(A2.27a)}$$

$$\dot{x}_2 = -x_1 - x_2 + x_2^3 \qquad \text{(A2.27b)}$$

This system has one equilibrium point at the origin and the eigenvalues are $\lambda_1 = -0.5 + j3.12 \quad and \quad \lambda_2 = -0.5 - j3.12$. Since the real parts of both

eigenvalues are negative the equilibrium is stable. A graph of the solution is shown in Figure A2.6.

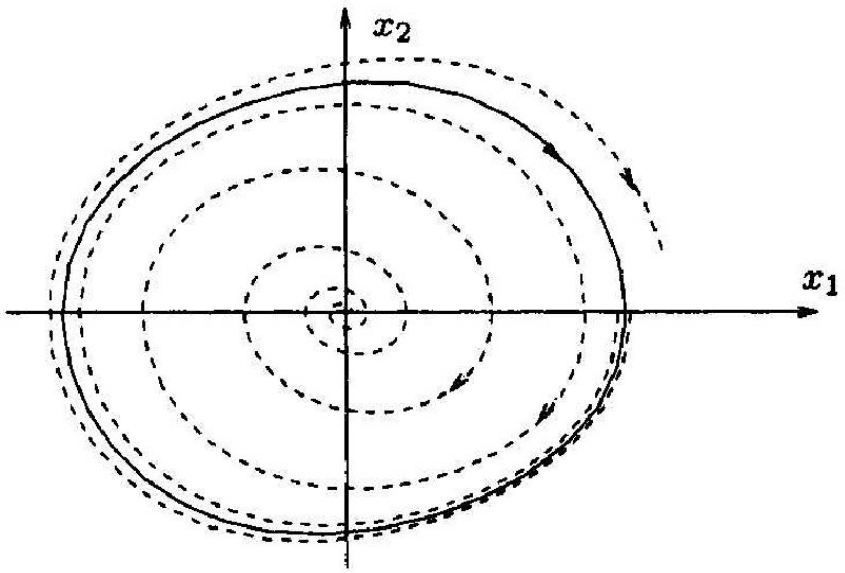

Figure A2.6 – Unstable Limit Cycle [4]

On the positive x-axis we can see a critical point at $\tilde{x}_1 = 3.685$. Trajectories starting on the x-axis at points less than the critical value spiral towards the equilibrium point at the origin and those starting on the x-axis at point greater than the critical value diverge. At the critical value there is an unstable limit cycle. It is unstable because trajectories starting near the critical value either spiral in towards the equilibrium at the origin or diverge away from the limit cycle. The stable manifold of this limit cycle is the limit cycle itself and its unstable manifold is all of the remaining state space.

A2.5 Bifurcation Theory.

When smooth, continuous changes occur in the parameters of a nonlinear system, sudden changes in the response of the system can occur. Bifurcation theory studies such changes. Voltage collapse in a power system is due to such bifurcations.

Consider the following family of smooth ordinary differential equations (ODEs).

$$\dot{x} = f(x, p) \qquad \text{(A2.28)}$$

x is a state vector of dimension $(n \times 1)$ and p is a parameter vector of dimension $(k \times 1)$. For any given value of p, the equilibrium points x^* of equation (A1.28) is given by:

$$f(x^*, p) = 0 \qquad \text{(A2.29)}$$

ie. for each possible value of p, there is one or more equilibrium points x^*. Therefore it can be said that equation (A2.29) defines the k-dimensional equilibrium manifold of the system in (A2.28) in $(n+k)$-dimensional state and parameter space. This can be visualised in 3-dimensions by taking one state vector x and two parameters p_1 and p_2. p_1 and p_2 form the two horizontal axes and x forms the vertical axis. All possible values of p will form a 1-dimensional curve (a line) on the horizontal plane. For each value on this curve there is one or more equilibrium value for the state variable x. These equilibrium values of x are measured along the vertical x-axis. Thus we obtain a two dimensional surface (this is the dimension k of the parameter vector) of equilibrium points which is the equilibrium manifold.

Now consider an equilibrium point $x^{(1)}$ of equation (A2.28) which corresponds to the parameter values p_0. The Jacobian at this point is assumed to be non-singular.

ie. $\det f_x(x^{(1)}, p_0) \neq 0$. (A2.30)

In this case it can be mathematically shown that there is a unique smooth function given by:

$$x^* = g^{(1)}(p) \quad satisfying \quad x^{(1)} = g^{(1)}(p_0). \tag{A2.31}$$

This equation gives a branch of the equilibrium points of the system of equation (A2.28) as a function of p.

Now consider that equation (A2.28) has another equilibrium point $x^{(2)}$ for the same value p_0 of p. Then as above,

$$\det f_x(x^{(2)}, p_0) \neq 0. \tag{A2.32}$$

And there is a unique smooth function:

$$x^* = g^{(2)}(p) \quad satisfying \quad x^{(2)} = g^{(2)}(p_0). \tag{A2.33}$$

Equation (A2.33) gives another branch of equilibrium points of the system (A2.28) as a function of p.

When these two branches of equilibrium points intersect each other a **bifurcation** is formed. At such a bifurcation point, the Jacobian $f_{(x)}$ is singular.

The following example taken from [4] illustrates the concept of bifurcation. Consider the first order (one state variable) system with one scalar parameter ($p = \mu$) given by:

$$\dot{x} = x^2 - 2x + 1.1 - \mu \tag{A2.34}$$

Figure A2.7 shows the plot of the two branches of equilibrium points $g^{(1)}(\mu) \quad and \quad g^{(2)}(\mu)$ in state and parameter space.

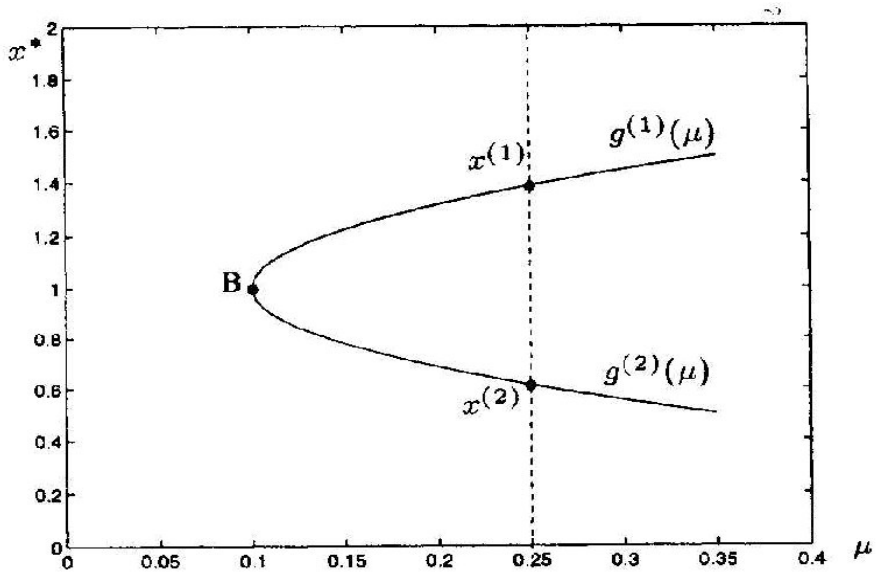

Figure A2.7 – Equilibria Bifurcation [4]

It is seen that these two branches intersect at the bifurcation point B given by $(\mu = 0.1, x^* = 1.0)$. At this bifurcation point $\frac{\partial f}{\partial x} = 0$. It has been shown with rigorous mathematics that a bifurcation occurs at a point in parameter space where the qualitative structure of the system in (A2.28) changes for a small variation of the parameter vector p. [4] gives a list of properties a change in any one of which constitutes a bifurcation:

1. Number of equilibrium points.
2. Number of limit cycles
3. Stability of equilibrium points or limit cycles.
4. Period of periodic solutions.

Voltage stability analysis can be performed by considering bifurcations that occur in single parameter families of ODEs. The two types of bifurcations in such systems are the Saddle Node Bifurcation (SNB) and the Hopf Bifurcation (HB).

A1.5.1 Saddle Node Bifurcations.

Considering a single parameter family of ODEs given by:

$$\dot{x} = f(x, \mu), \tag{A2.35}$$

its equilibrium condition is given by:

$$f(x, \mu) = 0. \tag{A2.36}$$

At a saddle node bifurcation of this system, two branches of equilibria meet at a point such as the point B in Fig. A2.7. At this bifurcation the equilibrium becomes a saddle node and therefore it is called a **Saddle Node Bifurcation** (**SNB**). Therefore the necessary conditions for an SNB are equation (A2.36) and the following equation.

$$\det f_x(x^*, \mu) = 0 \tag{A2.37}$$

Equation (A2.37) constitutes (n+1) equations in (n+1) variables (x and μ). However all points satisfying these necessary conditions are not SNB points. Considering a scalar system, the sufficient conditions for a saddle node bifurcation are:

$$f(x^*, \mu) = 0 \tag{A2.38a}$$

$$\frac{\partial f}{\partial x} = 0 \tag{A2.38b}$$

$$\frac{\partial f}{\partial \mu} \neq 0 \qquad \text{(A2.38c)}$$

$$\frac{\partial^2 f}{\partial x^2} \neq 0 \qquad \text{(A2.38d)}$$

The conditions (A2.38a,b) are the same as the conditions (A2.36) and (A2.37) applied for the case of a single state variable x and a single parameter μ. Conditions (A2.38c,d) are called the **transversality conditions**. Condition (A2.38c) is the condition for the existence of a smooth local function, $\mu = h(x)$, at the bifurcation point (μ_0, x_0). The geometrical interpretation of this is that the equilibrium manifold (A2.38a) intersects the line $x = x_0^*$ transversally at the bifurcation point. Condition (A2.38d) is the condition that locally, the equilibrium manifold remains on one side of the line $\mu = \mu_0$. It is also seen that that conditions (A2.38a-d) are also sufficient conditions for a maximum or minimum of μ on the manifold given by equation (A2.38a). An example of three systems taken from reference [4] illustrates the above. Consider the following three first order systems with a single parameter whose equilibria are graphed in the μ x plane in Figure A2.8.

$$\dot{x} = x^2 + \mu \qquad \text{(A2.39a)}$$

$$\dot{x} = x^3 + \mu \qquad \text{(A2.39b)}$$

$$\dot{x} = x^2 + \mu^3 \qquad \text{(A2.39c)}$$

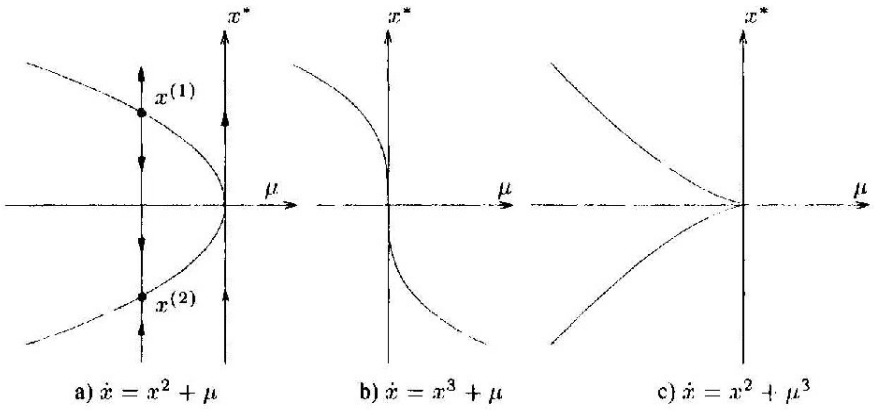

Fig. A2.8 – a) Sufficient Conditions for SNB, b) Violation of (A1.38d), c) Violation of (A1.38c) [4]

All three systems have an equilibrium point at $\mu_0 = x^*_0 = 0$ satisfying the condition $\frac{\partial f}{\partial x} = 0$. Equation (A2.39a) has a saddle node bifurcation at the origin, refer to Figure A2.8a. Equation (A2.39b) violates the condition (A2.38d), refer to Figure A 2.8b and equation (A2.39c) violates the condition (A2.38c), see fig. A 2.8c. However in general, in single parameter families, equilibria satisfying condition (A2.38b) will also satisfy conditions (A2.38c,d) and therefore are SNB points.

The system represented by equation (A2.39a) with an SNB at $\mu = 0$, has two equilibrium points for $\mu < 0$, one equilibrium point at $\mu = 0$ and no equilibrium points for $\mu > 0$. The equilibrium point at $\mu = 0$ is a saddle node and the time response or trajectories of the system is similar to that shown in Figure A2.1 but the time scale is reversed. For a given negative value of μ and for negative initial conditions of x, the trajectories converge to the equilibrium point $x^* = 0$; whereas for positive initial conditions x_0 of x, the trajectories explode in finite time given by $\beta_{x_0} = \frac{1}{x_0}$. Now considering the equilibrium points for $\mu < 0$,

Let $\mu = -a^2$ where $a > 0$.

Then the equilibrium points are given by,

$x^{(1)} = a$ and $x^{(2)} = -a$.

The Jacobian of A2.39a is,

$$\frac{\partial f}{\partial x} = 2x^*.$$

Therefore considering its eigenvalues, $x^{(1)} = +a$ is an unstable equilibrium and $x^{(2)} = -a$ is a stable equilibrium. Thus for a first order system, at a saddle node bifurcation, two points of equilibrium, one stable and the other unstable coalesce and disappear.

Conversely, if μ decreases slowly, from a value greater than its bifurcation value μ_0, then at the SNB point, two equilibria emerge simultaneously.

The above can be generalised for a multivariable system as follows. At an SNB two equilibrium points coalesce and disappear or emerge simultaneously. One of these points has an eigenvalue with a positive real part and the other an eigenvalue with a negative real part both becoming zero at the SNB. In such a multivariable system, if all the other eigenvalues, except the one becoming zero at the SNB, have eigenvalues with zero negative parts, then one of the equilibria coalescing at the SNB is stable and the other is unstable.

Figure A2.8a shows with arrows, the trajectories approaching the stable equilibrium $x^{(2)}$ and the trajectories departing from the unstable equilibrium $x^{(1)}$. It is seen that the trajectories with initial conditions $x_0 < a$ converge to the stable equilibrium point $x^{(2)} = -a$ and trajectories with initial conditions $x_0 > a$ explode after a finite interval of time. Thus the region of attraction of the stable equilibrium point is bounded by the unstable equilibrium. This is its

stable manifold in the multivariable case. It is also seen that the region of attraction contracts or shrinks as the SNB point is approached.

At the saddle node bifurcation point at the origin the stable manifold of the saddle node is the negative x-axis and the unstable manifold of the saddle node is the positive x-axis. Therefore the entire x-axis forms the center manifold of the saddle node. Since the system has only one state variable x, the entire state space is the center manifold.

It was mentioned above that in single parameter families of ODEs, the equilibrium points satisfying the necessary conditions represented by equations (A2.36) and (A2.37) are in general SNBs. In multiparameter families (where p is a $(k \times 1)$ vector) it should be noted that the points satisfying the necessary conditions for an SNB forms a $(k - 1)$-dimensional manifold in the $(n + k)$-dimensional state and parameter space while the points violating the sufficient conditions for an SNB form $(k - 2)$-dimensional submanifolds lying on the above manifold.

If the parameter vector moves along a given curve such as when the k parameters depend on a scalar μ, ie. $p = p(\mu)$, then the multiparameter problem reduces to a single parameter problem and the equilibrium points satisfying the necessary conditions represented by equations (A2.36) and (A2.37) are in general SNBs.

The following observations can be made regarding SNBs and equilibrium manifolds. At an SNB point the manifold of equilibrium points folds with respect to the parameter space. For example the curve of Figure A2.8a folds with respect to the μ axis at the SNB point. When SNB points are projected onto the k-dimensional parameter space, it forms a hypersurface of dimension (k - 1) called a bifurcation surface. The bifurcation surface is the boundary of the feasibility region, which is the region in parameter space for which equilibrium points exist. When an equilibrium point goes through a saddle

node bifurcation, the number of projection points of the equilibrium manifold on parameter space changes by two. For example in Figure A2.8a, the feasibility region is the negative μ axis bounded by the SNB point $\mu = 0$. When the system consists of multivariables, a saddle node bifurcation occurs at an equilibrium with a zero eigenvalue and this equilibrium point satisfies the transversality conditions. The curve in n-dimensional state space that is tangential to the right eigenvector of the zero eigenvalue is the center manifold of the saddle node. The center manifold consists of a stable manifold and an unstable manifold that are separated by the equilibrium point. Refer to Figure A2.2c.

A2.5.2 Hopf Bifurcations.

A saddle node bifurcation is characterised by a zero eigenvalue and at such a bifurcation the response of the system is monotonic. The point at which a SNB occurs is easily found by equating the Jacobian at the equilibrium point to zero, ie. $\det f_x(x^*, \mu) = 0$. A Hopf bifurcation occurs in nonlinear systems when a parameter variation forces a pair of complex eigenvalues to cross the imaginary axis in the complex plane. When this happens an oscillatory instability occurs in the system due to the interaction of the equilibrium point with a limit cycle. It has been shown mathematically that the necessary condition for a Hopf bifurcation (HB) is the existence of an equilibrium with purely imaginary eigenvalues. However as in the case of SNBs, not all equilibrium points satisfying the necessary condition are HBs, though most are. In cases where the real part of the critical eigenvalue pair does not change sign after going to zero are not Hopf bifurcations. Two types of Hopf bifurcations are defined in reference [4] as follows.

Subcritical HB: an unstable limit cycle existing prior to the bifurcation shrinks and eventually disappears as it coalesces with a stable equilibrium point at the bifurcation. After the bifurcation, the equilibrium point becomes unstable resulting in growing oscillations.

Supercritical HB: a stable limit cycle is generated at the bifurcation and a stable equilibrium point becomes unstable with increasing amplitude oscillations, which are eventually attracted by the stable limit cycle.

These two types of HBs are illustrated in Figure A2.9a,b.

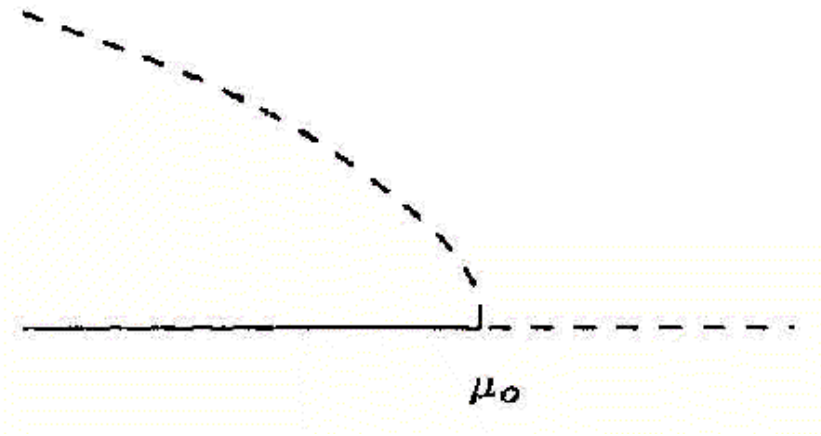

Figure A2.9a - Subcritical Hopf Bifurcation [4]

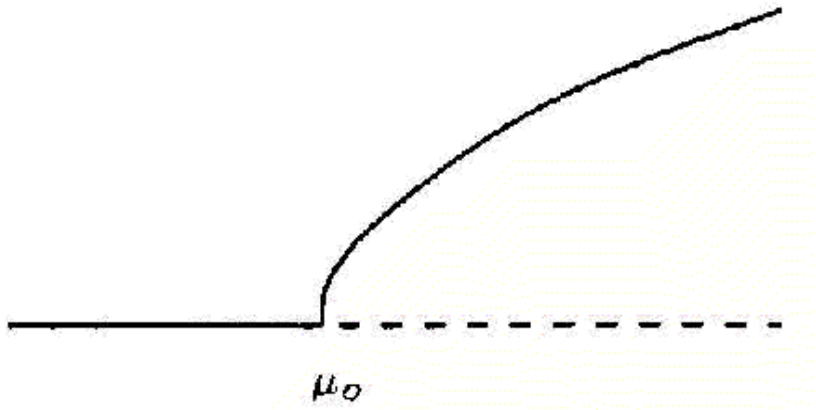

Figure A2.9b – Supercritical Hopf Bifurcation [4]

The abscissa in Figure A2.9 is the parameter value μ with μ_0 as its bifurcation value. The ordinate is the amplitude of the limit cycle. The straight line represents the possible equilibrium points and the curved line represents the amplitude of the limit cycle. Solid lines represent stable equilibria and stable limit cycles. The dashed lines represent unstable equilibria and unstable limit cycles.

In Figure A2.9a it is seen that the amplitude of the unstable limit cycle decreases as the parameter value approaches the bifurcation value. The limit cycle disappears at the bifurcation value and the equilibrium point becomes unstable as seen by the dashed line. Prior to bifurcation the region of attraction of the equilibrium is bounded by the stable manifold of the unstable equilibrium. After bifurcation the trajectories are unbounded with oscillations of increasing amplitude. It is seen from the figure that the branch of limit cycles emanating at the bifurcation exist only for values of the parameter less than its bifurcation value. Hence the adjective subcritical. In Figure A2.9b there is no limit cycle prior to bifurcation but a stable limit cycle is generated at bifurcation. Therefore after bifurcation any trajectories starting near the unstable equilibrium are attracted by the stable limit cycle with bounded oscillations. In practice just prior to bifurcation, the trajectories have lightly damped oscillations and after bifurcation, the trajectories are attracted by the limit cycle. Both these are unacceptable from a power system operation point of view.

A2.6 Differential - Algebraic Systems of Equations.

Differential - Algebraic systems of equations consist of differential equations, which also include algebraic variables and are subject to a set of algebraic constraints. These are important in voltage stability analysis since multiple time scale systems reduce to differential algebraic systems after time scale decomposition, which is a mathematical method used to solve multiple time scale systems.

A2.6.1 Equilibrium Points and Stability in Differential – Algebraic Systems.

Differential – Algebraic systems are of the following form.

$$\dot{x} = f(x, y, p) \tag{A2.40a}$$

$$0 = g(x, y, p) \tag{A2.40b}$$

The equations represent n differential equations and m algebraic equations, which are assumed smooth. x is a vector of n state variables, y is a vector of m algebraic variables and p is a vector of k parameter variables. A manifold called the constraint manifold of dimension (n+k) is defined by the m algebraic equations in the (n+m+k)-dimensional space of the state, algebraic and parameter variables x, y and p. The following method using the implicit function theorem is used in the analysis of differential algebraic systems.

At a point (x, y, p) where the algebraic Jacobian $g_y(x, y, p)$ is non-singular, the implicit function theorem states that there exists a locally unique smooth function of the following form.

$$\dot{x} = F(x, p) \tag{A2.41}$$

It is seen that the algebraic variables have been eliminated from this function and such a function exists for all points in (n+m+k)-dimensional, state, algebraic and parameter space where the algebraic Jacobian g_y is nonsingular. Therefore the theorem of existence and uniqueness referred to at the beginning of this appendix implies that there is a unique time solution to the above differential-algebraic equations at all points where the Jacobian g_y is nonsingular. For a given parameter vector p, the domain of F in state space is denoted by U_p. U_p is bounded by points for which the Jacobian g_y is singular and may also be bounded by any hard limits on the state variables.

Now using a method similar to the one shown in Section A2.2, for a given value of p, the equilibrium points are given by the solution of the following system of equations.

$$f(x, y, p) = 0 \qquad \text{(A2.42a)}$$

$$g(x, y, p) = 0 \qquad \text{(A2.42b)}$$

To determine the stability of equilibrium points the above system is linearised as follows.

$$\begin{bmatrix} \Delta\dot{x} \\ 0 \end{bmatrix} = J \begin{bmatrix} \Delta x \\ \Delta y \end{bmatrix} \qquad \text{(A2.43)}$$

Where $J = \begin{bmatrix} f_x & f_y \\ g_x & g_y \end{bmatrix}$ (A2.44)

is known as the unreduced Jacobian.

When g_y is nonsingular, Δy can be eliminated from equation (A2.43) (note that equation (A2.43) is a pair of simultaneous equations) and doing so we obtain:

$$\Delta\dot{x} = [f_x - f_y g_y^{-1} g_x]\Delta x \qquad \text{(A2.45)}$$

Therefore the state matrix of the linearised system is:

$$A = F_x = [f_x - f_y g_y^{-1} g_x] \qquad \text{(A2.46)}$$

The expression for A is known as the Schur complement of the algebraic equation Jacobian g_y in the unreduced Jacobian J. A is also referred to as the reduced Jacobian. Now we may draw the following conclusions.

- The eigenvalues of the state matrix A determine the stability of the equilibrium point of the differential-algebraic system for a given value of p.

- In state and algebraic variables space, the stable and unstable manifolds of the equilibrium point lie on the constraint manifold.

- Bifurcations occur in a differential-algebraic system as the parameter vector p is varied.

Note is made of Schur's determinant formula for nonsingular g_y:

$$\det J = \det g_y . \det [f_x - f_y g_y^{-1} g_x] = \det g_y . \det A \qquad \text{(A2.47)}$$

From this we see that for nonsingular g_y, when the state matrix A becomes singular so does the unreduced Jacobian J. Therefore the necessary condition for a saddle-node bifurcation, which is g_y becoming singular, is also the condition that the unreduced Jacobian J becomes singular.

A2.6.2 Singularity Induced Bifurcations.

The simultaneous solution of the algebraic constraint equations (A2.40b) and the singularity condition for the algebraic equation Jacobian given by:

$$\det g_y (x, y, p) = 0 \qquad \text{(A2.48)}$$

give the points on a hypersurface called the **impasse surface** with dimension (n+k-1) and lying on the constraint manifold. This surface cannot be crossed by the trajectories of the system and divides the impasse surface into different regions called **causality regions**. The projection of the impasse surface, for a given parameter vector p, onto the state space defines an (n-1)-dimensional surface denoted S_p. This surface S_p consists of the algebraic equation singularity points and bounds the domain U_p for a given value of the vector p. As p is varied the domain U_p, on which the differential equation (A2.41) is

defined, contracts and expands. Now consider an initial condition of the differential-algebraic system with coordinates (x_0, y_0, p_0) whose projection on state space is x_0 (x_0 is in the domain U_{p_0}). From the theorem of existence and uniqueness of solutions discussed in Section A2.1, the following conclusions can be drawn.

- Some solutions have an upper bound β and some solutions have a lower bound α on their interval of existence.

- As $t \to \beta$, solutions with an upper bound on the interval of existence either go to infinity or terminate on the boundary of U_p. The singularity surface forms part of this boundary.

- As $t \to \alpha$, solutions with a lower bound on the interval of existence either go to infinity or emerge from the boundary of U_p, the singularity surface forming part of this boundary.

Therefore the singularity surface contains points from which trajectories emerge or converge on in finite time.

The k-dimensional equilibrium manifold and the impasse surface of a differential-algebraic system lie on the constraint manifold. The points at which the equilibrium manifold and the impasse surface cross satisfy both the singularity condition (A2.48) and the equilibrium conditions (A2.42a,b) and therefore are of interest. When a family of equilibrium points approach the impasse surface, the determinant of the algebraic equation Jacobian g_y becomes progressively very small and therefore by equation (A2.47), the reduced Jacobian A becomes very large. When this happens at least one of the eigenvalues of the state matrix A tends to infinity and on the other side of the impasse surface but on the equilibrium surface, the equilibrium points also have an eigenvalue tending to infinity but of opposite sign. Therefore the stability properties change as the equilibrium passes through the singularity

surface, giving rise to a bifurcation. Such a bifurcation is called a **singularity induced bifurcation**. This is illustrated by the following example.

Consider the differential-algebraic system represented by the following equations:

$$\dot{x} = z - y \sin x \qquad \text{(A2.49a)}$$

$$0 = -0.5z - y^2 + y \cos x \qquad \text{(A2.49b)}$$

Where y > 0, z is a scalar parameter and n = m = k = 1. Therefore state and parameter space has dimension n + m + k = 3, constraint manifold has dimension n + k = 2 and the impasse surface has dimension n + k – 1 = 1. Figure A2.10 shows the constraint manifold, the equilibrium manifold and the impasse surface.

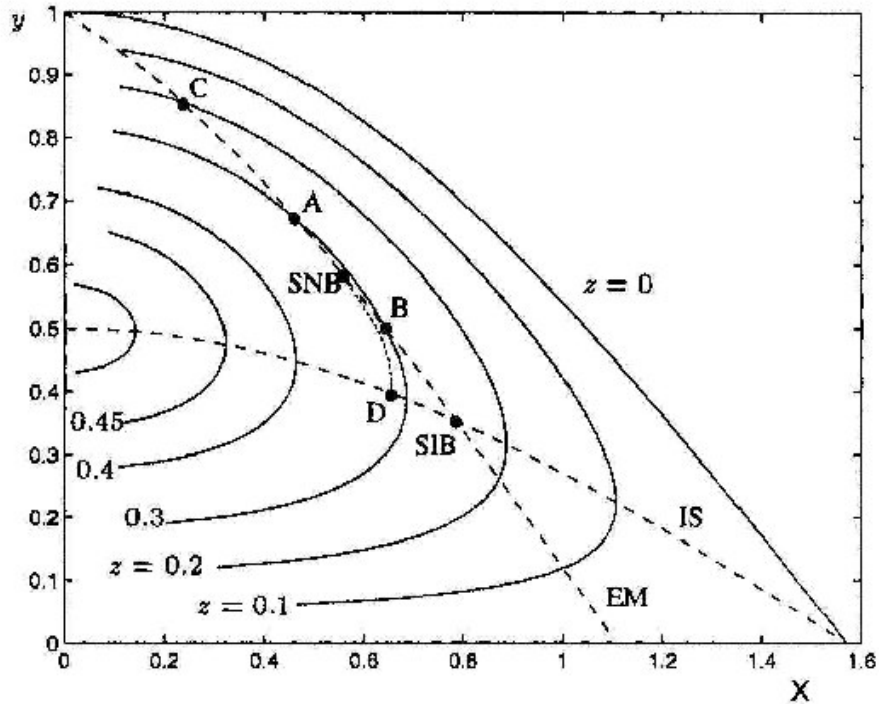

Figure A2.10 -Singularity Induced Bifurcation [4]

The three dimensional state and parameter space is shown with the z-axis perpendicular to the x-y plane, ie. the z-axis is perpendicular to the plane of the paper. Equation (A2.49b) defines the 2-dimensional constraint manifold and is represented by the contours in solid lines for different values of z. The impasse surface, a 1-dimensional curve in this case, is defined by the equation (A2.49b) and the singularity condition given by:

$$g_y = \frac{\partial g}{\partial y} = -2y + \cos x = 0 \qquad \text{(A2.50)}$$

It is shown marked IS on Figure A2.10 and lies on the 2-D constraint manifold. The constraint manifold is divided into two causality regions by the impasse surface. The equilibrium manifold is defined by the equation (A2.49b) and the equation:

$$z - y\sin\theta = 0 \qquad \text{(A2.51)}$$

If z is eliminated from equations (A2.49b) and (A2.51), the following equation is obtained.

$$y = \cos x - 0.5\sin x \qquad \text{(A2.52)}$$

Using equations (A2.51) and (A2.52) the equilibrium manifold, a 1-dimensional curve in this case, is drawn as shown in fig. A2.10 and marked EM. This too lies on the 2-dimensional constraint manifold. If the equations for the constraint manifold (A2.49b), the impasse curve (A2.50) and the equilibrium manifold (A2.51) are solved simultaneously, the point of intersection of the impasse curve (IS) and the equilibrium manifold (EM) on the constraint manifold is obtained and is shown as SIB. This is a singularity induced bifurcation and its coordinates are $(x = \pi/4, y = \sqrt{2}/4, z = 0.25)$. The point (0, 1, 0), where the parameter z = 0, lies on the equilibrium manifold and therefore is an equilibrium point. It is also a stable equilibrium. Now if the parameter z is slowly increased, the equilibrium point moves

slowly uphill along the equilibrium manifold EM till it reaches the point SNB. For any further increase of z there is no equilibrium and the point SNB is a saddle-node bifurcation, a point at which a stable equilibrium such as the point A coalesces with an unstable equilibrium such as the point B. Once this SNB is reached, the trajectory will depart from equilibrium along the unstable manifold of the SNB till it reaches the algebraic singularity point D, which lies on the impasse surface IS and is not an equilibrium.

A2.7 Multiple Time Scale Systems of Differential Equations.

Some systems, including power systems, have dynamics evolving in different time scales. That is these systems have dynamics evolving in slow and fast time scales. Such systems are represented as follows.

$$\dot{x} = f(x, y) \tag{2.6a}$$

$$\varepsilon \dot{y} = g(x, y) \tag{2.6b}$$

Where x is a vector of slow states, y is a vector of fast states and ε is a small number.

In singular perturbation or time scale decomposition, the method used to study such systems, it is assumed that $\varepsilon \to 0$. Then the system reduces to a differential algebraic system as follows.

$$\dot{x}_s = f(x_s, y_s) \tag{2.6c}$$

$$0 = g(x_s, y_s) \tag{2.6d}$$

This system contains only slow state variables and can be studied by the methods used for differential algebraic systems. It is assumed in the analysis that the fast dynamics are stable and that they have died out.

Appendix 3

Appendix 3 in accompanying CD.

Appendix 4

PUBLISHED PAPERS

1. Transactions IEEE Pakistan – Accepted for Publication

VOLTAGE INSTABILITY IN POWER SYSTEMS, ITS ANALYSIS AND PREDICTION USING ARTIFICIAL INTELLIGENCE METHODS

K. J. T. N. Fernando* and A. Kalam*

*Faculty of Health, Engineering and Science
Victoria University of Technology
Footscray, Victoria, Australia.

Abstract:

Before the restructuring of the electricity industry adequate redundancy was built into power systems for voltage instability to be a major problem. Only rotor angle stability was considered in the operation and expansion of power systems. With the introduction of the new electricity market resulting in reduced investment and altered load patterns, particularly increasing load in areas with weak transmission and generation capacity, voltage stability has come into prominence. Unlike rotor angle stability, voltage stability requires mathematical theory and concepts that are difficult and not normally covered in undergraduate electrical engineering courses. This paper explains the theory of voltage instability and methods used to analyse the problem and proposes artificial intelligence methods for its prediction in power systems.

1. Introduction.

A major outage in North America on 14th August 2003 causing major blackouts in Midwest and Northeast United States and Ontario, Canada has been at least partially due to voltage collapse according to the US-Canada Power System Outage Task Force Report [13]. A recent outage due to voltage instability has also been reported in Sri Lanka [14]. References [15, 16] describe the application of voltage stability theory to analyze the South-Brazilian and Ecuadorian Power Systems and how the results thus obtained agreed with operational experience where voltage collapse has been experienced before.

Thus voltage stability is not merely a theoretical construct but reality for which there was no urgency till recent times when power systems became more and more stressed. Therefore as power systems become more complex as well as operate in more stressed states, in addition to presently used security assessment methods, methods for voltage security assessment are also needed.

Theories to explain and analyze voltage stability are now being developed. [1]. Voltage instability results in voltages in parts of the system or the entire system becoming unstable or collapsing altogether causing collapse of the power system. It is different to low voltages experienced in certain parts of the network during certain conditions, when, though some voltages are low, the system is operating at a stable point.

Mathematics of dynamical systems that studies such concepts as dynamics of and bifurcations in dynamical systems and singular perturbation, [2-10], is used in the study of voltage stability. Computer programs are now available for solution and visualization of solutions. [11] and Matlab. There is also a voltage stability specific computer program called UWPFLOW that solves voltage stability specific problems.[12]. Extensive use of this program was made in the research for this paper along with Phaser.[11].

2 Some Useful Definitions.

The following two definitions of stability of a power system are given in [17].

1. *An operating point of a power system is small disturbance stable if, following any small disturbance, the power system state returns to be identical or close to the pre-disturbance operating point.*

2. *An equilibrium of a power system model is asymptotically stable if, following any small disturbance, the power system state tends to the equilibrium.*

The second definition assumes that the power system is modelled by, a set of differential equations.

Voltage instability is defined in [1] as follows.

Voltage instability stems from the attempt of load dynamics to restore power consumption beyond the capacity of the combined transmission and generation system.

3 Voltage Instability

A power system operating under stable conditions keeps continuously evolving. During this process some or all of the following take place in the system. The load changes; generators and induction motors go through electromechanical transients; static VAR compensators, (SVCs), activate; on load tap changers in transformers activate; shunt capacitors are switched on and off; automatic load recovery takes place following faults; faulted components of the power system are isolated; faulted transmission and distribution lines auto-reclose; excitation limiters activate etc. Thus a power system under load is a dynamical system. During this dynamics, if the power system is to remain stable, the operating point or the equilibrium point of the system has to track a stable point in state space. However the transmission system has a limited capacity for power transmission and generators have a limited generating capacity, on reaching these limits the system can go into voltage instability. At the point of going into voltage instability, the stable point of operation that existed before disappears. Thus the power system undergoes a transient and during this transient, the voltages decline monotonically causing a voltage collapse. It is to be noted that the state of a power system operating with low voltages but at a stable point, (i.e. there is no dynamic collapse of the voltages), does not constitute a voltage stability problem.

4. The dynamics of a loaded power system.

The dynamics of a loaded power system can be represented by a system of non-linear ordinary differential equations, which can be written as:

$\dot{x} = f(x)$.

Where $\dot{x} = \frac{dx}{dt}$, t is time and x is a (nx1) vector.

The vector x represents the state of the system at a given time and is known as the state vector. Systems of this type are known as dynamical systems.

Such dynamical systems can be solved analytically only in a very limited number of cases, however given initial conditions for the state variables, the equations can be solved by numerical integration. The geometric theory of ordinary differential equations allows the study of the behaviour of dynamical systems without resort to integration.

5. Evaluation of a power system for voltage stability.

There are a few computer programs available for the evaluation of voltage stability. Typically they perform continuation power flows, see [17], using detailed steady state models of the various power system elements. Because of their ability to model the power system elements in detail they can be used to determine the progression of steady state points as system conditions change. Thus for example a voltage sensitive load can be modelled as the system conditions change and successive power flows performed.

The authors used the UWPFLOW program to perform continuation power flow studies on the IEEE 14 bus test system (see Fig. 1) to obtain the point of (system) collapse loading, the power system nose curves related to voltage collapse and sufficient loading points during the continuation power flow study to train artificial neural networks (ANN"S).

There is a number of voltage stability indices used to measure proximity to voltage collapse, [17]. In the research presented in this paper the additional amount of load that could be utilised, at each point during the continuation power flow, before voltage collapse, known as the **loading margin** is utilised.

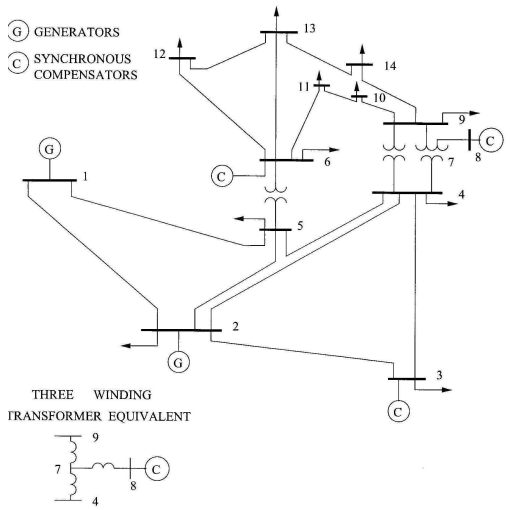

Fig. 1 IEEE 14 Bus Test System

The data for the system shown in IEEE data format is shown in Table 1.

IEEE 14 Bus Test System Bus Data

1	Bus 1	1	HV	1	1	3	1	0	0	0	0	0	0	1.06	100	-100	0	0 0
2	Bus 2	2	HV	1	1	2	1.045	0	21.7	12.7	40	0	0	1.045	50	-40	0	0 0
3	Bus 3	3	HV	1	1	2	1.01	0	94.2	19	0	0	0	1.01	40	0	0	0 0
4	Bus 4	4	HV	1	1	0	1	0	47.8	-3.9	0	0	0	0	0	0	0	0 0
5	Bus 5	5	HV	1	1	0	1	0	7.6	1.6	0	0	0	0	0	0	0	0 0
6	Bus 6	6	LV	1	1	2	1.07	0	11.2	7.5	0	0	0	1.07	24	-6	0	0 0
7	Bus 7	7	ZV	1	1	0	1	0	0	0	0	0	0	0	0	0	0	0 0
8	Bus 8	8	TV	1	1	2	1.09	0	0	0	0	0	0	1.09	24	-6	0	0 0
9	Bus 9	9	LV	1	1	0	1	0	29.5	16.6	0	0	0	0	0	0	0	0.19 0
10	Bus 10	10	LV	1	1	0	1	0	9	5.8	0	0	0	0	0	0	0	0 0
11	Bus 11	11	LV	1	1	0	1	0	3.5	1.8	0	0	0	0	0	0	0	0 0
12	Bus 12	12	LV	1	1	0	1	0	6.1	1.6	0	0	0	0	0	0	0	0 0
13	Bus 13	13	LV	1	1	0	1	0	13.5	5.8	0	0	0	0	0	0	0	0 0
14	Bus 14	14	LV	1	1	0	1	0	14.9	5	0	0	0	0	0	0	0	0 0

IEEE 14 Bus Test System Branch Data

1	2	1	1	1	0	0.01938	0.05917	0.0528	0	0	0	0	0	0	0	0	0	0 0 0
1	5	1	1	1	0	0.05403	0.22304	0.0492	0	0	0	0	0	0	0	0	0	0 0 0
2	3	1	1	1	0	0.04699	0.19797	0.0438	0	0	0	0	0	0	0	0	0	0 0 0
2	4	1	1	1	0	0.05811	0.17632	0.034	0	0	0	0	0	0	0	0	0	0 0 0
2	5	1	1	1	0	0.05695	0.17388	0.0346	0	0	0	0	0	0	0	0	0	0 0 0
3	4	1	1	1	0	0.06701	0.17103	0.0128	0	0	0	0	0	0	0	0	0	0 0 0
4	5	1	1	1	0	0.01335	0.04211	0	0	0	0	0	0	0	0	0	0	0 0 0
4	7	1	1	1	0	0	0.20912	0	0	0	0	0	0	0.978	0	0	0	0 0 0
4	9	1	1	1	0	0	0.55618	0	0	0	0	0	0	0.969	0	0	0	0 0 0
5	6	1	1	1	0	0	0.25202	0	0	0	0	0	0	0.932	0	0	0	0 0 0
6	11	1	1	1	0	0.09498	0.1989	0	0	0	0	0	0	0	0	0	0	0 0 0
6	12	1	1	1	0	0.12291	0.25581	0	0	0	0	0	0	0	0	0	0	0 0 0
6	13	1	1	1	0	0.06615	0.13027	0	0	0	0	0	0	0	0	0	0	0 0 0
7	8	1	1	1	0	0	0.17615	0	0	0	0	0	0	0	0	0	0	0 0 0
7	9	1	1	1	0	0	0.11001	0	0	0	0	0	0	0	0	0	0	0 0 0
9	10	1	1	1	0	0.03181	0.0845	0	0	0	0	0	0	0	0	0	0	0 0 0
9	14	1	1	1	0	0.12711	0.27038	0	0	0	0	0	0	0	0	0	0	0 0 0
10	11	1	1	1	0	0.08205	0.19207	0	0	0	0	0	0	0	0	0	0	0 0 0
12	13	1	1	1	0	0.22092	0.19988	0	0	0	0	0	0	0	0	0	0	0 0 0
13	14	1	1	1	0	0.17093	0.34802	0	0	0	0	0	0	0	0	0	0	0 0 0

Table 1 IEEE 14 Bus Data in IEEE Data Format

Each branch in the 14 bus system was treated as a double circuit line and the following contingencies were chosen in addition to the full system. In each case after the base case power flow analysis a continuation power flow analysis with progressive small increases in load was performed. Thus a large number of operating points for a number of possible operating conditions of the power system are obtained.

1. One circuit, buses 1 to 2, out.
2. One circuit, buses 1 to 5, out.
3. One circuit, buses 6 to 11, out.
4. One circuit, buses 6 to 12, out.
5. One circuit, buses 10 to 11, out.
6. One circuit, buses 12 to 13, out.
7. One circuit, buses 13 to 14, out.

The nose curves for the most affected buses, 6, 7, 9 & 11, during the continuation power flow for the full system drawn using 220 points on the curve are shown in Fig. 2. Similar curves were obtained for other operating conditions or contingencies.

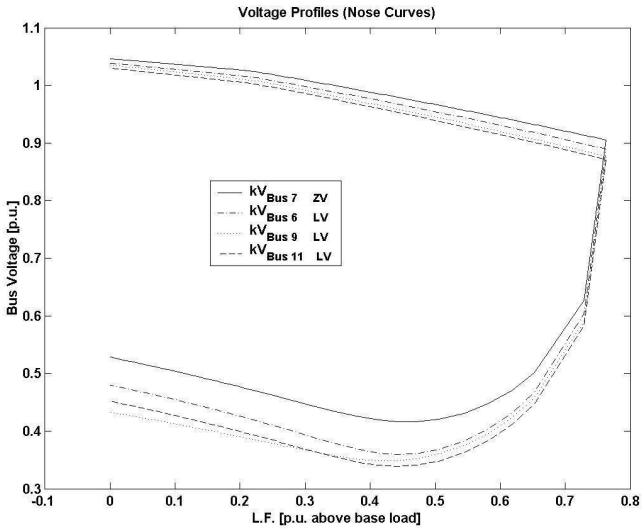

Figure 2 Nose Curves for the Full 14 Bus System

For each of the eight cases, including the case of all circuits connected, the loading margin was calculated at each loading point up to the voltage collapse point which is the nose of the curve. These points were divided into adjacent groups of three, the first group being the set of points furthest from voltage collapse. For the purpose of training ANN's, each point in each group was assigned a vector that indicates the severity of loading of the power system as follows.

$[1\ 0\ 0]^T$ The system is safe from voltage collapse.
$[0\ 1\ 0]^T$ Caution needed during further loading.
$[0\ 0\ 1]^T$ Extreme caution needed, system approaching voltage collapse.

Altogether 1390 load points were obtained from all the continuation power flow simulations together with the bus voltages for the weakest buses. The P & Q loads and voltages of the seven weakest buses namely buses 6, 9, 10, 11, 12, 13 & 14 were chosen as the training inputs of the ANN's. Thus each ANN has 21 inputs.

6. Artificial Neural Network Training.

After a study of artificial neural networks, [18, 19, 20], **Multilayer Perceptrons** that use backpropagation were chosen as the most suitable. Networks of different architectures using different learning functions, as explained below, were trained and evaluated for suitability. The Matlab Neural Network Toolbox was used for the training.

6.1. ANN Architectures Selected.

The notation, R-S1-S2-S3….., where R is the number of inputs and S1, S2 etc are the number of neurons in layer 1, layer 2 etc is used to represent the structure of each network. The following architectures were tested for suitability. For definitions of training functions, learning functions, transfer functions and the term epochs etc please see [18, 21].

1. 21-25-3 with Trainlm training function and Learngdm learning function, layer 1 Logsig transfer function, layer 2 Purelin transfer function trained for 1000 epochs.
2. As above but with layer 1 Tansig transfer function, layer 2 Purelin transfer function.
3. As in 1 but with layer 1 Tansig, layer 2 Tansig.

4. As in 1 but with layer 1 Tansig, layer 2 Purelin and training function Traincgf.
5. 21-30-3 layer 1 Tansig, layer 2 Purelin and the rest as in 1.
6. 21-35-3 rest as in 5.
7. 21-25-3 using automated regularisation {21] with the training function Trainbr. Layer 1 Tansig transfer function, layer 2 Purelin transfer function. For this method the training set and the target set need to be preprocessed and the results postprocessed [21].
8. 21-50-3. The rest same as in 7.
9. 21-25-25-3. The rest same as in 7 and with the additional layer also with Tansig transfer function.

7. Results.

Analysis of the results by simulating the trained networks using sets of results from the various continuation power flows and comparing them with the expected targets shows that the network architecture represented in 9 above gives the best results and therefore is the most suitable. 3-D graphs generated in Matlab for visualisation of the errors is shown for two of the above networks including network 9 are shown below.

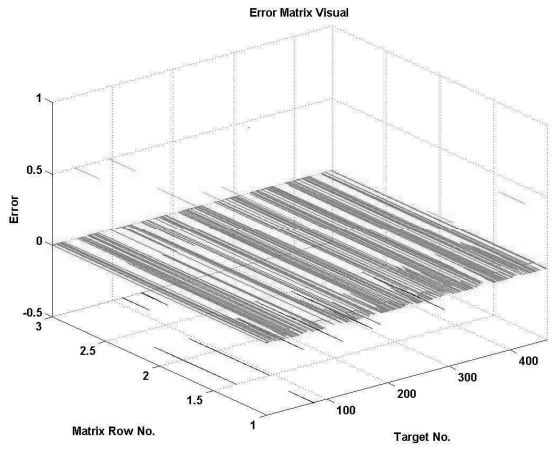

Figure 3 Error Visualisation for the ANN Architecture 3

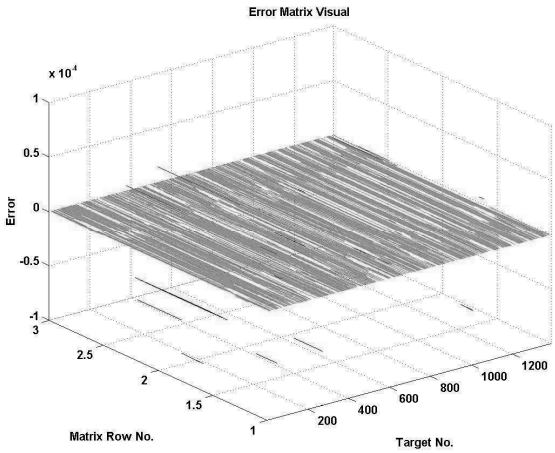

Figure 4 Error Visualisation for the ANN Architecture 9

Figure 3 shows a number of errors of the order of less than 1.0 for a number of outputs while the number of error in Figure 3 for the architecture 9 is much less and only of the order of less than 0.0001.

8. Conclusion.

Therefore it is concluded that an Artificial Neural Network of the architecture represented as 9 in paragraph 6.1 is very suitable for the prediction of pending voltage instability in a power system. A number of such networks need to be trained to take into account seasonal changes in load patterns. It would be possible for such a network to be embedded in dedicated hardware. Inputs such as the values of voltages and loads at weak buses can then be fed directly into this hardware utilising an existing SCADA system at suitable intervals of time. The output of the ANN would be an indication of voltage stability of the system for the system operator.

9. References.

[1]T. Van Cutsem and C. Vournas, Voltage Stability of Electric Power Systems. Boston: Kluwer Academic Publishers, 2001.

[2]W. E. Boyce and R. C. DePrima, Elementary Differential Equations and Boundary Value Problems. New York: John Wiley & Sons Inc., 1992

[3]J. Cronin and R. E. O'Malley, "Analysing Multiscale Phenomena Using Singular Perturbation Methods," in Proceedings of Symposia in Applied Mathematics, vol. 56. Providence, Rhode Island: American Mathematical Society, 1998.

[4]J. K. Hale and H. Kocak, Dynamics and Bifurcations. New York: Springer-Verlag, 1991.

[5]J. Kevorkian and J. D. Cole, Perturbation Methods in Applied Mathematics. New York: Springer-Verlag, 1985.

[6]J. Kevorkian and J. D. Cole, Multiple Scale and Singular Perturbation Methods, vol. 114. New York: Springer, 1996.

[7]P. V. Kokotovic, H. K. Khalil, and J. O'Reilly, Singular Perturbation Methods in Control: Analysis and Design. New York: Academic Press Harcourt Brace Jovanovich, Publishers, 1986.

[8]R. E. O'Malley, Introduction to Singular Perturbations. New York: Academic Press, 1974.

[9]I. Percival and D. Richards, Introduction to Dynamics. Cambridge, London, New York: Cambridge University Press, 1982.

[10]A. L. Rabenstein, Introduction to Ordinary Differential Equations. New York: Academic Press, 1972.

[11]H. Kocak, et. al., "Phaser." USA: WWW. Phaser.com, pp. A Universal Simulator for Dynamical Syatems.

[12]C. Canizares, "UWPFLOW." Waterloo: Canizares, Claudio, pp. Solves voltage stability problems.

[13]U.-C. P. S. O. T. Force, "Final Report on the August 14, 2003 Blackout in the United States and Canada: Causes and Recommendations," 2004.

[14]N. Mithulananthan and S. C. Srivastava, "Investigation of a Voltage Collapse Incident in Sri Lanka's Power System," presented at EMPD'98, Singapore, 1998.

[15]A. A. P. Lerm, C. Canizares, and A. S. e Silva, "Multi-parameter Bifurcation Analysis of the South-Brazilian Power System," IEEE Transactions in Power Systems, 2002.

[16]C. Canizares, "On Bifurcations, Voltage Collapse and Load Modeling," IEEE Transactions in Power Systems, vol. 10, pp. 512-522, 1995.

[17]C. Canizares, "Voltage Stability Assessment: Concepts, Practices and Tools," IEEE/PES, 2003.

[18]M. T. Hagan, H. B. Demuth, M. Beale, "Neural Network Design," Asia: Thomson, Undated.

[19]F. M. Ham, I. Kostanic, "Principles of Neurocomputing for Science & Engineering," Boston: McGraw Hill, 2001.
[20]K. Warwick, A. Ekwue, R. Aggarwal, "Artificial Intelligence Techniques in Power Systems," London: IEE, 1997.
[21]H. Demuth, M. Beale, "Neural Network Toolbox," USA: The Mathworks Inc., 2001.

2. Australian Universities Power Engineering Conference 2006 – Published

MATHEMATICS OF VOLTAGE INSTABILITY IN POWER SYSTEMS

K. J. T. N. Fernando* and A. Kalam*

*Faculty of Health, Engineering and Science
Victoria University of Technology
Footscray, Victoria, Australia.

Abstract:

Before the restructuring of the electricity industry adequate redundancy was built into power systems for voltage instability to be a major problem. Only rotor angle stability was considered in the operation and expansion of power systems. With the introduction of the new electricity market resulting in reduced investment and altered load patterns, particularly increasing load in areas with weak transmission and generation capacity, voltage stability has come into prominence. Unlike rotor angle stability, voltage stability requires mathematical theory and concepts that are difficult and not normally covered in undergraduate electrical engineering courses. This paper is an exposition of this mathematics.

1. INTRODUCTION

1.1 Some Useful Definitions.

Voltage stability is defined in [1] as follows.

An operating point of a power system is small disturbance stable if, following any small disturbance, the power system state returns to be identical or close to the pre-disturbance operating point.
An equilibrium of a power system model is asymptotically stable if, following any small disturbance, the power system state tends to the equilibrium.

It is defined in [2] as follows.

Voltage instability stems from the attempt of load dynamics to restore power consumption beyond the capacity of the combined transmission and generation system.

1.2 Voltage Instability.

A power system operating under stable conditions keeps continuously evolving. The load changes; generators and induction motors go through electromechanical transients; static VAR compensators, (SVCs), activate etc. Thus a power system under load is a dynamical system. During this dynamics, the operating point or the equilibrium point of the system has to track a stable point in state space. However the transmission system has a limited capability and on reaching this limit, the system can go into voltage instability. At the point of going into voltage instability, the stable point of operation that existed before disappears. A power system operating with low voltages but at a stable point does not constitute a voltage stability problem.

The following example taken from [1] but solved in greater detail is an elementary example of how voltage instability takes place.

1.3 Voltage Instability in an Elementary DC Power System.

Consider a simple DC power system fed by a DC power source of 1V. The line resistance is 0.5Ω, the load is a variable resistor and I is the current drawn by the load.

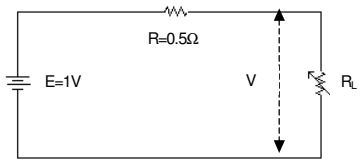

Fig. 1.1 An Elementary DC Power System.

The load resistance R_L is automatically varied to achieve an assumed maximum power demand of 0.55W according to the differential equation:

$$\dot{R}_L = I^2 R_L - 0.55 \quad (1.1)$$

According to elementary circuit theory, the maximum transferable power P_{max} is given by:

$$P_{\max} = \frac{E^2}{4R} = 0.5W \quad (1.2)$$

However in this example the maximum power demand is 0.55W.

The trajectory of the load resistance given by the solution of the differential equation (1.1) with an initial condition of $R_L = 4.5\Omega$ is shown in figure 1.2.

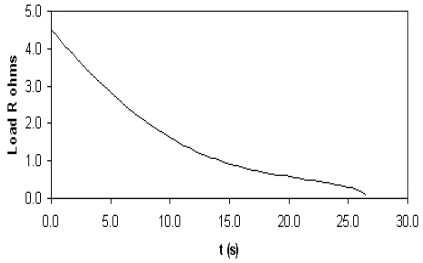

Fig.1.2 Trajectory of the Load Resistance.

The variations of the load voltage and load power are shown in figures1.3 & 1.4.

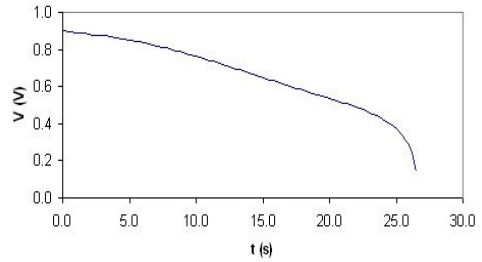

Fig. 1.3 Variation of Load Voltage.

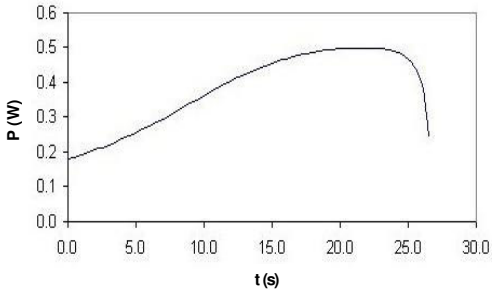

Fig.1.4 Variation of Load Power

It is seen from figures 1.3 & 1.4 that voltage instability or collapse takes place when the demand for power increases beyond the maximum deliverable power of 0.5 W.

The dynamics of a loaded power system can be represented by a system of non-linear ordinary differential equations, which can be written as:

$$\dot{x} = f(x) \qquad (1.3) \qquad (1.3)$$

Where usually $\dot{x} = \frac{dx}{dt}$ where t is time, x is a $(n \times 1)$ vector and $f_i, (i = 1, 2, ...n)$ are generally non-linear functions of $x_i, (i = 1, 2, ...n)$. The vector x represents the state of the system at a given time and is known as the state vector. Systems of this type are known as dynamical systems.

Such dynamical systems can be solved analytically only in a very limited number of cases, however given initial conditions for the state variables, the equations can be solved by numerical integration. The geometric theory of ordinary differential equations allows the study of the behaviour of dynamical systems without resort to integration.

2. SCALAR AUTONOMOUS DIFFERENTIAL EQUATIONS

Many of the concepts of the geometry of solutions of ordinary differential equations can be understood by a study of scalar autonomous differential equations.

Consider an equation of the form (1.3):

$$\dot{x} = f(x) \qquad (2.1) \qquad (2.1)$$

This equation is scalar if x is one dimensional and autonomous if $f(x)$ is independent of t.

2.1 Solution of Scalar Autonomous Differential Equations.

When solving an equation of the type (2.1), often the interest is in a specific solution that passes through an initial value x_0 at time t_0. Such a problem is called an initial value problem. Therefore the initial value problem may be expressed as:

$$\dot{x} = f(x), \qquad x(t_0) = x_0 \tag{2.2}$$

But in many cases it is impossible to perform the required integration though numerical integration using a computer program can give a solution. However the interest in most cases is in the qualitative behaviour of dynamical systems and this can be studied by geometrical methods.

Example 2.1

Consider the following initial value problem.

$$\dot{x} = x^2, \qquad x(0) = x_0 \tag{2.3}$$

The solution is:

$$x(t) = \frac{x_0}{1 - x_0 t}$$

On examination of this solution certain conclusions can be drawn regarding the behaviour of $x(t)$, see [2]. For $x_0 > 0$, the solution is valid or defined only on the interval $\left(-\infty, \frac{1}{x_0}\right)$; for $x_0 = 0$, the solution is defined on the interval $(-\infty, +\infty)$ and for $x_0 < 0$, the solution is defined only on the interval $\left(\frac{1}{x_0}, +\infty\right)$. Trajectories of the solution of the equation (2.3) for the initial values $x_0 = -1.5, -1.0, -0.5, 0.0, 0.5, 1.0 \,\&\, 1.5$ are shown in Fig. 2.1.

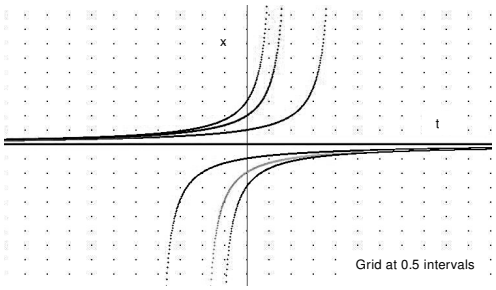

Fig. 2.1 Trajectories of $\dot{x} = x^2$

It is now evident that a solution to an initial value problem has an interval of validity of its solution. This interval is called the maximal interval of existence and may be infinite in some cases. It is usually represented as $I_{x_0} \equiv (\alpha_{x_0}, \beta_{x_0})$ where $\alpha_{x_0} < t < \beta_{x_0}$.

Sometimes it is convenient to represent the solution $x(t)$ to the initial value problem of equation (2.1) as $\varphi(t, x_0)$.

The following theorem, called the theorem of existence and uniqueness of solutions, given without proof, establishes the conditions for the existence and uniqueness of solutions to initial value problems.

Theorem 2.1 The Theorem of Existence and Uniqueness of Solutions.

If $f(x)$ is continuous in the domain U, a sub set of the domain of real numbers R, then there exists a solution $\varphi(t, x_0)$ for all x_0 in U with a maximal interval of existence of $I_{x_0} \equiv (\alpha_{x_0}, \beta_{x_0})$ dependent on x_0.

If in addition to the above, the first derivative of $f(x)$ is continuous in U, then the solution $\varphi(t, x_0)$ is unique in I_{x_0}.

2.2 The Direction Fields, Vector Fields, Orbits and Phase Portraits of Differential Equations.

The geometry of the flow of a differential equation can be studied by a study of its direction field, vector field and phase portraits.

The right hand side of equation (2.1) gives the slope of the trajectory of its solution in the (t, x)-plane at any given point. Figure 2.2 below shows a collection of line segments representing the slope at different points on the (t, x)-plane for $\dot{x} = -x$. The collection of such line segments is called the direction field, see [3]. The direction field is always tangential to the given trajectory.

Now since $f(x)$ is independent of x, along every line parallel to the t-axis on the (t, x)-plane, the direction field has the same slope. If this slope is projected on to the x-axis with its direction indicated, the vector field or the velocity field is obtained. See Fig. 2.2.

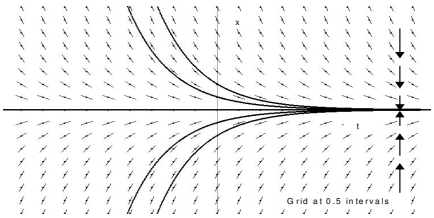

Fig. 2.2 Direction Field and Vector Field of $\dot{x} = -x$.

The orbit $\gamma(x_0)$ of the trajectory of a differential equation passing through the initial condition x_0 is the projection of that trajectory between $t = \alpha_{x_0}$ and $t = \beta_{x_0}$ on to the x-axis.

The positive orbit $\gamma^+(x_0)$ of the trajectory of a differential equation is the projection of that trajectory between $t = 0$ and $t = \beta_{x_0}$ on to the x-axis.

The negative orbit $\gamma^-(x_0)$ of the trajectory of a differential equation is the projection of that trajectory between $t = \alpha_{x_0}$ and $t = 0$ on to the x-axis.

The Fig. 2.3 shows the orbits for $\dot{x} = -x$ passing through a positive initial value.

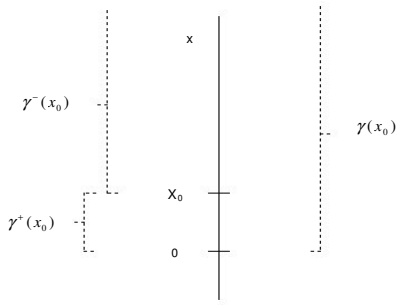

Fig. 2.3 Orbits Through x_0 of $\dot{x} = -x$.

On the orbit $\gamma(x_0)$, arrows can be inserted to indicate the direction in which its solution $\varphi(t, x_0)$ is changing as time t increases. The collection of all the orbits together with the arrows gives the phase portrait of the differential equation. See Fig. 2.4.

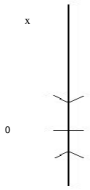

Fig. 2.4 Phase Portrait of $\dot{x} = -x$

2.3 Equilibrium Points of Scalar Autonomous Differential Equations.

An equilibrium point also known as a critical point, usually represented by $\overline{x}$, of a differential equation occurs at a point where $f(x) = 0$. A system on reaching a critical point stays at that point for all time. However any given equilibrium point may or may not be stable.

2.4 Methods of Drawing the Orbits and Phase portraits of Differential Equations. (See [3]).

The graph of x Vs $f(x)$ gives an easy method of drawing the orbits with the direction of motion and therefore the phase portrait of a differential equation. When $f(x) > 0$, the solution increases in t and therefore approaches an equilibrium point or $+\infty$ as $t \to \beta_{x_0}$. When $f(x) < 0$, the solution decreases in t and therefore approaches an equilibrium point or $-\infty$ as $t \to \beta_{x_0}$.

In the second method the potential function, $F(x)$ of equation (2.1) is defined as follows.

$\dot{x} = f(x) = -\dfrac{d}{d(x)} F(x)$. Therefore,

$$F(x) = -\int_0^x f(s)ds\,.$$

Now if a graph of the potential function $F(x)$ is drawn, its extreme points, that is, its maxima and minima, will be the equilibrium points.. If a particle is imagined to travel freely along this graph, the likely direction in which it travels will give the phase portrait.

Following figures illustrates the two methods.

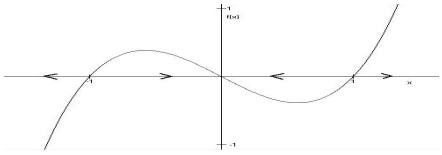

Fig. 2.5a Phase Portrait of $\dot{x} = -x + x^3$ Using the Function $f(x) = -x + x^3$.

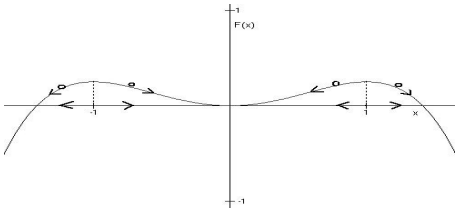

Fig. 2.5b Phase Portrait of $\dot{x} = -x + x^3$ Using the Potential Function $F(x) = x^2/2 - x^4/4$.

On examination of the above graphs certain conclusions can be drawn on the behaviour of the differential equation.

The differential equation has equilibrium points at $x = -1, 0 \& +1$. The equilibrium point at $x = 0$ is stable. The equilibrium points at $x = -1 \& +1$ are unstable.

2.5 Stability of Equilibrium Points.

An equilibrium point $\overline{x}$ is stable if all solutions to the differential equation starting near $\overline{x}$ stay near to it. An equilibrium point is asymptotically stable if all solutions near $\overline{x}$ tend to $\overline{x}$ as $t \to \infty$.

Theorem 2.2

If $\overline{x}$ is an equilibrium point of $\dot{x} = f(x)$ and $f'(x)$ exists, that is, $f(x)$ is differentiable, then, $\overline{x}$ is asymptotically stable if $f'(\overline{x}) < 0$ and unstable if $f'(\overline{x}) > 0$.

When $f'(\overline{x}) \neq 0$, the equilibrium point is called a hyperbolic equilibrium point and when $f'(\overline{x}) = 0$, the equilibrium is called a nonhyperbolic point.

2.6 Bifurcations in Differential Equations.

Bifurcation of its differential equations is a very important aspect of voltage instability in power systems. The behaviour of these differential equations represents the behaviour of the power system.

Consider the behaviour of the following differential equation.

$$\dot{x} = c + x^2 = F(c, x) \qquad (2.3)$$

Where c is a real number variable parameter. The graph of this equation for c=0, passes through the origin (0, 0) which is an equilibrium point. When other values are assigned to c, the resultant graph is similar to the graph with c=0, but with the x-axis shifted vertically by –c. See Fig. 2.6.

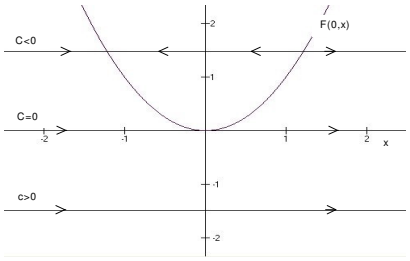

Fig. 2.6 Phase Portraits of $\dot{x} = c + x^2$ for different values of c.

Using method 1 of 2.4, the phase portrait of equation (2.3) can be drawn for different values of c as shown. For $c < 0$, there are two equilibrium points, for $c > 0$, there are no equilibrium points and for $c = 0$, there is one equilibrium point, the origin. Now for small variations of c around 0, the number of equilibrium points change suddenly. Such a value of the parameter is called a bifurcation value, the equation being at a bifurcation point causing a saddle node bifurcation.

3. SECOND ORDER AUTONOMOUS DIFFERENTIAL EQUATIONS. (See [3]).

3.1 Linear Harmonic Oscillator.

Consider the linear harmonic oscillator represented by the following equation.

$$\dot{x}_1 = x_2 \qquad (3.1)$$
$$\dot{x}_2 = -x_1$$

The vector field and the phase portraits of this equation for initial values (x_1, x_2) = (1.0, 1.0), (0.75, 0.75), (0.5, 0.5) are as shown in Fig. 3.1.

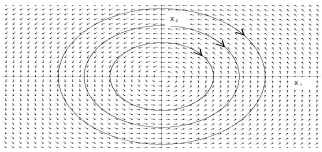

Fig. 3.1 Vector Field and Phase Portraits of Linear Harmonic Oscillator.

The equation has an equilibrium point at (0, 0) and the orbits for nearby initial conditions are circular orbits round this equilibrium point. Such an equilibrium point is stable but not asymptotically stable and is called a center.

3.2 Van der Pol Oscillator.

Consider the Van der Pol oscillator represented by the following equation.

$$\dot{x}_1 = x_2 \qquad (3.2)$$
$$\dot{x}_2 = (1.0 - x_1^2)x_2 - x_1$$

The phase portraits of this equation for initial values (x_1, x_2) = (-0.1, 0.1), (-2.0, 2.0), (2.0, -2.0) are as shown in Fig. 3.2.

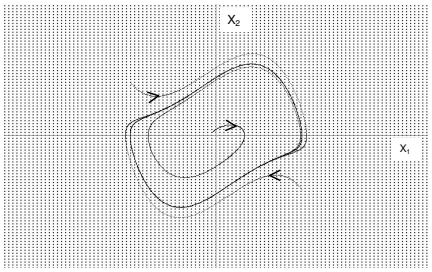

Fig. 3.2 Phase Portraits of Van der Pol Oscillator.

It is seen that this equation has an isolated periodic solution called a limit cycle. All trajectories starting at any initial condition approach this limit cycle.

3.3 Linear Product System.

Consider the linear product system represented by the following equation.

$$\dot{x}_1 = ax_1 \qquad (3.3)$$
$$\dot{x}_2 = bx_2$$

The phase portraits for b<a<0, b=a<0 and a<0<b are shown in Figs. 3.3a,b &c.

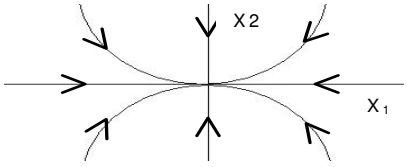

(a) b<a<0

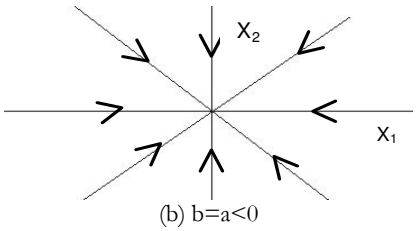

(b) b=a<0

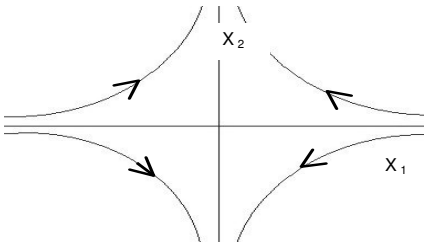

(c) a<0<b

Fig. 3.3 Phase Portraits of the Linear Product System

It is seen that for b<a<0, both $x_1(t)$ and $x_2(t) \rightarrow 0$ exponentially as $t \rightarrow \infty$. For b=a<0, they tend to 0 along straight lines. Therefore the equilibrium point is called a stable node. For a<0<b, the origin is still an equilibrium point but all orbits other than the point orbit at the origin leave the origin as shown in Fig. 3.3c. Such an equilibrium point is called a saddle.

In a power system often the state varies as parameters vary. This variation in parameters can cause voltage collapse. A very simple case is a product system where λ is the parameter:

$$\dot{x}_1 = \lambda + x_1^2 \qquad (3.4)$$
$$\dot{x}_2 = -x_2$$

For such a system it can be shown that for $\lambda < 0$, there are two equilibriums, one a node and the other a saddle. As λ is varied and reaches 0, the equilibriums coalesce. As λ is further increased making $\lambda > 0$, the equilibrium disappears. Such a bifurcation is called a saddle node bifurcation.

3.4 Hopf Bifurcation.

Consider the single parameter system below.

$$\dot{x}_1 = x_2 + x_1(\lambda - x_1^2 - x_2^2) \qquad (3.5)$$
$$\dot{x}_2 = -x_1 + x_2(\lambda - x_1^2 - x_2^2)$$

It can be shown by drawing the phase portraits, that in such a system, when $\lambda \leq 0$, all solutions spiral in to the origin as $t \rightarrow \infty$ and when $\lambda > 0$ all solutions spiral in to a periodic orbit, that is a limit cycle. Such a bifurcation is called a Hopf bifurcation.

4. STABILITY IN SYSTEMS OF NON-LINEAR DIFFERENTIAL EQUATIONS

In the analysis of power systems to determine voltage stability one comes across more complicated systems of non-linear differential equations. Following rules, given without proof, can be used to determine their stability. See [2], [4] and [5].

Consider the dynamical system represented by the equation (1.3). Let $\bar{x}$ be an equilibrium point. Then the Jacobian A of $f(x)$, which is a matrix, is defined as follows.

$$A = \frac{\partial f}{\partial x}(at\ x = \overline{x}) = f_x(\overline{x}) \tag{4.1}$$

Now, the eigenvalues of the matrix A give a method of determining the stability as follows.

If all the eigenvalues of $f_x(\overline{x})$ (the Jacobian) have negative real parts, then the equilibrium point $\overline{x}$ is asymptotically stable.
If at least one eigenvalue of $f_x(\overline{x})$ has a positive real part, then the equilibrium point $\overline{x}$ is unstable.
If some eigenvalues of $f_x(\overline{x})$ have positive real parts and the others have negative real parts, then the unstable equilibrium point $\overline{x}$ is called a saddle.
If $f_x(\overline{x})$ has a zero eigenvalue, then the unstable equilibrium point $\overline{x}$ is called a saddle node.
If $f_x(\overline{x})$ has a pair of complex conjugate eigenvalues, then the equilibrium point $\overline{x}$ is called a center. A center is stable but not asymptotically stable.

When a power system is modelled as a dynamical system for the study of voltage stability one comes across all the above types of stability and instability. The above is an introduction to the mathematics of voltage instability and the more complex topics such as differential algebraic systems, which may be used for modelling power systems, require further study.

REFERENCES

[1] IEEE/PES Power System Stability Subcommittee Special Publication, "Voltage Stability Assessment, Procedures and Guides", IEEE, USA, 2001.

[2] Thierry Van Cutsem and Costas Vournas, "Voltage Stability of Electric Power Systems", Kluwer Academic Publishers, Boston, London, Dordrecht, 2001.

[3] Jack K. Hale and Huseyin Kocak, "Dynamics and Bifurcations", Springer-Verlag, New York, 1991.

[4] Ian Percival and Derek Richards, "Introduction to Dynamics", Cambridge University Press, Cambridge, London, New York, 1982.

[5] William E. Boyce and Richard C. DiPrima, "Elementary Differential Equations and Boundary Value Problems", John Wiley & Sons, Inc., New York, 1992.

3. Australian Universities Power Engineering Conference 2008 – Published

VOLTAGE INSTABILITY IN POWER SYSTEMS AND THE USE OF ARTIFICIAL INTELLIGENCE METHODS FOR ITS PREDICTION

K. J. T. N. Fernando* and A. Kalam*

*Faculty of Health, Engineering and Science
Victoria University of Technology
Footscray, Victoria, Australia.

Abstract:

Before the restructuring of the electricity industry adequate redundancy was built into power systems for voltage instability to be a major problem. Only rotor angle stability was considered in the operation and expansion of power systems. With the introduction of the new electricity market resulting in reduced investment and altered load patterns, particularly increasing load in areas with weak transmission and generation capacity, voltage stability has come into prominence. Unlike rotor angle stability, voltage stability requires mathematical theory and concepts that are difficult and not normally covered in undergraduate electrical engineering courses. This paper explains briefly the theory of voltage instability and the use of artificial intelligence methods for its prediction in power systems.

I INTRODUCTION

Major power system outages due to voltage instability round the world are described in [16-19].

Theories to explain and analyze voltage stability are now being developed [4, 20]. Voltage instability results in voltages in parts of the system or the entire system becoming unstable or collapsing altogether causing collapse of the power system. It is different to low voltages experienced in certain parts of the network during certain conditions, when, though some voltages are low, the system is operating at a stable point.

Mathematics of dynamical systems [5-13] is used in the study of voltage stability. Computer programs are now available for solution and visualization of solutions, PHASER [14], UWPFLOW [15] and MATLAB. UWPFLOW is voltage stability specific.

II SOME RELEVANT DEFINITIONS

The following two definitions of stability of a power system are given in [20].

3. *An operating point of a power system is small disturbance stable if, following any small disturbance, the power system state returns to be identical or close to the pre-disturbance operating point.*

4. *An equilibrium of a power system model is asymptotically stable if, following any small disturbance, the power system state tends to the equilibrium.*

The second definition assumes that the power system is modelled by, a set of differential equations.

Voltage instability is defined [4] as follows.

Voltage instability stems from the attempt of load dynamics to restore power consumption beyond the capacity of the combined transmission and generation system.

III VOLTAGE INSTABILITY, THE MECHANISM

A power system operating under stable conditions keeps continuously evolving. During this process some or all of the following take place in the system. The load changes; generators and induction motors go through electromechanical transients; static VAR compensators, (SVCs), activate; on load tap changers in transformers activate; shunt capacitors are switched on and off; automatic load recovery takes place following faults; faulted components of the power system are isolated; faulted transmission and distribution lines auto-reclose; excitation limiters activate etc. Thus a power system under load is a dynamical system. During this dynamics, if the power system is to remain stable, the operating point or the equilibrium point of the system has to track a stable point in state space. However the transmission system has a limited capacity for power transmission and generators have a limited generating capacity, on reaching one or more of these limits the system can go into voltage instability. At the point of going into voltage instability, the stable point of operation that existed before disappears. Thus the power system undergoes a transient and during this transient, the voltages decline monotonically causing a voltage collapse. It is to be noted that the state of a power system operating with low voltages but at a stable point, (i.e. there is no dynamic collapse of the voltages), does not constitute a voltage stability problem.

IV THE DYNAMICS OF A LOADED POWER SYSTEM

The dynamics of a loaded power system can be represented by a system of non-linear ordinary differential equations as follows:

$\dot{x} = f(x)$.

Where $\dot{x} = \frac{dx}{dt}$, t is time and x is a (nx1) vector.

The vector x represents the state of the system at a given time and is known as the state vector. Systems of this type are known as dynamical systems. Such dynamical systems can be solved analytically only in a very limited number of cases, however the geometric theory of ordinary differential equations allows the study of the behaviour of dynamical systems without resort to integration.

V A SIMPLE POWER SYSTEM

Consider a simple power system as follows.

A single PV or constant voltage or slack bus with a single generator connected to it supplying a constant power factor PQ load consisting of real and reactive parts equal to p(1+jk).

Let the impedance of the line be $(0 + jX)$ as resistance is neglected. Then, if I is the line current and $(S = p + jq)$ is the load power, it can be shown that [4, 20]:

$$V = E - jXI \qquad (1) \qquad (1)$$

$$S = \frac{j}{X}(EV\cos\delta + jEV\sin\delta - V^2) \qquad (2a\&b)$$

$$\therefore p = -\frac{EV}{X}\sin\delta$$

and

$$q = -\frac{V^2}{X} + \frac{EV}{X}\cos\delta$$

The above equations are written on the assumption of quasi-steady-state in which case they reduce to power flow equations.

If real power p is chosen as the slowly varying parameter and V and δ are chosen as the state vector, the variation of the magnitude of V with p is as shown in Figure 1. Such a diagram where one of the state variables is plotted against the slowly varying parameter, p in this case, is called a **bifurcation diagram or a nose curve**.

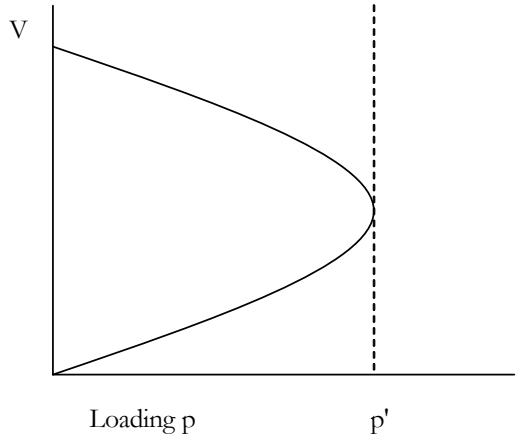

Figure 1 Bifurcation Diagram of State V Vs Parameter p

It is seen from the bifurcation diagram that for loads less than p' there are two equilibria, one at high voltage and therefore low current and the other at low voltage and high current. In practice the high voltage equilibrium is the more stable and the equilibrium at which a power system operates. As the slowly varying parameter, power p, is increased at the load

bus, the two equilibria come closer and coalesce at the critical power p' which is a **saddle node bifurcation**. Beyond p' the power system has no equilibrium points and cannot be operated. At p' voltage collapse occurs.

In a real power system the state space would be multidimensional consisting of hundreds if not thousands of states.

VI EVALUATION OF THE IEEE 14 BUS TEST SYSTEM FOR VOLTAGE STABILITY

Most available computer programs perform continuation power flows [20] using detailed steady state models of the various power system elements. Because of their ability to model the power system elements in detail they can be used to determine the progression of steady state points as system conditions change. The authors used the UWPFLOW program to perform continuation power flow studies on the IEEE 14 bus test system (refer to Figure 2) to obtain the **point of (system) collapse loading**, the power system nose curves related to voltage collapse and sufficient loading points during the continuation power flow study to train artificial neural networks (ANN'S).

Out of the available voltage stability indices used to measure proximity to voltage collapse [20], in the research presented in this paper, the additional amount of load that could be utilised at each point during the continuation power flow, before voltage collapse, known as the **loading margin** is utilised.

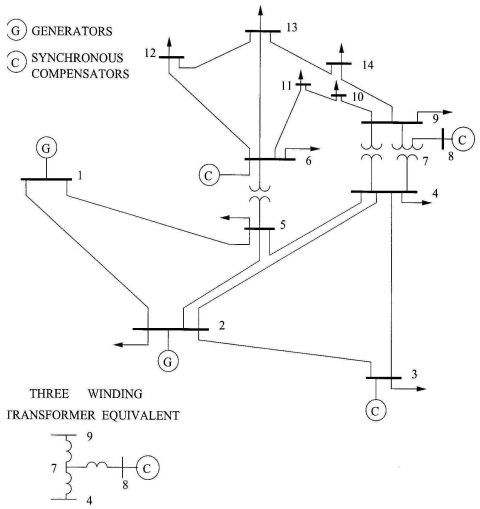

Figure 2 IEEE 14 Bus Test System

The data for the system, shown in IEEE data format, is shown in Table 1.

IEEE 14 Bus Test System Bus Data

1	Bus 1	1	HV	1	1	3	1	0	0	0	0	0	0	1.06	100	-100	0	0	0
2	Bus 2	2	HV	1	1	2	1.045	0	21.7	12.7	40	0	0	1.045	50	-40	0	0	0
3	Bus 3	3	HV	1	1	2	1.01	0	94.2	19	0	0	0	1.01	40	0	0	0	0
4	Bus 4	4	HV	1	1	0	1	0	47.8	-3.9	0	0	0	0	0	0	0	0	0
5	Bus 5	5	HV	1	1	0	1	0	7.6	1.6	0	0	0	0	0	0	0	0	0
6	Bus 6	6	LV	1	1	2	1.07	0	11.2	7.5	0	0	0	1.07	24	-6	0	0	0
7	Bus 7	7	ZV	1	1	0	1	0	0	0	0	0	0	0	0	0	0	0	0
8	Bus 8	8	TV	1	1	2	1.09	0	0	0	0	0	0	1.09	24	-6	0	0	0
9	Bus 9	9	LV	1	1	0	1	0	29.5	16.6	0	0	0	0	0	0	0	0.19	0
10	Bus 10	10	LV	1	1	0	1	0	9	5.8	0	0	0	0	0	0	0	0	0
11	Bus 11	11	LV	1	1	0	1	0	3.5	1.8	0	0	0	0	0	0	0	0	0
12	Bus 12	12	LV	1	1	0	1	0	6.1	1.6	0	0	0	0	0	0	0	0	0
13	Bus 13	13	LV	1	1	0	1	0	13.5	5.8	0	0	0	0	0	0	0	0	0
14	Bus 14	14	LV	1	1	0	1	0	14.9	5	0	0	0	0	0	0	0	0	0

IEEE 14 Bus Test System Branch Data

1	2	1	1	1	0	0.01938	0.05917	0.0528	0	0	0	0	0	0	0	0	0	0	0
1	5	1	1	1	0	0.05403	0.22304	0.0492	0	0	0	0	0	0	0	0	0	0	0
2	3	1	1	1	0	0.04699	0.19797	0.0438	0	0	0	0	0	0	0	0	0	0	0
2	4	1	1	1	0	0.05811	0.17632	0.034	0	0	0	0	0	0	0	0	0	0	0
2	5	1	1	1	0	0.05695	0.17388	0.0346	0	0	0	0	0	0	0	0	0	0	0
3	4	1	1	1	0	0.06701	0.17103	0.0128	0	0	0	0	0	0	0	0	0	0	0
4	5	1	1	1	0	0.01335	0.04211	0	0	0	0	0	0	0	0	0	0	0	0
4	7	1	1	1	0	0	0.20912	0	0	0	0	0	0	0.978	0	0	0	0	0
4	9	1	1	1	0	0	0.55618	0	0	0	0	0	0	0.969	0	0	0	0	0
5	6	1	1	1	0	0	0.25202	0	0	0	0	0	0	0.932	0	0	0	0	0
6	11	1	1	1	0	0.09498	0.1989	0	0	0	0	0	0	0	0	0	0	0	0
6	12	1	1	1	0	0.12291	0.25581	0	0	0	0	0	0	0	0	0	0	0	0
6	13	1	1	1	0	0.06615	0.13027	0	0	0	0	0	0	0	0	0	0	0	0
7	8	1	1	1	0	0	0.17615	0	0	0	0	0	0	0	0	0	0	0	0
7	9	1	1	1	0	0	0.11001	0	0	0	0	0	0	0	0	0	0	0	0
9	10	1	1	1	0	0.03181	0.0845	0	0	0	0	0	0	0	0	0	0	0	0
9	14	1	1	1	0	0.12711	0.27038	0	0	0	0	0	0	0	0	0	0	0	0
10	11	1	1	1	0	0.08205	0.19207	0	0	0	0	0	0	0	0	0	0	0	0
12	13	1	1	1	0	0.22092	0.19988	0	0	0	0	0	0	0	0	0	0	0	0
13	14	1	1	1	0	0.17093	0.34802	0	0	0	0	0	0	0	0	0	0	0	0

Table 1 IEEE 14 Bus Data in IEEE Data Format

Each branch in the 14 bus system was treated as a double circuit line and the following contingencies were chosen in addition to the full system:

8. One circuit, buses 1 to 2, out.
9. One circuit, buses 1 to 5, out.
10. One circuit, buses 6 to 11, out.
11. One circuit, buses 6 to 12, out.
12. One circuit, buses 10 to 11, out.
13. One circuit, buses 12 to 13, out.
14. One circuit, buses 13 to 14, out.

The nose curves for the most affected buses, 6, 7, 9 & 11, during the continuation power flow for the full system drawn using 220 points on the curve are shown in Figure 3. Similar curves were obtained for other operating conditions or contingencies.

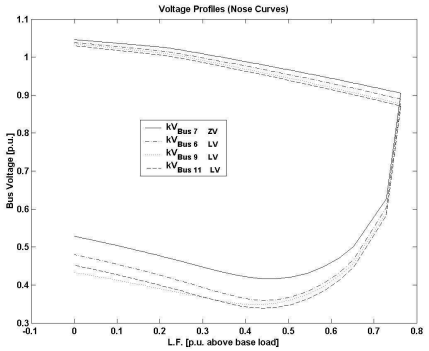

Figure 3 Nose Curves for the Full 14 Bus System

For each of the eight cases, including the case of all circuits connected, the loading margin was calculated at each loading point up to the voltage collapse point which is the nose of the curve. These points were divided into adjacent groups of three, the first group being the set of

points furthest from voltage collapse. For the purpose of training ANN's, each point in each group was assigned a vector that indicates the severity of loading of the power system as follows.

$[1\ 0\ 0]^T$ The system is safe from voltage collapse.
$[0\ 1\ 0]^T$ Caution needed during further loading.
$[0\ 0\ 1]^T$ Extreme caution needed, system approaching voltage collapse.

Altogether 1390 load points were obtained from all the continuation power flow simulations together with the bus voltages for the weakest buses. The P & Q loads and voltages of the seven weakest buses namely buses 6, 9, 10, 11, 12, 13 & 14 were chosen as the training inputs of the ANN's. Thus each ANN has 21 inputs.

VII ARTIFICIAL NEURAL NETWORK TRAINING

After a study of artificial neural networks [1, 3, 70], **Multilayer Perceptrons** that use backpropagation were chosen as the most suitable. Networks of different architectures using different learning functions, as explained below, were trained and evaluated for suitability. The Matlab Neural Network Toolbox was used for the training.

A. ANN Architectures Selected.

The notation, R-S1-S2-S3….., where R is the number of inputs and S1, S2 etc are the number of neurons in layer 1, layer 2 etc is used to represent the structure of each network. The following architectures were tested for suitability. For definitions of training functions, learning functions, transfer functions and the term epochs etc refer to [2, 3].

10. 21-25-3 with Trainlm training function and Learngdm learning function, layer 1 Logsig transfer function, layer 2 Purelin transfer function trained for 1000 epochs.
11. As above but with layer 1 Tansig transfer function, layer 2 Purelin transfer function.
12. As in 1 but with layer 1 Tansig, layer 2 Tansig.
13. As in 1 but with layer 1 Tansig, layer 2 Purelin and training function Traincgf.
14. 21-30-3 layer 1 Tansig, layer 2 Purelin and the rest as in 1.
15. 21-35-3 rest as in 5.
16. 21-25-3 using automated regularisation [2] with the training function Trainbr. Layer 1 Tansig transfer function, layer 2 Purelin transfer function. For this method the training set and the target set need to be preprocessed and the results postprocessed [2].
17. 21-50-3. The rest same as in 7.
18. 21-25-25-3. The rest same as in 7 and with the additional layer also with Tansig transfer function.

VII RESULTS

Analysis of the results by simulating the trained networks using sets of results from the various continuation power flows but not used in training and comparing them with the expected targets shows that the network architecture represented in 9 above gives the best results and therefore is the most suitable. A 3-D graph generated in Matlab for visualisation of the errors is shown in Figure 4 for network 9.

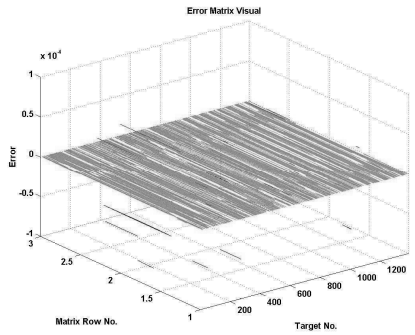

Figure 4 Error Visualisation for the ANN Architecture 9

The errors are only of the order of less than 0.0001.

VIII CONCLUSIONS

Therefore it is concluded that an Artificial Neural Network of the architecture represented as 9 in Section VII A is suitable for the prediction of pending voltage instability in a power system. A number of such networks need to be trained to take into account seasonal changes in load patterns. It would be possible for such a network to be embedded in dedicated hardware. Inputs such as the values of voltages and loads at weak buses can then be fed directly into this hardware utilising an existing SCADA system at suitable intervals of time. The output of the ANN would be an indication of the proximity to voltage instability of the power system.

IX NOTES

The topic of voltage stability being one that has come into prominence only recently the following notes are considered appropriate to place the research in its proper context.

1. A literature survey has revealed that there are no published papers for the prediction of voltage instability in power systems. This could be due to the commercial sensitivities of publishing data for real-life power systems and the novelty of the topic.
2. For the network used, the authors obtained 1390 operating points of the power system and the training of ANN's required up to 1000 epochs for each ANN architecture used. This makes the process very labour intensive and hence the selection of the IEEE 14 Bus Test System for analysis.

REFERENCES

[1] C. Canizares, "On Bifurcations, Voltage Collapse and Load Modeling," IEEE Transactions in Power Systems, vol. 10, pp. 512-522, 1995.

[2] U.-C. P. S. O. T. Force, "Final Report on the August 14, 2003 Blackout in the United States and Canada: Causes and Recommendations," 2004.

[3] A. A. P. Lerm, C. Canizares, and A. S. e Silva, "Multi-parameter Bifurcation Analysis of the South-Brazilian Power System," IEEE Transactions in Power Systems, 2002.

[4] N. Mithulananthan and S. C. Srivastava, "Investigation of a Voltage Collapse Incident in Sri Lanka's Power System," presented at EMPD'98, Singapore, 1998.

[5] C. Canizares, "Voltage Stability Assessment: Concepts, Practices and Tools," IEEE/PES, 2003.

[6] T. Van Cutsem and C. Vournas, Voltage Stability of Electric Power Systems. Boston: Kluwer Academic Publishers, 2001.
[7] W. E. Boyce and R. C. DePrima, Elementary Differential Equations and Boundary Value Problems. New York: John Wiley & Sons Inc., 1992.
[8] J. Cronin and R. E. O'Malley, "Analysing Multiscale Phenomena Using Singular Perturbation Methods," in Proceedings of Symposia in Applied Mathematics, vol. 56. Providence, Rhode Island: American Mathematical Society, 1998.
[9] J. K. Hale and H. Kocak, Dynamics and Bifurcations. New York: Springer-Verlag, 1991.
[10] J. Kevorkian and J. D. Cole, Perturbation Methods in Applied Mathematics. New York: Springer-Verlag, 1985.
[11] J. Kevorkian and J. D. Cole, Multiple Scale and Singular Perturbation Methods, vol. 114. New York: Springer, 1996.
[12] P. V. Kokotovic, H. K. Khalil, and J. O'Reilly, Singular Perturbation Methods in Control: Analysis and Design. New York: Academic Press Harcourt Brace Jovanovich, Publishers, 1986.
[13] R. E. O'Malley, Introduction to Singular Perturbations. New York: Academic Press, 1974.
[14] I. Percival and D. Richards, Introduction to Dynamics. Cambridge, London, New York: Cambridge University Press, 1982.
[15] A. L. Rabenstein, Introduction to Ordinary Differential Equations. New York: Academic Press, 1972.
[16] H. Kocak, et. al., "Phaser." USA: WWW. Phaser.com, pp. A Universal Simulator for Dynamical Syatems.
[17] C. Canizares, "UWPFLOW." Waterloo: Canizares, Claudio, pp. Solves voltage stability problems.
[18] M. T. Hagan, H. B. Demuth, and M. Beale, Neural Network Design. Boston, USA: PWS Publishing Company, 1996.
[19] F. M. Ham and I. Kostanic, Principles of Neurocomputing for Science & Engineering. Boston, USA: McGraw Hill, 2001.
[20] Various, Artificial Techniques in Power Systems. London: The Institution of Electrical Engineers, 1997.
[21] H. B. Demuth and M. Beale, Neral Network Toolbox for Use with Matlab - User's Guide. Natick, USA: The Mathworks Inc., 2001.

BIBLIOGRAPHY

[1] Various, *Artificial Techniques in Power Systems*. London: The Institution of Electrical Engineers, 1997.
[2] H. B. Demuth and M. Beale, *Neral Network Toolbox for Use with Matlab - User's Guide*. Natick, USA: The Mathworks Inc., 2001.
[3] M. T. Hagan, H. B. Demuth, and M. Beale, *Neural Network Design*. Boston, USA: PWS Publishing Company, 1996.
[4] T. Van Cutsem and C. Vournas, *Voltage Stability of Electric Power Systems*. Boston: Kluwer Academic Publishers, 2001.
[5] W. E. Boyce and R. C. DePrima, *Elementary Differential Equations and Boundary Value Problems*. New York: John Wiley & Sons Inc., 1992.
[6] J. Cronin and R. E. O'Malley, "Analysing Multiscale Phenomena Using Singular Perturbation Methods," in *Proceedings of Symposia in Applied Mathematics*, vol. 56. Providence, Rhode Island: American Mathematical Society, 1998.
[7] J. K. Hale and H. Kocak, *Dynamics and Bifurcations*. New York: Springer-Verlag, 1991.
[8] J. Kevorkian and J. D. Cole, *Perturbation Methods in Applied Mathematics*. New York: Springer-Verlag, 1985.
[9] J. Kevorkian and J. D. Cole, *Multiple Scale and Singular Perturbation Methods*, vol. 114. New York: Springer, 1996.
[10] P. V. Kokotovic, H. K. Khalil, and J. O'Reilly, *Singular Perturbation Methods in Control: Analysis and Design*. New York: Academic Press Harcourt Brace Jovanovich, Publishers, 1986.
[11] R. E. O'Malley, *Introduction to Singular Perturbations*. New York: Academic Press, 1974.
[12] I. Percival and D. Richards, *Introduction to Dynamics*. Cambridge, London, New York: Cambridge University Press, 1982.
[13] A. L. Rabenstein, *Introduction to Ordinary Differential Equations*. New York: Academic Press, 1972.
[14] H. Kocak, et. al., "Phaser." USA: WWW. Phaser.com, pp. A Universal Simulator for Dynamical Syatems.
[15] C. Canizares, "UWPFLOW." Waterloo: Canizares, Claudio, pp. Solves voltage stability problems.
[16] U.-C. P. S. O. T. Force, "Final Report on the August 14, 2003 Blackout in the United States and Canada: Causes and Recommendations," 2004.
[17] N. Mithulananthan and S. C. Srivastava, "Investigation of a Voltage Collapse Incident in Sri Lanka's Power System," presented at EMPD'98, Singapore, 1998.
[18] A. A. P. Lerm, C. Canizares, and A. S. e Silva, "Multi-parameter Bifurcation Analysis of the South-Brazilian Power System," *IEEE Transactions in Power Systems*, 2002.
[19] C. Canizares, "On Bifurcations, Voltage Collapse and Load Modeling," *IEEE Transactions in Power Systems*, vol. 10, pp. 512-522, 1995.

[20] C. Canizares, "Voltage Stability Assessment: Concepts, Practices and Tools," IEEE/PES, 2003.
[21] P. Kundur and e. al., "Definition and Classification of Power System Stability," *IEEE Transactions in Power Systems*, vol. 19, 2004.
[22] V. Ajjarapu, "A Study of Dynamic Aspects Related to Voltage Collapse in Power Systems," presented at 28th Conference on Decision and Control, Tampa, Florida, 1989.
[23] V. Ajjarapu, "Nonlinear Static and Dynamical Aspects of Power Systems: A Bifurcation Approach," *Unknown (IEEE)*, 1992.
[24] D. J. Hill, "On the Equilibria of Power Systems with Nonlinear Loads," *IEEE Transactions on Circuits and Systems*, vol. 36, 1989.
[25] D. J. Hill and I. M. Y. Mareels, "Stability Theory for Differential/Algebraic Systems with Application to Power Systems," *IEEE Transactions on Circuits and Systems*, vol. 37, 1990.
[26] V. Ajjarapu, "Application of Bifurcation and Continuation Methods for the Analysis of Power System Dynamics," *Unknown (IEEE)*, 1995.
[27] V. Ajjarapu and B. Lee, "Nonlinear Oscillations and Voltage Collapse Phenomenon in Electrical Power Systems," *Unknown (IEEE)*, 1990.
[28] V. Ajjarapu and B. Lee, "A General Approach to Study Static and Dynamic Aspects of Voltage Instability," presented at 31st Conference on Decision and Control, Tucson, Arizona, 1992.
[29] V. Ajjarapu and B. Lee, "Bifurcation Theory and its Application to Nonlinear Dynamical Phenomena in an Electrical Power System," *IEEE Transactions in Power Systems*, vol. 7, 1992.
[30] B. Lee and V. Ajjarapu, "Factors to be Considered in the Study of Voltage Stability of Structure Preserving Power System Model," *Unknown (IEEE)*, 1993.
[31] A. A. P. Lerm, C. Canizares, F. A. B. Lemos, and A. S. e Silva, "Multi-parameter Bifurcation Analysis of Power Systems," presented at North American Power Symposium, Cleveland, Ohio, 1998.
[32] V. Ajjarapu and Z. Feng, "A Novel Approach for Voltage Collapse Analysis and Control," *Unknown (IEEE)*, 1998.
[33] C. Canizares, "Application of Optimization to Voltage Collapse Analysis," presented at IEEE/PES Summer Meeting, San Diego, 1998.
[34] W. Rosehart, C. Canizares, and V. H. Quintana, "Optimal Power Flow Incorporating Voltage Collapse Constraints," *University of Waterloo, Canada. Internally Published.*
[35] C. Canizares and F. L. Alvarado, "Point of Collapse and Continuation Methods for Large AC/DC Systems," *IEEE Transactions in Power Systems*, vol. 8, pp. 1-8, 1993.
[36] C. Canizares, F. L. Alvarado, C. L. DeMarco, I. Dobson, and W. F. Long, "Point of Collapse Methods Applied to AC/DC Power Systems," *IEEE Transactions in Power Systems*, vol. 7, 1992.
[37] C. Canizares, A. C. Z. de Souza, and V. H. Quintana, "Comparison of Performance Indices for Detection of Proximity to Voltage Collapse," *IEEE Transactions in Power Systems.*

[38] C. Canizares, A. C. Z. de Souza, and V. H. Quintana, "Improving Continuation Methods for Tracing Bifurcation Diagrams in Power Systems," presented at Bulk Power System Voltage Phenomena - III Seminar, Davos, Switzerland, 1994.

[39] C. Canizares, N. Mithulananthan, A. Berizzi, and J. Reeve, "On the Linear Profile of Indices for the Prediction of Saddle-Node and Limit-Induced Bifurcation Points in Power Systems," *IEEE Transactions on Circuits and Systems*, 2003.

[40] V. Ajjarapu and C. Christy, "The Continuation Power Flow: A Tool for Steady State Voltage Stability Analysis," *IEEE Transactions in Power Systems*, vol. 7, 1992.

[41] V. Ajjarapu and C. Christy, "The Application of a Locally Parameterised Continuation Technique to the Study of Steady State Voltage Stability," *Unknown (IEEE)*, Unknown.

[42] A. C. Z. de Souza, C. Canizares, and V. H. Quintana, "New Techniques to Speed Up Voltage Collapse Computations Using Tangent Vectors," *IEEE Transactions in Power Systems*, 1996.

[43] Z. Feng, V. Ajjarapu, and B. Long, "Identification of Voltage Collapse Through Direct Equilibrium Tracing," *IEEE Transactions in Power Systems*, vol. 15, 2000.

[44] C. Guoyun, D. J. Hill, and R. Hui, "Continuation of Local Bifurcations for Power System Differential-Algebraic Equation Stability Model," *IEE Proceedings on Generation Transmission and Distribution*, vol. 152, 2005.

[45] Q. Wang, H. Song, and V. Ajjarapu, "Continuation-Based Quasi-Steady-State Analysis," *IEEE Transactions in Power Systems*, vol. 21, 2006.

[46] D. Yang and V. Ajjarapu, "An Overview of Critical Eigenvalue Tracing and Decoupled Time Domain Simulation in Power System Analysis," *Unknown (IEEE)*, 2005.

[47] Y. Zhou and V. Ajjarapu, "Identification and Tracing of Voltage and Oscillatory Stability Margins," *Unknown (IEEE)*, 2002.

[48] Y. V. Makarov, D. J. Hill, and Z.-Y. Dong, "Computation of Bifurcation Boundaries for Power Systems: A New Delta-Plane Method," *IEEE Transactions on Circuits and Systems*, vol. 47, 2000.

[49] X. Wen and V. Ajjarapu, "Critical Eigenvalue Trajectory Tracing for Power System Oscillatory Stability Assessment," *Authors from Iowa State University*.

[50] D. Yang and V. Ajjarapu, "Critical Eigenvalues Tracing for Power System Analysis via Continuation of Invariant Subspaces and Projected Arnoldi Method," *IEEE Transactions in Power Systems*, vol. 22, 2007.

[51] W. Rosehart, C. Canizares, and V. H. Quintana, "Effect of Detailed Power System Models in Traditional and Voltage Stability Constrained Optimal Power Flow Problems," *IEEE Transactions in Power Systems*, 2002.

[52] B. Lee and V. Ajjarapu, "Invariant Subspace Parametric Sensitivity (ISPS) of Structure-Preserving Power System Models," *IEEE Transactions in Power Systems*, vol. 11, 1996.
[53] N. Mithulananthan, C. Canizares, and J. Reeve, "Indices to Detect Hopf Bifurcations in Power Systems," presented at NAPS-2000, Waterloo, Ontario, 2000.
[54] C. L. DeMarco and C. Canizares, "A Vector Energy Function Approach for Security Analysis of AC/DC Systems," *IEEE Transactions in Power Systems*, vol. 7, pp. 1001-1011, 1992.
[55] C. L. DeMarco and T. J. Overbye, "An Energy Based Security Measure for Assessing Vulnerability to Voltage Collapse," *IEEE Transactions in Power Systems*, vol. 5, 1990.
[56] A. Halim, K. Takahashi, and B. Kermanshahi, "Lyapunov Function for Robust Voltage Stability Analysis Considering Perturbation Location," *Unknown (IEEE)*, 1998.
[57] A. Halim, K. Takahashi, and B. Kermanshahi, "Dynamic Voltage Stability Analysis Using Lyapunov Function Method," presented at 8th International Conference on Harmonics and Quality of Power, ICHQP'98, Athens, Greece, 1998.
[58] N. Narasimhamurthi and M. Musavi, "A Generalised Energy Function for Transient Stability Analysis of Power Systems," *IEEE Transactions on Circuits and Systems*, vol. CAS-31, 1984.
[59] T. J. Overbye and C. L. DeMarco, "Voltage Security Enhancement Using Energy Based Sensitivities," *IEEE Transactions in Power Systems*, vol. 6, 1991.
[60] N. A. Tsolas, A. Arapostathis, and P. Varaiya, "A Structure Preserving Energy Function for Power System Transient Stability Analysis," *IEEE Transactions on Circuits and Systems*, vol. CAS-32, 1985.
[61] N. Narasimhamurthi, "On the Existence of Energy Function for Power Systems with Transmission Losses," *IEEE Transactions on Circuits and Systems*, vol. CAS-31, 1984.
[62] J. Zhao, H. Li, H. Jia, N. He, Z. Tang, Y. Zhang, and H. Fu, "A Real-Time Monitor Framework for Static Voltage Stability of Power System," *Unknown (IEEE)*.
[63] A. C. Z. de Souza, J. C. S. de Souza, and A. M. L. da Silva, "On-Line Voltage Stability Monitoring," *IEEE Transactions in Power Systems*, vol. 15, 2000.
[64] S. T. Kurita A., "The Power System Failure on July 23, 1987 in Tokyo," presented at 27th Conference on Decision and Control, Tokyo, 1988.
[65] o. L. R. f. D. P. IEEE Task Force, "Load Representation for Dynamic Performance Analysis," in *IEEE/PES Winter Meeting*. New York, USA: IEEE, USA, 1992.
[66] o. L. R. f. D. P. IEEE Task Force, "Standard Load Models for Power Flow and Dynamic Performance Simulation," in *IEEE/PES Summer Meeting*. San Francisco, California, USA: IEEE, USA, 1994.

[67] W. W. Price, K. A. Wirgau, A. Murdoch, J. V. Mitsche, E. Vaahedi, and M. A. El-Kady, "Load Modeling for Power Flow and Transient Stability Computer Studies," *IEEE Transactions in Power Systems*, vol. 3, 1988.

[68] J. N. Fernando, "Electrical Energy Transactions in a Spot Price Based Electrical Industry," in *School of Electrical & Computer Systems Engineering*, vol. Master of Engineering by Research. Melbourne, Australia: RMIT University, 2001.

[69] T. Kohonen, "An Introduction to Neural Computing," *Neural Networks*, vol. 1, pp. 3 - 16, 1988.

[70] F. M. Ham and I. Kostanic, *Principles of Neurocomputing for Science & Engineering*. Boston, USA: McGraw Hill, 2001.

[71] S. Lee and R. M. Kil, "Multilayer Feedforward Potential Function Network," presented at Proceedings of the International Conference on Neural Networks, 1988.

[72] R. P. Lippmann, "An Introduction to Computing with Neural Nets," *Acoustics, Speech, and Signal Processing Magazine*, vol. 4, pp. 4 - 22, 1987.

[73] D. E. Rumelhart, G. E. Hinton, and J. L. McClelland, *Parallel Distributed Processing: Explorations in the Microstructure of Cognition, Vol. 1, Foundations*, 1986.

[74] G. E. Hinton, "Connectionist Learning Procedures," *Artificial Intelligence*, vol. 40, pp. 185 - 232, 1989.

[75] Y. le Cun, "A Theoretical Framework for Backpropagation," *Proceedings of the Connectionist Models Summer School*, pp. 21-28, 1998.

[76] B. Widrow and M. A. Lehr, "30 Years of Adaptive Neural Networks: Perceptron, Madaline, and Backpropagation," *Proceedings of the IEEE*, vol. 78, pp. 1415-1442, 1990.